9950-752

FINAL REPORT

CONTRACT 955935

THERMACORE, INC.

LANCASTER, PENNSYLVANIA

STUDY OF A HEAT REJECTION SYSTEM

FOR THE

NUCLEAR ELECTRIC PROPULSION (NEP) SPACECRAFT

NOVEMBER, 1982

PRINCIPAL INVESTIGATOR

DONALD M. ERNST

Prepared For:

JET PROPULSION LABORATORY
CALIFORNIA INSTITUTE OF TECHNOLOGY
PASADENA, CALIFORNIA

"This work was performed for the Jet Propulsion Laboratory, California Institute of Technology sponsored by the National Aeronautics and Space Administration under Contract NAS 7-100"

TECHNICAL CONTENT STATEMENT

"This report contains information prepared by Thermacore, Inc. under subcontract. Its content is not necessarily endorsed by the Jet Propulsion Laboratory, California Institute of Technology or the National Aeronautics and Space Administration."

ABSTRACT

This report covers the testing and evaluation of two different heat pipe radiator elements; one intended for use with the power conversion subsystem of the NASA funded Nuclear Electric Propulsion (NEP) Spacecraft and one intended for use with the DOE funded Space Power Advanced Reactor (SPAR) system.

The NEP radiator heat pipe was designed, fabricated and processed by Thermacore under JPL subcontract 955100. The stainless steel/sodium heat pipe was 4.42 meters long and had a 2 cm diameter. Thermal performance testing at 920 K showed a non-limited power level of 3560 watts, well in excess of the design power of 2600 watts. This test verified the applicability of screen arteries for use in long radiator heat pipes.

The SPAR radiator heat pipe was designed and fabricated by LANL under DOE sponsorship and subsequently shipped to Thermacore for loading and processing. The titanium/potassium heat pipe was 5.5 meters long and had a semicircular crossection with a 4 cm diameter. Thermal performance testing at 775 K showed a maximum power level of 1.86 kW, somewhat short of the desired 2.6 kW beginning of life design requirement. The reduced performance was shown to be the result of the inability of the evaporator wall wick (shot blasted evaporator wall) to handle the required liquid flow.

In addition to testing the radiator heat pipes, Thermacore's A37 computer code was improved so that the predicted heat pipe performance is in equilibrium with the environment the heat pipe is in. The test data for the NEP radiator heat pipe was correlated using A37. LANL's HTPIPE computer code was compared to Thermacore's A37 and the differences

discussed with LANL. Both codes are very similar but A37 was shown to be more versatile and shows better agreement with test data.

TABLE OF CONTENTS

FIGURES

FIGURES
(continued)

TABLES

1. INTRODUCTION

This report covers work done by Thermacore, Inc., Lancaster, PA, under Contract 955935, "The Study of a Heat Rejection System for the Nuclear Electric Propulsion (NEP) Spacecraft." The work was performed between December 1980 and October 1981.

The work effort had three interrelated tasks, which are presented as sections of this report. They are: (1) Performance testing of the radiator heat pipe fabricated under Contract 955100, (2) Heat pipe computer modeling and the comparison of computer code A-37 with LANL's HTPIPE Code, and (3) The loading, processing and testing of a LANL supplied titanium heat pipe radiator element for the SPAR system.

2. PERFORMANCE TESTING

The 4.4 meter long stainless steel/sodium heat pipe fabricated under Contract 955100 is described in detail in the JPL Subcontract 955100 Final Report[1]. During the performance testing described below, the 4.4 meter long heat pipe was inadvertently operated beyond the heat pipe's capability for the operating temperature. This damaged the evaporator wick. Following unsuccessful attempts to reestablish full performance, the test was terminated, and work was begun on the fabrication of a second heat pipe. Following the fabrication of an evaporator which was to eliminate the possibilities of evaporator hot spots, as had occurred with the first heat pipe, the development of the second heat pipe was terminated at JPL's request as the program was redirected from a conductively coupled heat source to converter to a radiation coupled system. The program objective was changed and work began on the loading, processing and testing of the LANL supplied titanum/potassium heat pipe.

2.1 Background and Heat Pipe Description

The 4.4 meter long heat pipe was fabricated to demonstrate technology rather than to represent a particular NEP system radiator element. This particular test was to qualify the design of screen wick arteries and the validity of the computer model. For example, if the heat pipe was used with thermionics, the envelope material would likely be Niobium so as to interface properly with the collector. Alternatively, if high temperature thermoelectrics were the energy conversion devices, then either a Niobium or stainless steel envelope could be employed. If the radiator temperature was reduced 200 K to 720 K, then titanium could be used. The choice of stainless steel/

sodium was made as a cost effective and convenient means of demonstrating the screen wick artery technology.

Likewise, the actual dimension of the heat pipe was different than a true radiator element. The nominal design of a radiator element was 2 cm OD by 0.025 cm wall by the required length for the evaporator, adiabatic and condenser (2M to 5M total) sections. The heat pipe fabricated for testing used a 2.09 cm ID x 2.67 cm OD envelope which was readily available. The length was limited by the existing vacuum system 4.8 meters long.

The heat pipe is seen in its test rack prior to testing in Figure 1. Figure 2 is a close up of the 25 cm evaporator end, and Figure 3 shows the open arteries in the condenser prior to final closure of the heat pipe envelope. Table 1 gives the details of the heat pipe dimensions and wick structures. The nominal external evaporator temperature of a thin walled heat pipe is 920 K with a 20 K total ΔT at the design power of 2600 watts. The as fabricated heat pipe had a 36 K ΔT at 2600 watts due to its heavier stainless steel wall.

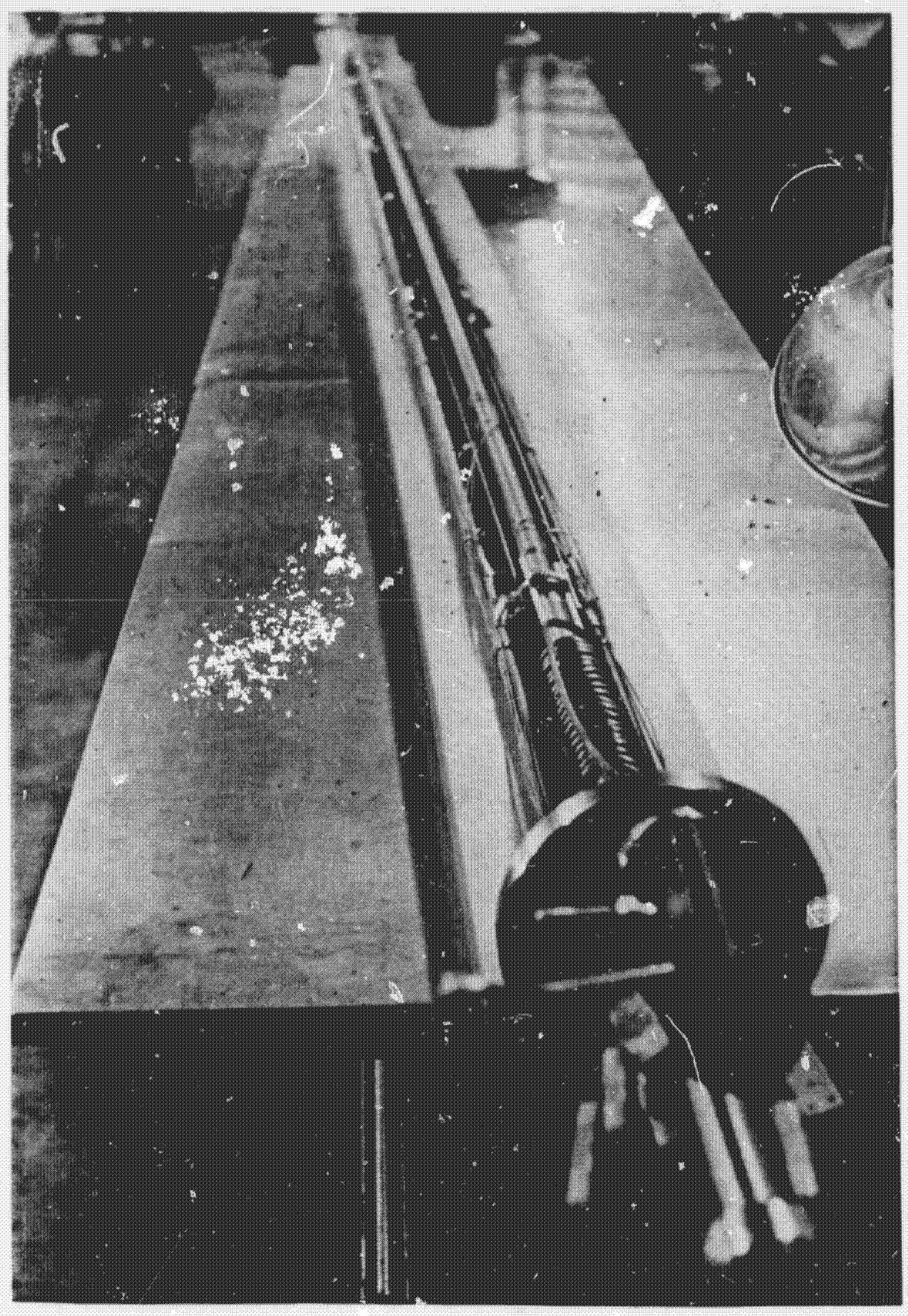

Fig. 1. Radiator Heat Pipe Ready For Test

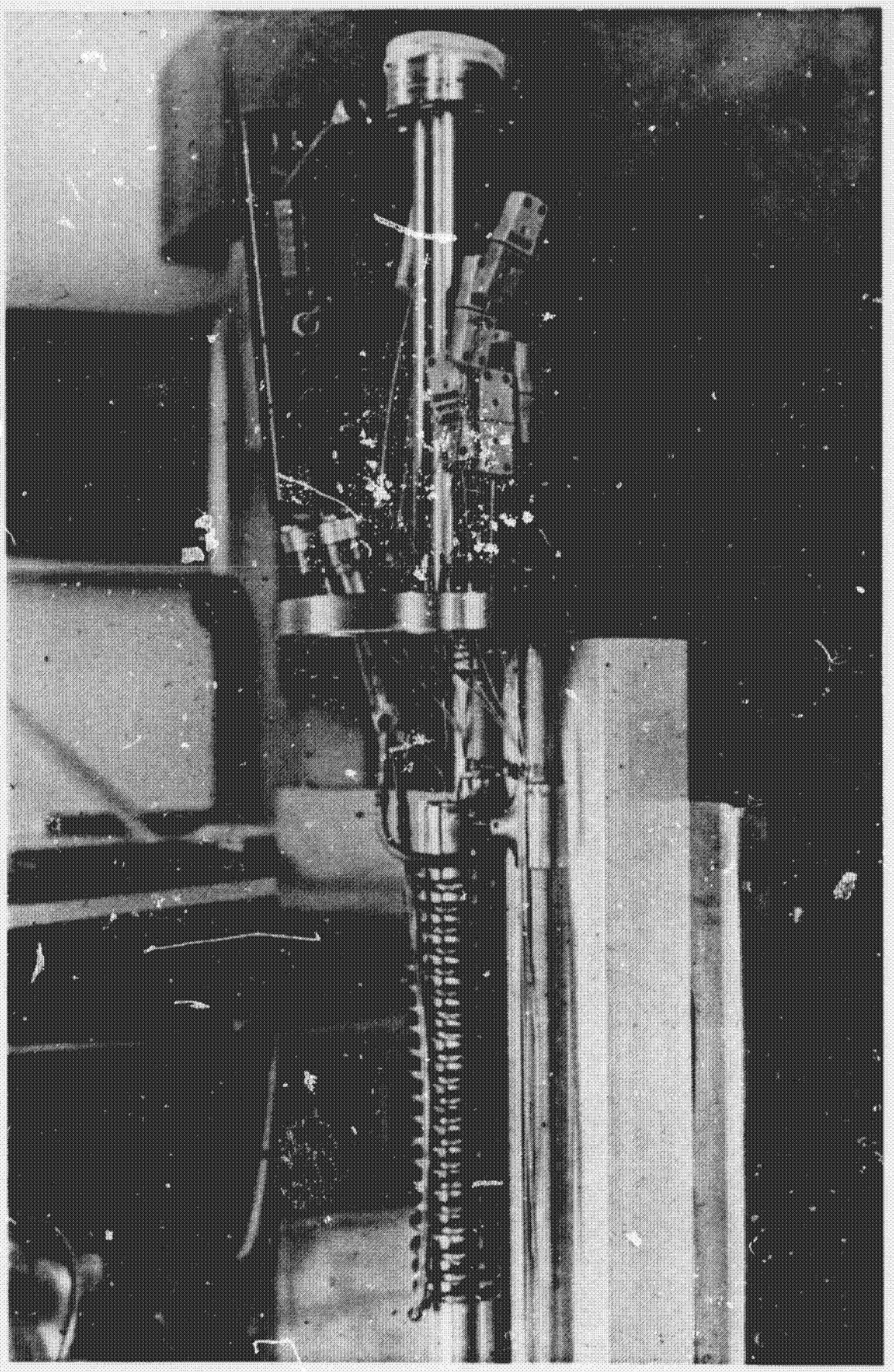

Fig. 2. Heat Pipe Evaporator With RF Coil And Instrumentation

Fig. 3. Arteries In Radiator Heat Pipe Condenser

TABLE 1

HEAT PIPE RADIATOR ELEMENT DESIGN

Evaporator	28 cm
Condenser	408 cm
Outside Diameter	2.67 cm
Inside Diameter	2.09 cm
Wall Thickness	0.29 cm
Material	304L SS (3/4" IPS Sch 40)
Wall Wick	2 wraps - 200 mesh
Number of Arteries	2
Artery Wick	2 wraps - 200 mesh
Fluid	Sodium

Nominal Operating Temperatures at 2600 watts

Evaporator - 935 K (920 K equivalent for thin wall Nb)

Condenser High - 915 K (913 K equivalent for thin wall Nb)

Condenser Low - 912 K (910 K equivalent for thin wall Nb)

Design Power - 2600 watts, ΔT = 23 K (10 K)

Maxium Power - 5300 watts, ΔT = 46 K (23K)

2.2 Performance Testing

The meaningful performance test results are seen in Table 2. The test numbers indicate the order in which the tests were carried out. For example, Tests 1-1 and 1-2 were performed within the same time frame where no changes were made to the heat pipe. Following test set 1, the second set of test data were taken with three additional thermocouples placed on the condenser. The third set was taken following the cleaning of the vacuum system and the fourth and fifth sets were taken after all thermocouples were resecured to the heat pipe. A second group of thermocouples was placed on the heat pipe for the sixth test set; however, they were unshielded and the RF interfered with their readings.

Figure 4 shows the location of the thermocouples on the heat pipe and the location of the heat pipe within the water cooled calorimeter. Figure 5 shows the best fit curve for total power transferred by the heat pipe versus RF amps.

Figure 6 shows the vacuum system in which the heat pipe was tested. Figure 7 shows the thermometers used to measure the cooling water temperature rise on which calorimetric measurements were made to establish the heat pipe's power performance.

Exact comparison of the measured test data to the theoretical design performance at the design temperature is not possible because the combined radiating area and emissivity of the heat pipe was greater than the design condition. From Table 2 one sees that in tests 2-3 and 2-4 the radiant load was 2635 and 2698 watts respectively at nominal minimum condenser temperatures of 831K and 853K. The total load was 2735 and 2803 watts. These two data points are in excess of the

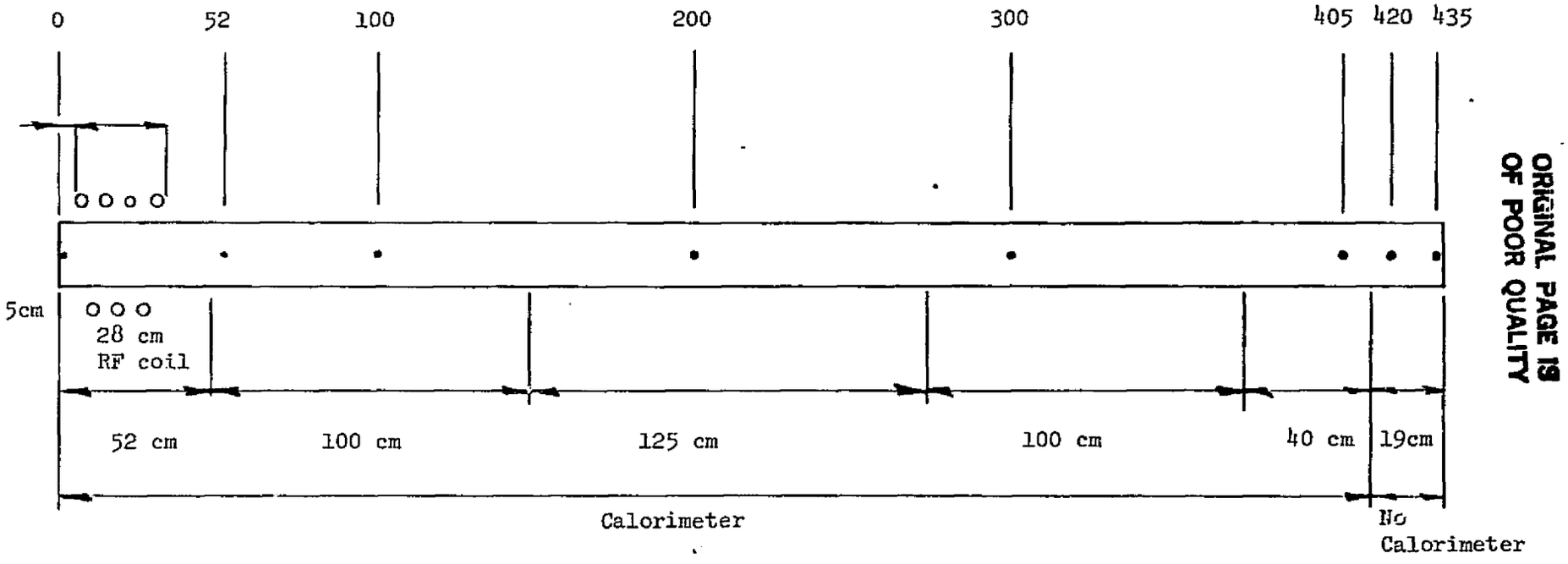

Fig. 4. Thermocouple, RF Coil And Calorimeter Locations

Figure 5 - Total Heat Pipe Power vs RF Current

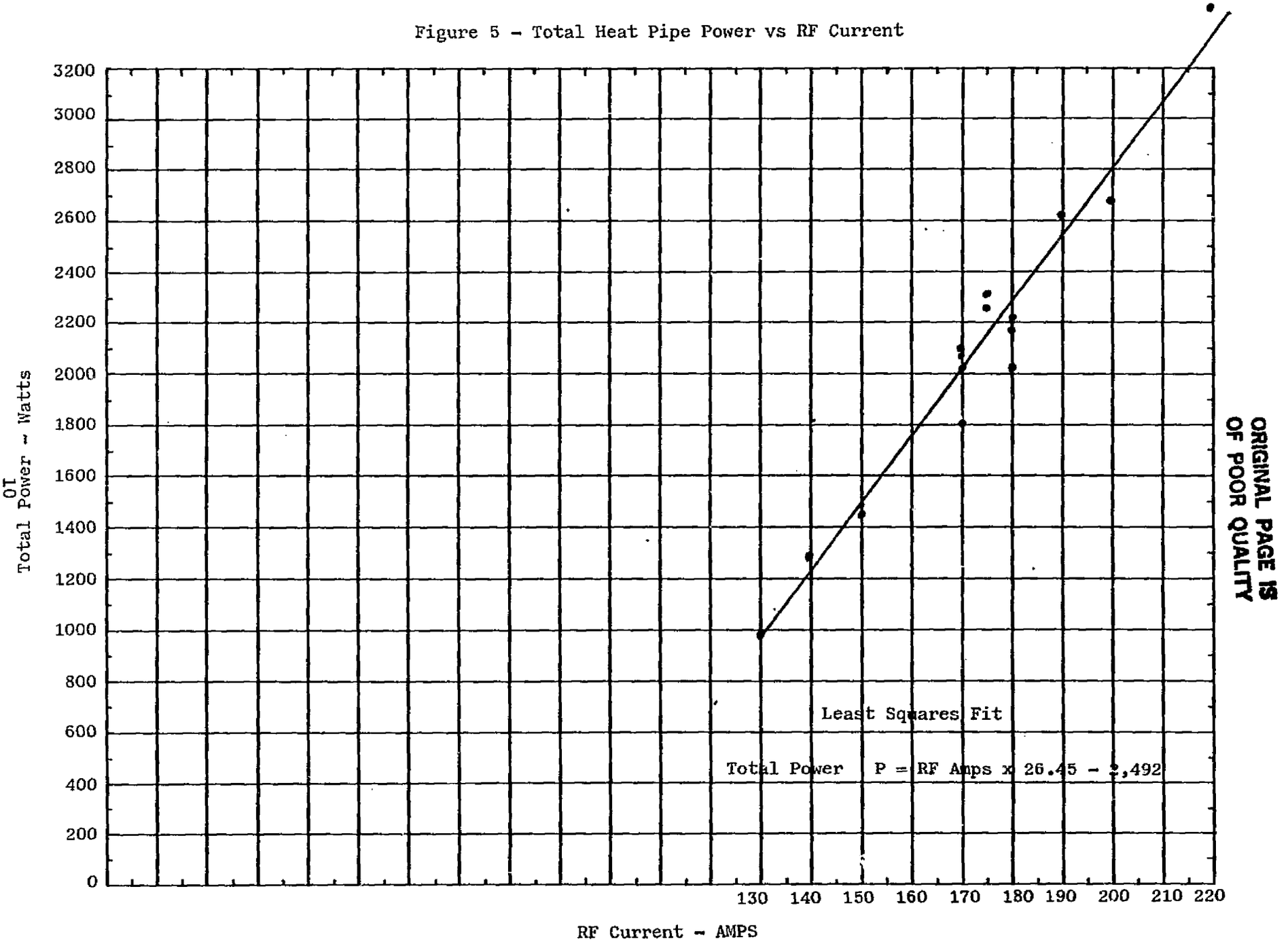

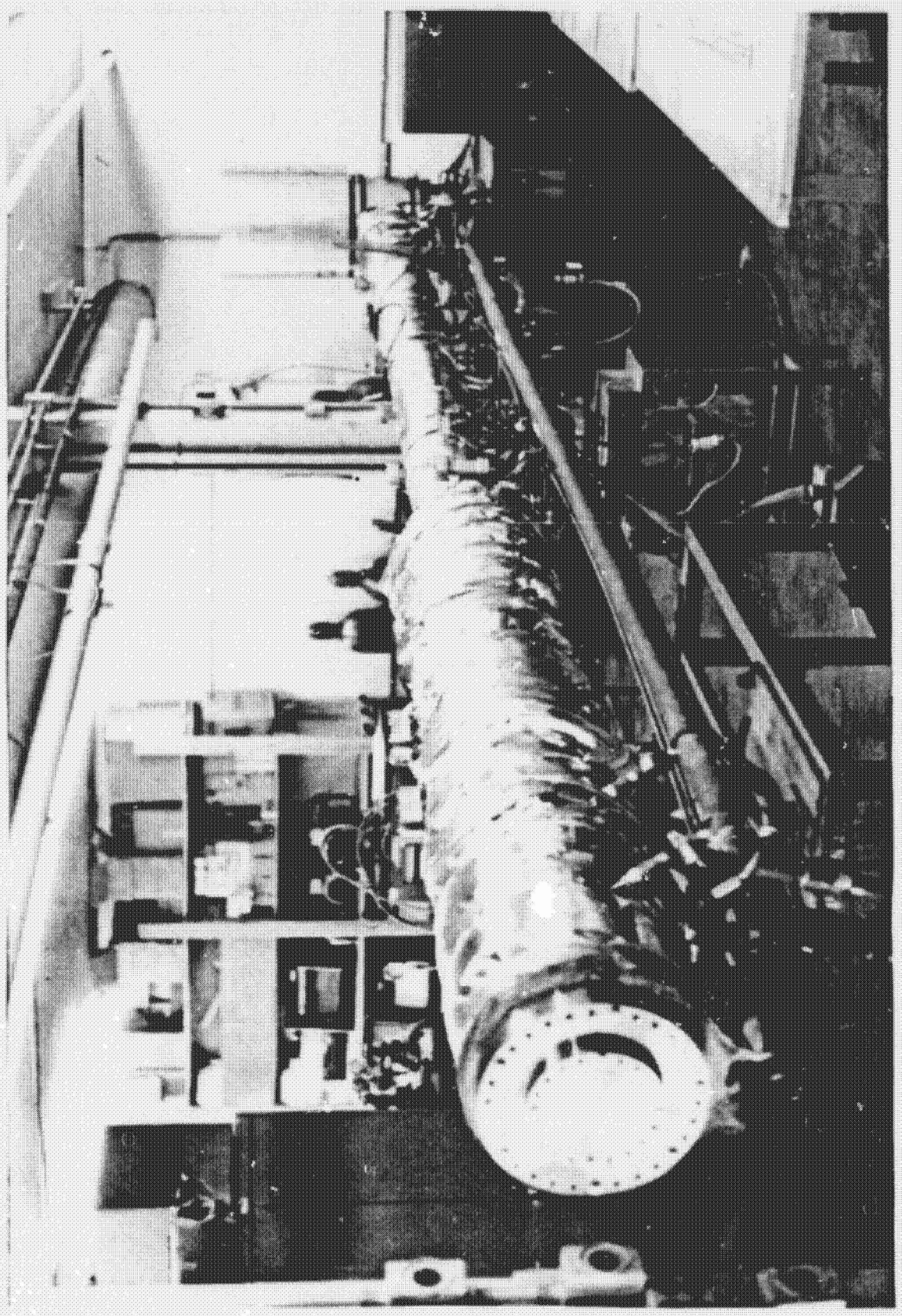

Fig. 6. Vacuum System For Heat Pipe Testing

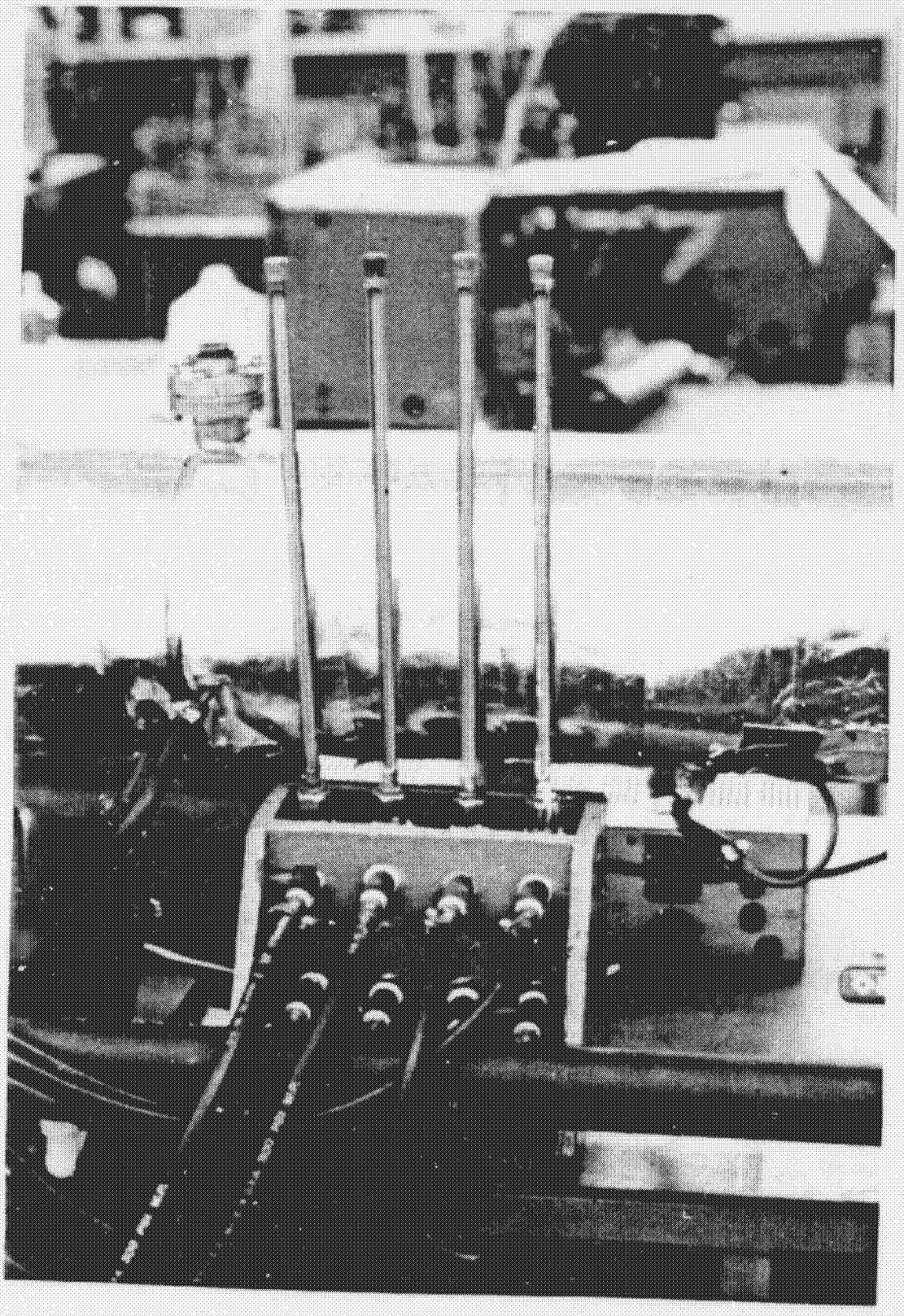

Fig. 7. Instrumentation Used For Calorimetric Measurements

TABLE 2

4.4 METER LONG TEST DATA

Test #	RF Amps	Power-Watts Rad.	Cond.	Total	EVAPORATOR 1	EVAPORATOR 1	CONDENSER THERMOCOUPLE LOCATION FROM EVAPORATOR – CM 52.2	52.5	100.5	103.5	200.5	207	300.3	303.5	405	420	435
1-2	220				602	–	606	622	624	624	625	613	608	624	–	–	–
2-5	220	3446	114	3560	656	–	620	635	606	635	642	630	627	617	622	600	627
2-4	200	2698	105	2803	627	–	573	588	564	588	574	579	580	578	578	558	580
1-1	190				563	–	563	576	558	580	568	570	551	568			
2-2	190				604	–	552	571	542	563	572	558	558	544	557	536	558
2-3	190	2635	100	2735	612	–	563	579	551	570	580	565	564	556	564	540	558
2-1	180				580	–	540	556	526	548	554	540	538	520	540	512	530
3-3	180	2217															
4-6	180	2029	96	2125	584	584	550	568	562	559	546	546	537	537	526	520	532
4-7	180	2187	98	2285	584	584	552	572	564	564	551	551	540	540	536	526	538
5-3	175	2213	98	2311	586	588	560	556	566	558	556	552	540	529	531	530	538
5-4	175	2173	97	2270	584	584	558	554	564	555	553	549	537	526	529	528	535
3-2	170				504	–	527	540	519	494	533	526	512	492	474	485	494
4-4	170	1823	92	1915	574	574	538	554	543	543	525	525	512	512	502	498	508
4-5	170	2010	92	2102	576	576	540	555	544	544	530	530	518	518	500	502	514
5-2	170	2085	95	2180	581	582	555	550	556	550	547	541	530	520	522	520	528
6-2	170	2132	95	2227	581	581	561	550	557	547	546	541	530	521	523	520	526
3-1	160				496	–	516	534	508	487	516	509	489	468	440	455	227
4-3	150	1443	–	1443	556	556	536	522	525	525	500	500	464	464	378	323	107
5-1	150				553	554	534	525	530	525	514	505	473	470	454	429	188
6-1	150	1448	–	1448	560	561	555	526	530	524	514	503	474	465	420	418	175
4-2	140	1290	–	1290	550	550	532	514	518	518	494	490	448	448	91	40	36
4-1	130	976	–	976	542	542	529	527	507	507	483	478	376	239	17	17	17

required radiant power at 79 K and 59 K lower operating temperatures. Also, test No. 2-5 shows the heat pipe at the desired operating temperature of 920 K transferring a total of 3560 watts, of which 3446 is by radiation. Accordingly, one concludes that the screen artery heat pipe performed as designed, and as will be shown in Section 3, the predicted temperature profile for a given temperature and power is in good agreement with the measured data.

During the taking of the sixth set of test data, the heat pipe was operated as a variable conductance device in order to see what effects the presence of an inert gas in the heat pipe might have on the arteries. During this time, the temperature and power level was increased to near 900 C and 6 kW for a 2 meter long heat pipe. While at this condition, the inert gas was inadvertently pumped out and the heat pipe evaporator dried out and began to over heat. Prior to shutting down the RF heat input, as the sodium returned to the evaporator, high pressure pulses of superheated sodium vapor pushed the evaporator screen wick away from the wall.

Following cooling of the heat pipe, all subsequent attempts to regain proper operation of the heat pipe failed. Accordingly, a new heat pipe was begun.

2.3 Improved Evaporator Wick

Normally, to prevent local hot spots in the evaporator, the first layer of screen wick is sintered or bonded to the heat pipe wall. Unless a split/expanding mandrel is used it is difficult to bond to a SS envelope. Since SS has a high thermal expansion, an internal mandrel must have a greater thermal expansion. There are few such

materials. Accordingly, a sintered powder metal wick structure was to be fabricated in lieu of the first layer of screen. A photograph of the evaporator is seen in Figure 8. Although a well sintered evaporator was made, no heat pipe was fabricated using it, as the emphasis of the program was shifted to processing and testing of RAD3, the 5.5 meter long SPAR titanium Radiator Heat Pipe.

Along with sintering a metal powder to the heat pipe wall, a heat pipe cleaning schedule was introduced which included a dry hydrogen firing($\simeq$ -100 C dew point) at 900 C of the heat pipe evaporator.

The heat pipe evaporator was machined so that its diameter was .030 inches larger than the rest of the heat pipe. Using 200 x 400 mesh nickel powder, the ID of the evaporator was built up to its original diameter by sintering the nickel powder in place in dry hydrogen. This wick structure was felt to be capable of providing all of the circumferential liquid flow for the evaporator. Thus, the arteries and their circumferential wick need only make nominal contact with the sintered nickel in order to assure liquid distribution in the evaporator, and since the sintered wick would always be full, there would be no occurrence of hot spots due to poor fitting of the screen wick against the evaporator wall.

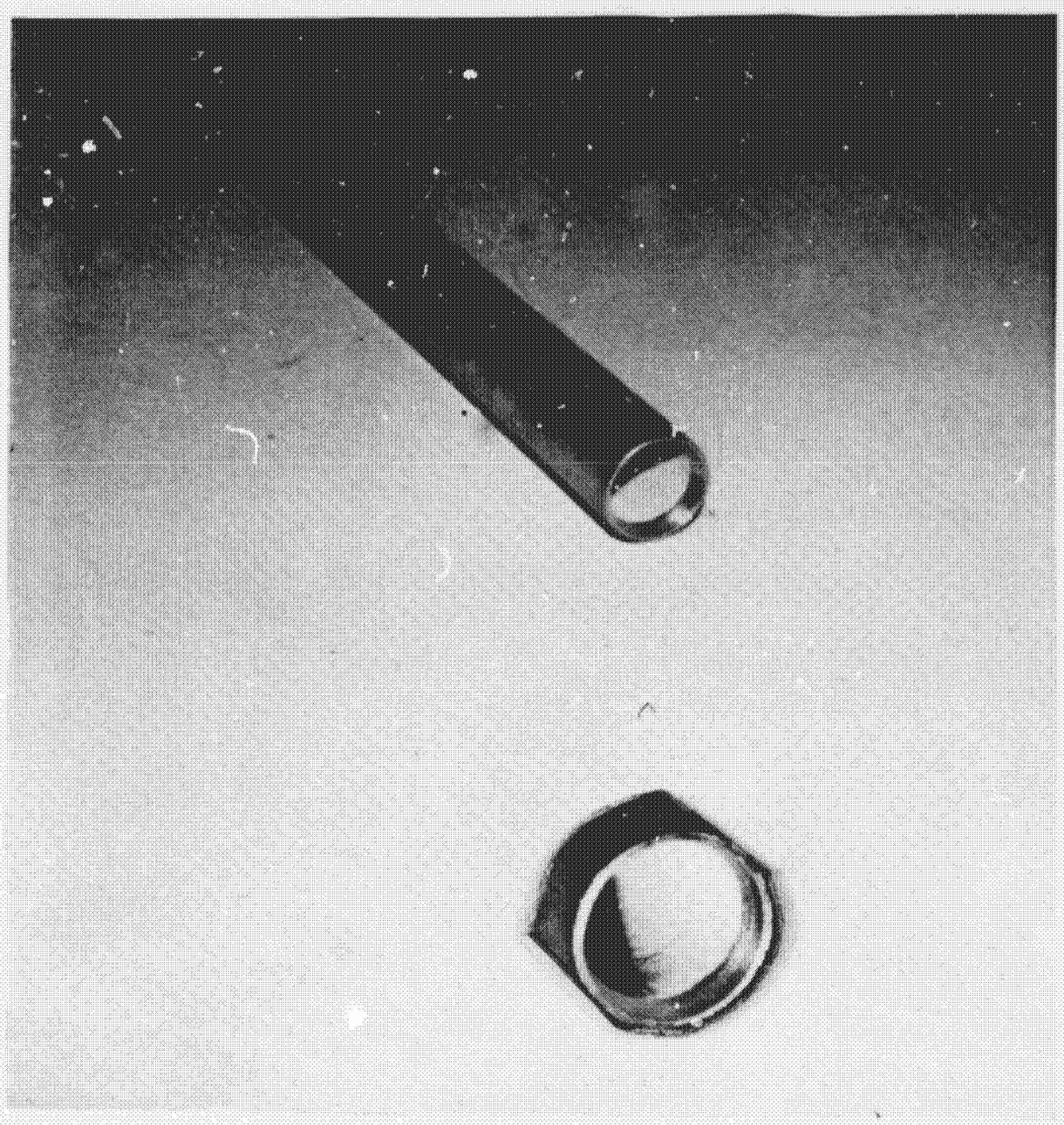

Fig. 8. Sintered Powder Metal Wick Evaporator

3. COMPUTER MODELING

Thermacore's heat pipe computer code A-37 is a comprehensive user interactive code for use in design analysis and empirical correlation of heat pipe test data. The code includes the most recent theoretical formulation for the vapor flow regimes within the evaporator, adiabatic and condenser zones. The code integrates over a user-specified number of increments in each of the three zones, making adjustment in the physical properties of the working fluid and wall and wick material as a function of temperature in each increment. One option includes the thermal equilibrium case where the throughput down the heat pipe is equal to the radiant and conductive load of the condenser as defined by the external condenser temperature and system parameters.

Additional items identified, but currently not included in the program include: non uniform heat loading in the evaporator, heat loss in the adiabatic zone, and their effect on power throughput and temperature profile. However, as will be shown below, A-37 is more comprehensive than LANL's heat pipe computer code HTPIPE[2].

3.1 A-37 Computer Code

Appendix A contains copies of the input and output statements for A-37. Figure A1 is a copy of the instructions. Figure A2 is a copy of the input data. Both the instructions and input data are self-explanatory. Following the inputting of the data, calculations are made; by following the printed instructions, the results can be printed out.

A3 is a copy of the six different performance evaluations. Items 1, 2 and 3 are calculated, using the best known mathematical formulations for the vapor flow, i.e. compressible effects on the vapor are included by mathematical integration. Items 4, 5 and 6 use simple Poiseuille flow equations that are continuously numerically integrated over a user-specified number of segments in each zone.

The stop-off (1 and 4) performance is that at a user-specified power, such as 2366 watts. The equilibrium condition (2 and 5) is the one power throughput at which the radiative and conductive power removal from the heat pipe condenser is equal to the power throughput for the given beginning temperature.

A-37 operates by adding increments to the user-specified starting power until it reaches a limit (e.g. viscous or sonic vapor velocity or capillary limit). The non-limited performance (3 and 6) is that power level which is one incremental power unit (5, 25, 100, 1000 watts) less than the power throughput which caused a limit to be reached.

The difference in calculated performance (ΔT and/or power throughput) shows the effect of integral (1, 2 and 3) versus numerical (4, 5 and 6) intergration. Experience has shown that the number of increments required in each section to achieve stable results is when the ΔT in a given increment is on the order of 1-3 degrees K. Additional increments can be used to correlate experimental results; however, the accuracy of the calculation is unchanged. Accordingly, if the heat pipe is operating in a mode where there is a ΔT of more than several degrees Kelvin observed in one of the three vapor zones, then the integrated results should be used for the best accuracy.

Table A4 shows the temperature profile and various vapor pressure

drops and power levels for the Number 5 equilibrium condition. In this case, one sees that the radiant power Q_1 from the condenser varies from 106 watts in the first segment to 104 watts in the last segment. This difference in radiant power is not large, but could be appreciable if the ΔT along the condenser were larger. Likewise, the significance of the 129 watts (Q(1)) conductive power is more pronounced at lower temperatures.

Table A5 shows the details of the heat pipe design, and Table A6 shows in detail the sum of the various pressure drops and temperatures at the end points of each heat pipe zone.

3.2 Correlation of Test Data

The data from test Numbers 4-6, 4-7, 5-3 and 5-4 of the sodium stainless steel heat pipe were chosen to be correlated with the A-37 code. These data were chosen as they are the most consistent within themselves, as the thermocouples were known to be held securely in place.

Table 3 shows the as taken and corrected test data. The as taken data is the external heat pipe temperature, while the corrected data allows for the ΔT thru the wall to obtain the vapor temperature. This is done so as to be able to compare the data to the computer printout of the integrated equilibrium case.

The temperature profile along the length of the heat pipe for the test data in Table 3 is seen in Figure 9, along with several A37 and HTPIPE computer generated temperature profiles for the test conditions. Curves #1-4 used Thermacore's sodium in A-37. Curve #1 is for an external evaporator temperature of 605 C and has a calculated equilibrium power throughput of 2275 watts. Curve #2 is for 603 C and 2232 watts, curve #3 is for 601 C and 2188 watts, and curve #4 is for 599 C and 2143 watts,

TABLE 3

TEST DATA USED

Location From Evap - cm		Evap 1	Evap 1	52.2	52.5	100.5	103.5	Condenser 200.5	Condenser 207	300.3	303.5	405	420	435
Corresponding Computer #		1	1	4	4	10	10.5	22.6	23.4	35	35.5	48	50	52
Test #	Total Power							AS TAKEN DATA						
4-6	2125	584	584	550	568	562	559	546	546	537	537	526	520	532
4-7	2285	584	584	552	572	564	564	551	551	540	540	536	526	538
5-3	2311	586	588	560	556	566	558	556	552	540	529	531	530	538
5-4	2270	584	584	558	554	564	555	553	549	537	526	529	528	535
							CORRECTED TO VAPOR TEMPERATURE							
4-6	2125	585	585	551	569	563	560	547	547	538	538	527	521	533
4-7	2285	585	585	553	573	565	565	552	552	541	541	537	527	539
5-3	2311	587	589	561	557	567	559	557	553	541	530	532	529	539
5-4	2276	585	585	559	555	565	556	553	550	538	527	530	529	536

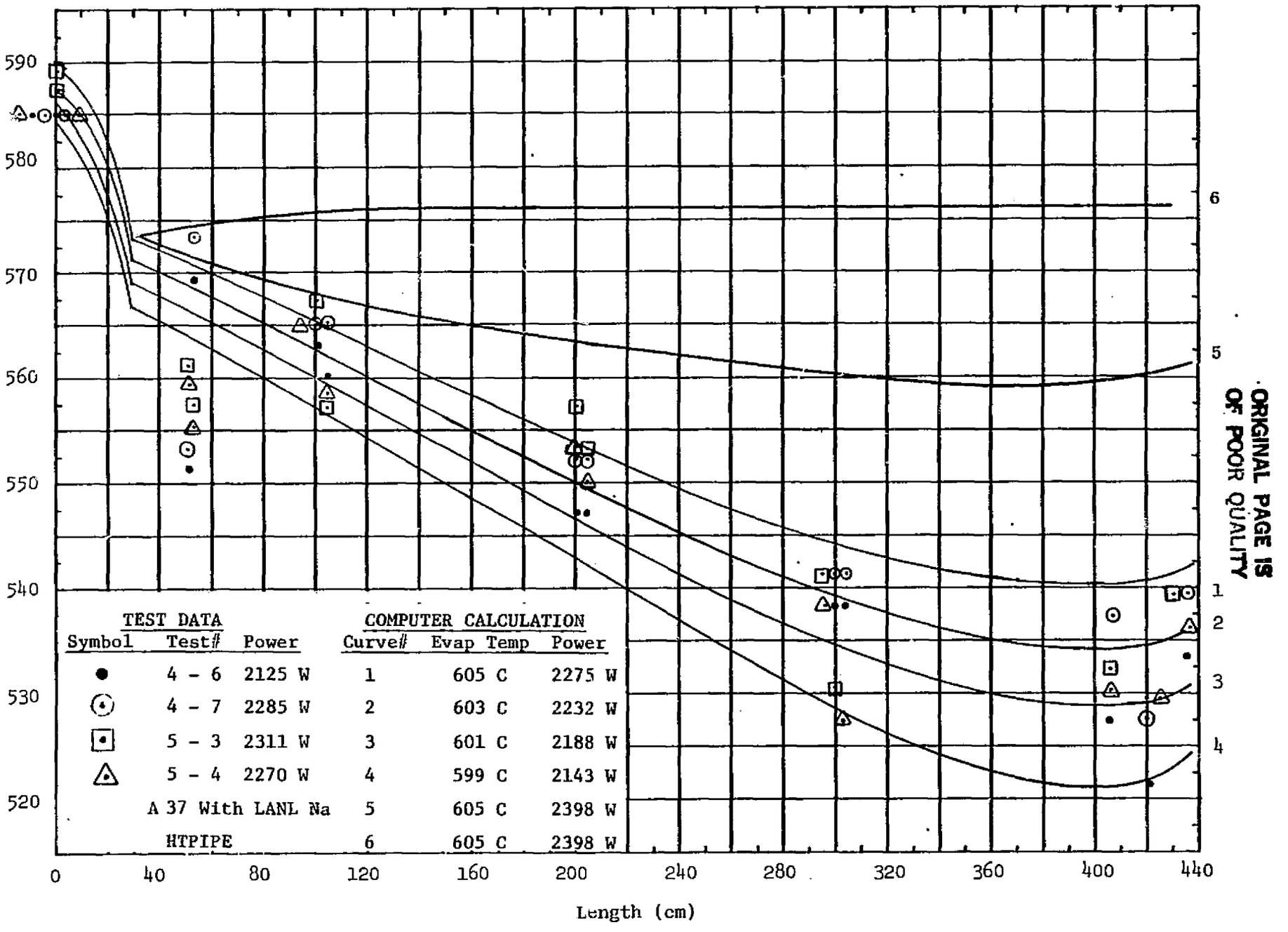

Fig. 9. Temperature Profile For Radiator Heat Pipe

curve #5 was generated in A-37 using LANL's sodium for an external evaporator temperature of 605 C and calculated an equilibrium power throughput of 2398 watts. Curve #6 is from HTPIPE at 605 C and 2398 watts.

The large differences seen between curve 1, 5 and 6 will be discussed in section 3.3. The computer calculations of Figure 9 were based on the heat pipe design of Table 1 and used an effective emissivity of 0.242 for the heat pipe, and a thermal conductive load with an area to length ratio of 0.992 cm^2/cm with a cold end temperature of 50 C.

Examination of Figure 9 shows reasonable agreement between the test data for the sodium/stainless steel heat pipe and the A-37 computer prediction. Each test number's data points seem to fall within a band of 2-3 K of the predicted curve with several notable exceptions. All but one set of these exceptions can be attributed to loose thermocouples which give rise to lower readings, or even high readings if the TC picks up RF heating directly.

The test data points at the 52 cm location (#4 point on condenser profile printout) is set of points that fall out of the norm. All but one point of eight fall outside of the 6 K computer generated temperature band. Further examination of the data would indicate that the two high points are in error, perhaps due to the TC's picking up RF, and the lower points are real data. This is logical as it seems hard to reason that seventy five percent of the data should come from loose thermocouples and be reasonably self-consistent.

If one assumes that the low TC readings are real, then there must be an explanation, i.e.,a physical phenomenon is taking place that the computer does not account for. This phenomenon is probably transonic flow in the first few centimeters of the condenser. Kemme[3], at LANL measured transonic velocity in a sodium heat pipe. Figure 10 shows Kemme's test data.

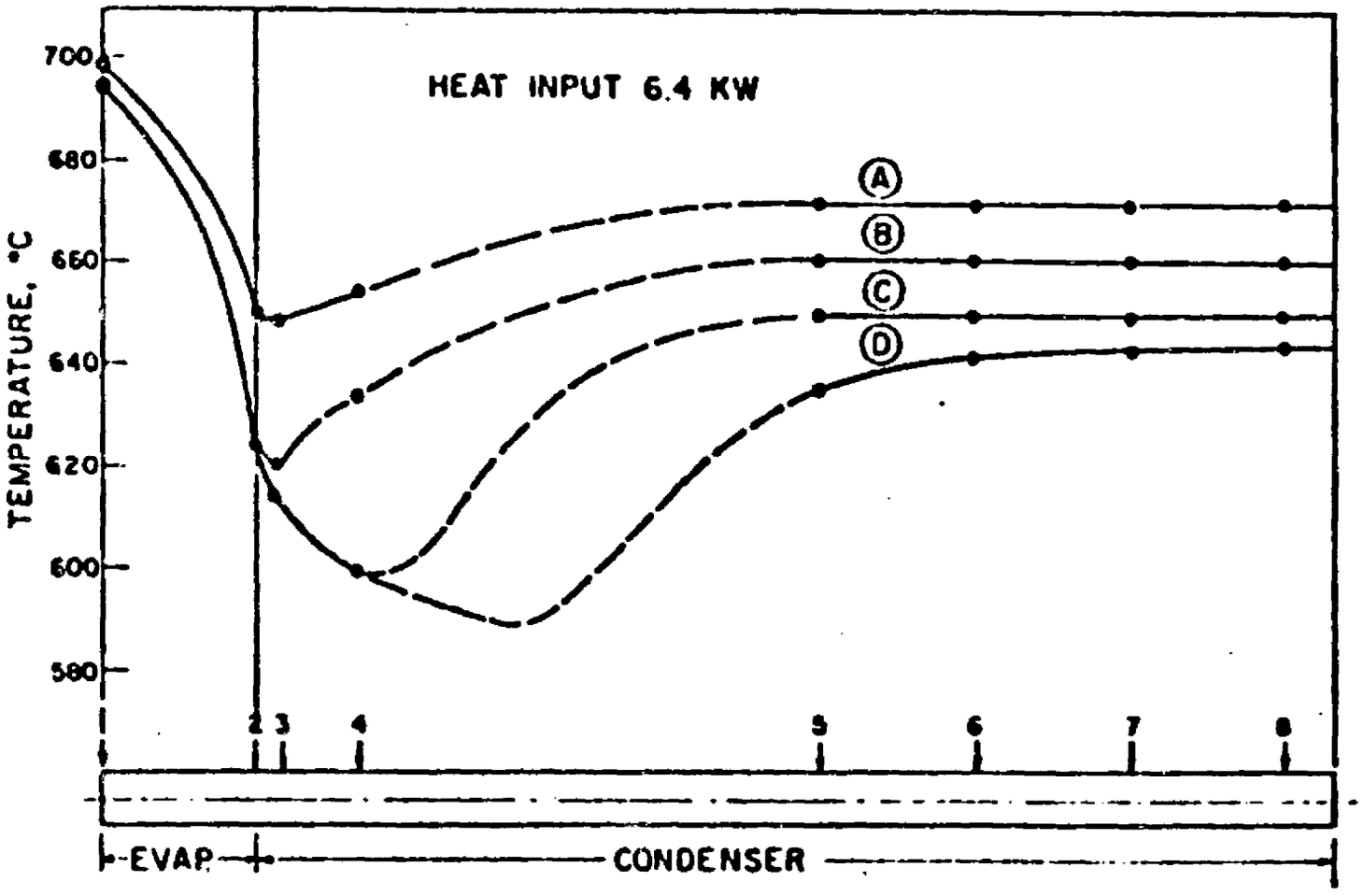

Fig. 10. Trans-sonic velocity conditions in a heat pipe.

The calculated Mach number in the vapor exit ranged from 0.395 at 606 C external temperature to 0.429 at 599 C. Thus one may question the possibility of transonic flow. However, a varition of several degrees K in starting temperature and/or a increase in power of 1 or 2% can increase the Mach number from near 0.5 to 1.0.

If transonic flow did occur, then the method by which the computer predicts the pressure drop in the evaporator is incorrect. The current computer code uses Busse's[4] formulation that includes a pressure coefficient, which varies from $\frac{\pi^2}{8}$ i.e. (1.234) at the beginning of the evaporator to 1.111 at the end of the evaporator at sonic conditions. This formulation does not allow for vapor velocities greater than Mach 1. Accordingly new evaporator and adiabatic vapor flow calculation rationale will be required for the prediction of transonic flow, possibly including the evaporator pressure coefficient.

Prenger and Kemme[5] at LANL have shown the need for using a pressure coefficient of 1.442, 1.558 and 2.719 in the evaporator to get analytical agreement with measured test data on the 2 meter long SPAR sodium heat pipe with a long adiabatic section. Transonic flow was not observed since the operating temperature was 1400 K. However, the pressure drop in the evaporator as inferred by the temperature drop did exceed that calculated using Busse's pressure coefficient.

Figure 11 is from Busse's paper and shows additional evidence of transonic flow with immediate recovery, followed by a decreasing condenser temperature with an additional small amount of recovery at the far end of the condenser. The cold end on Busse's data was attributed to a non-condensible gas.

Based on the above cited examples of transonic flow and the need for a different pressure coefficient correlation to get better agreement between experimental data and analytical prediction, there is a good

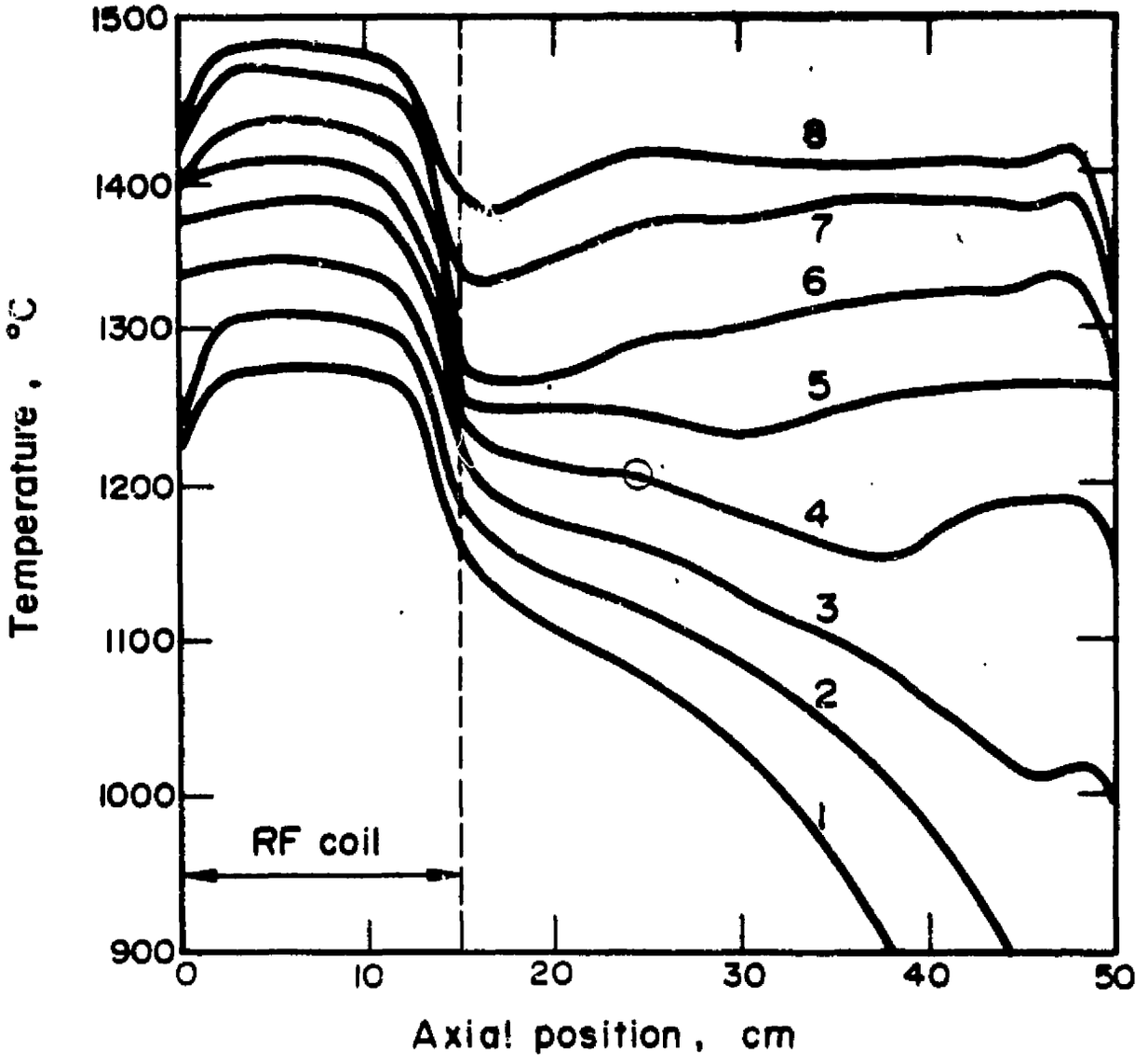

FIG. 11. Temperature distribution along a radiation cooled Nb-1Zr/Pb heat pipe of 10 mm o.d. and 500 mm length.

probability that the data points in Figure 9 are real, and that transonic flow was being observed.

Figure 12 is a replot of Figure 9, along with additional data points taken before/after the tests of Figure 9. Figure 12 is a plausible representation of what the actual temperature profile may have looked like. The curves of Figure 12 look somewhat like the transonic flow curves of Figures 10 and 11. The difference between the curves of Figures 10, 11 and 12 is the fact that all used different types of heat sinks, which alter the temperature profile from test to test.

If the low measured temperature at the first condenser TC are not due to transonic flow or loose thermocouples, then a third explanation may be the result of a turbulent eddy caused by one of the perforated clips used to hold the wick in place. The exact location of a clip in the area is not known, but the presence of a clip in the general area is known. If the clip ended between the thermocouple locations the first TC may have seen a reduced temperature due to increased flow over the clip, and the second TC may have seen an increased temperature due to pressure recovery past the clip.

No attempt was made to alter the calculation rationale of A-37. To include the effect of a clip is relatively simple; however, to include an increased pressure coefficient and/or transonic flow should be based on additional theoretical analysis and empirical correlation of the pressure coefficient along with providing the theoretical equations for transonic flow and calculation of the shock wave, all of which are interrelated. This is a recommended area for future work.

Considerable time was spent in getting agreement for the rest of the condenser temperature profile, i.e., the pressure recovery at the end of the condenser. This was accomplished by the modeling of

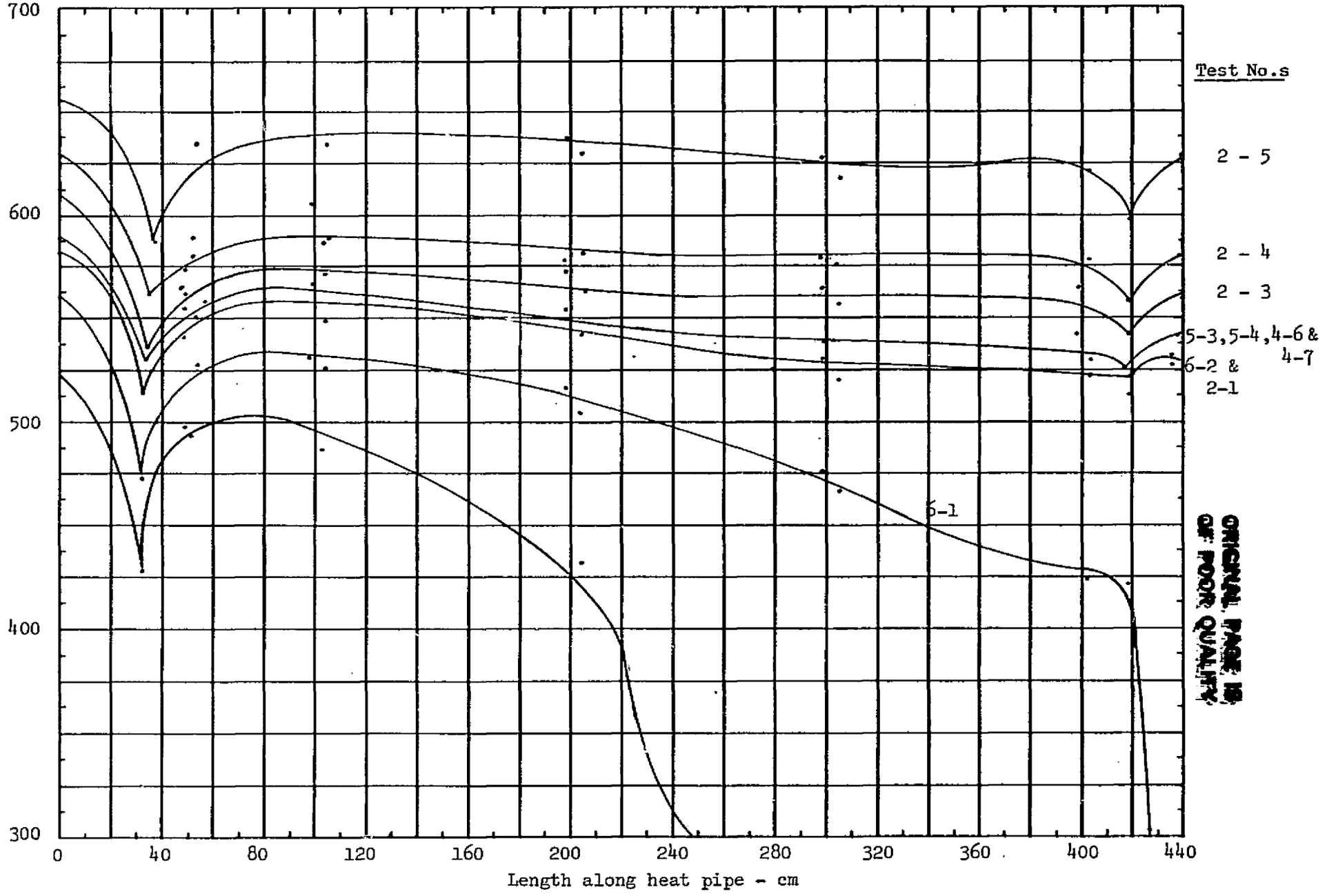

Fig. 12. Possible Temperature Profiles For Transonic Flow In Radiator Heat Pipe

conductive heat sinks in addition to the radiant heat sinks along the condenser at user-specified location.

3.3 Comparison of A-37 and HTPIPE

Thermacore's A-37 was compared to LANL's HTPIPE computer program by two methods. First, the calculational rationale was examined side by side, followed by comparing a set of computer printouts for equal heat pipes as seen in Figure 9.

A significant difference between the two programs is the language and accessibility. A-37 is a user interactive program for use in engineering design, data analysis and empirical correlation. The language is BASIC. HTPIPE.is written in Fortran and requires the use of a deck of punch cards or tape to input the data. Accordingly, to change a variable a new card or tape change is required. Alternatively, if a keyboard terminal is to be used, then the program must be called into EDITOR, changes made and the program recompiled.

Technically, there are differences also. A-37 uses as an input variable the beginning outside evaporator temperature and assumes it remains constant for different power throughputs down the heat pipe. This is generally the case in real situations, i.e., the evaporator temperature is fixed. HTPIPE fixes the evaporator - adiabatic vapor temperature - a temperature that can only be inferred by the measurement of the E-A wall temperature. However, by fixing this temperature, all other temperatures vary as the power varies; thus, to match a given desired power throughput at a given true external evaporator temperature, many trial runs may be needed.

In addition to being user interactive, A-37 calculates all desired information about a particular input design without the need for

additional input, other than the user answering a yes or no question as to whether or not something should be calculated or printed out. Each segment of HTPIPE must be treated as a separate computer run, i.e., max. power capability and temperature profile at a given power are calculated in two different portions of the program, requiring separate access rather than simultaneously.

Major differences also exist in calculation rationale. In A-37, the pressure drop in each increment is calculated from which a new pressure and temperature is calculated for the beginning of the next increment. The computer moves down the pipe summing up the ΔP's, calculating new pressures and temperatures until the end of the pipe is reached. Different mathematical formulas are used in each of the three major sections, the evaporator, adiabatic and condenser. HTPIPE calculates the pressure drop in the evaporator for a given power throughput. This ΔP is calculated using Busse's equation. From the E-A temperature, a beginning evaporator pressure and temperature is calculated, using the calculated ΔP. This ΔP is then divided by the number of evaporator increments, and the actual value of the ΔP in each increment is calculated using a mathematical series based on the vapor flow through the evaporator with uniform mass injection, i.e., no compensation for temperature changes takes place since Busse's equation assumes isothermal flow. However, since discrete pressures are calculated at each point, temperatures can be calculated. A-37 uses the same mathematical formula for mass flow, but allows all the physical properties to vary at each point. The use of Busse's equation for calculating the evaporator pressure drop is a very good approximation, provided the vapor flow in the evaporator is less than Mach 0.5.

A-37 allows for the pressure coefficient in the evaporator to

vary from 1.234 to 1.11, as does HTPIPE. However, neither program internally permits transonic flow to occur or has a rationale which calculates a larger pressure coefficient than 1.234.

Fundamentally the calculation of the pressure drop in the adiabatic zone is the same for both programs. However, A-37 has several options available which are not in HTPIPE. The calculation of the pressure drop and/or recovery in the condenser is treated quite differently by the two programs. In HTPIPE the condener profile either shows pressure recovery or all pressure loss, starting at the beginning of the condenser. No profile like those of Figure 9 can be calculated, i.e., first a pressure loss, followed by pressure recovery. HTPIPE assumes uniform heat removal from the condenser. A-37 allows for radiation to a user-specified environment along with the addition of conduction heat sinks at any place on the condenser.

The pressure profiles of Figure 9 are attributed to the water cooled heat sink at the end of the heat pipe. However, Busses's data in Figure 11 also show recovery at the far end of the condenser under various conditions. If one examines the viscous and inertial pressure components in the last increment of the condenser, the inertial component will generally be larger than the viscous components depending on the size of the increment. Thus, one assumes that there will always be a small upturn in pressure at the far end of the condenser as the last few molecules of working fluid strike the condenser wall, unless the heat pipe is in the viscous dominated range in which case the end temperature of the heat pipe is generally several hundred degress colder than the evaporator.

HTPIPE calculates the pressure recovery in the condenser as $-\frac{\pi^2}{8} \rho v^2$, the same magnitude but opposite sign as the evaporator.

A-37 uses $\rho V^2/\pi^2/8$. The reason for dividing by, rather than multiplying by the pressure coefficient is that both theory and experiment[6] have shown that with suction (condensation) the pressure drop (recovery) is less than with normal fluid flow. Therefore, to get a reduction in pressure drop, the pressure coefficient must be reduced, which for values near one may, in fact, be a reciprocal. The principal investigator of this program has spent considerable time examining the data of Yuan and Finkelstein[6] and believes that division by the pressure coefficient has a good theoretical foundation, which appears to be borne out by the relative good agreement of the data and curves of Figure 9 calculated using A-37.

A significant difference between the two programs are the values used for the physical properties of the working fluid. This is seen in Figure 9. Some fluids agree quite well; other fluids differ by significant amounts. Other differences occur in the fact that that in HTPIPE the physical properties of the particular wick must be put in, i.e., the thickness, pore radius and permeability. An A-37 user need only specify a particular wick structure; the properties are then calculated by a set of equations internal to the program. If the wick is non standard, then the wick properties can be put directly into the program through the input statements.

A-37 uses the conservative value for the capillary pore radius as first defined by Ernst[7], i.e., $r_c = 1/2N$ where N = mesh number. HTPIPE uses the half width of the opening between wires in a mesh screen which can, at times, be achieved but not on a reliable and repeatable basis. The use of other wick structures in which the pore radius is well defined or measured will not result in an overcalculation of the capillary force in HTPIPE. Thus, the expected performance of a

screen wick heat pipe in HTPIPE (using LANL's capillary pore radius) may result in an over-prediction of performance.

Overall, A-37 and HTPIPE are very similar. For performance calculations in a heat pipe with vapor flow less than 0.3 mach, the differences are minor. At high vapor flow (Mach $\geq$ 0.5), low vapor density (viscous range), and non-uniform heat removal from the condenser, A-37 provides a more comprehensive treatment. This is borne out by the curves of Figure 9 where the sodium/stainless steel test data were compaired to the computer generated curves of A37 and HTPIPE.

4. TITANIUM RADIATOR HEAT PIPE

RAD-3 is the first length titanium-potassium radiator heat pipe with a "D" crossection, built by LANL, for use with the closely coupled (conductively) SPAR system. Although LANL had the capability of fabricating the heat pipe, they did not have a vacuum system of sufficient length ($\gtrsim$5.5M) to process and test the heat pipe.

Following the testing of the 4.2 meter Sodium-SS Radiator heat pipe (as designed, fabricated and tested by Thermacore), a three way agreement was reached between Thermacore, NASA/JPL and LANL to have the LANL fabricated titanium radiator heat pipe envelope shipped tc Thermacore for potassium loading, processing and testing.

Appendix B contains a complete record and discussion of the loading, processing and testing of RAD-3 as compiled at Thermacore, and written by Steve P. Girrens of LANL. Prior to loading, processing and testing, several items needed to be completed. They were: design and build a fixture to support and hold the heat pipe level; develop an efficient RF coil which coupled well to the flat titanium heat pipe; and develop a means of connecting the stainless steel distillation pot to the titanium heat pipe.

4.1 RF Coil

RF heating was chosen as the means of heating the flat bottom titanium heat pipe as it was the only method which allowed the evaporator to be observed. A clear view of the evaporator was necessary to observe the onset of hot spots indicating the heat pipe limit at that operating condition.

Numerous RF coils were built and tested. Figure 13 shows a test of one of the coils on a flat titanium sheet. Figure 14 shows the selected RF coil design. The coil was made from rectangular waveguide tubing. It was 60 cm long, 5 cm wide and had four turns (8 legs). Figure 15 shows the RF coil in position under the heat pipe in the test rack.

4.2 Test Rack

Fabrication of the heat pipe was by welding three 180 cm long sections together. Accordingly, the heat pipe had a considerable bow in it. Figure 16 shows the titanium heat pipe as received by Thermacore. To properly hold the heat pipe in a level manner, a test fixture was designed and fabricated.

Ceramic rods were used to support the heat pipe, the ceramics being supported by stainless steel posts. Support posts were placed every twenty cm in the evaporator and every meter in the condenser. Figure 15 shows a typical support post including the lower support used to hold the RF coil in place.

Because of the length of the heat pipe, heating of the condenser was required for processing. Accordingly, ceramic beaded nichrome wire trace heaters were placed along the length of the heat pipe. These heaters and the Inconel sheathed thermocouples were held in place with SS spring clips, as seen in Figure 17.

4.3 Connection to Distillation Pot

Initially, a mechanical connection to the 1/4" OD titanium evacuation tube was to be made with a carbon steel swagelock fitting. However, thermal testing of the fitting showed that it leaked while at temperature and that after several cycles it leaked at room temperature. Accordingly, a titanium to titanium joint was required.

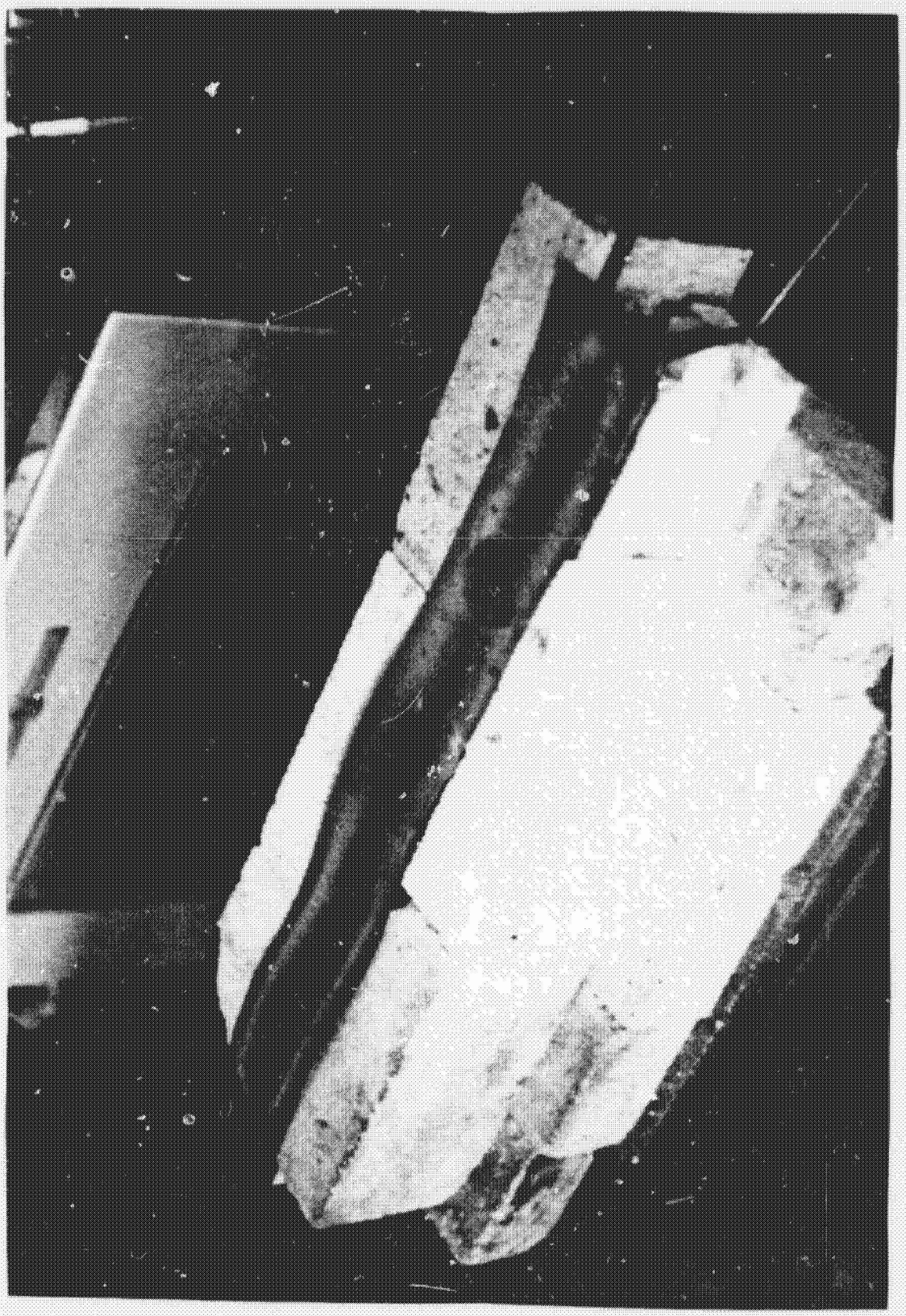

Fig. 13. RF Coil Test

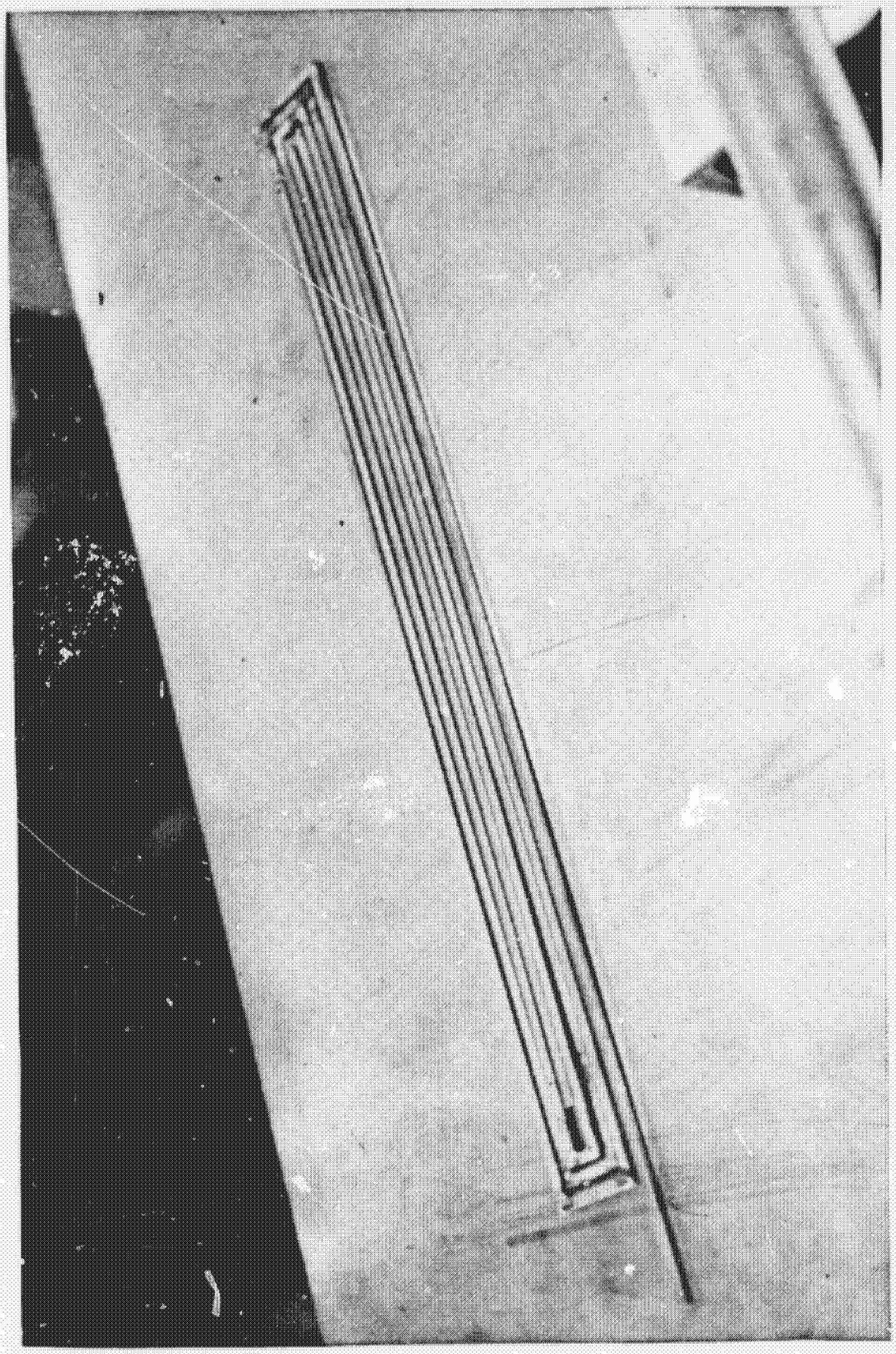

Fig. 14. Selected RF Coil Design

Fig. 15. RF Coil In Position

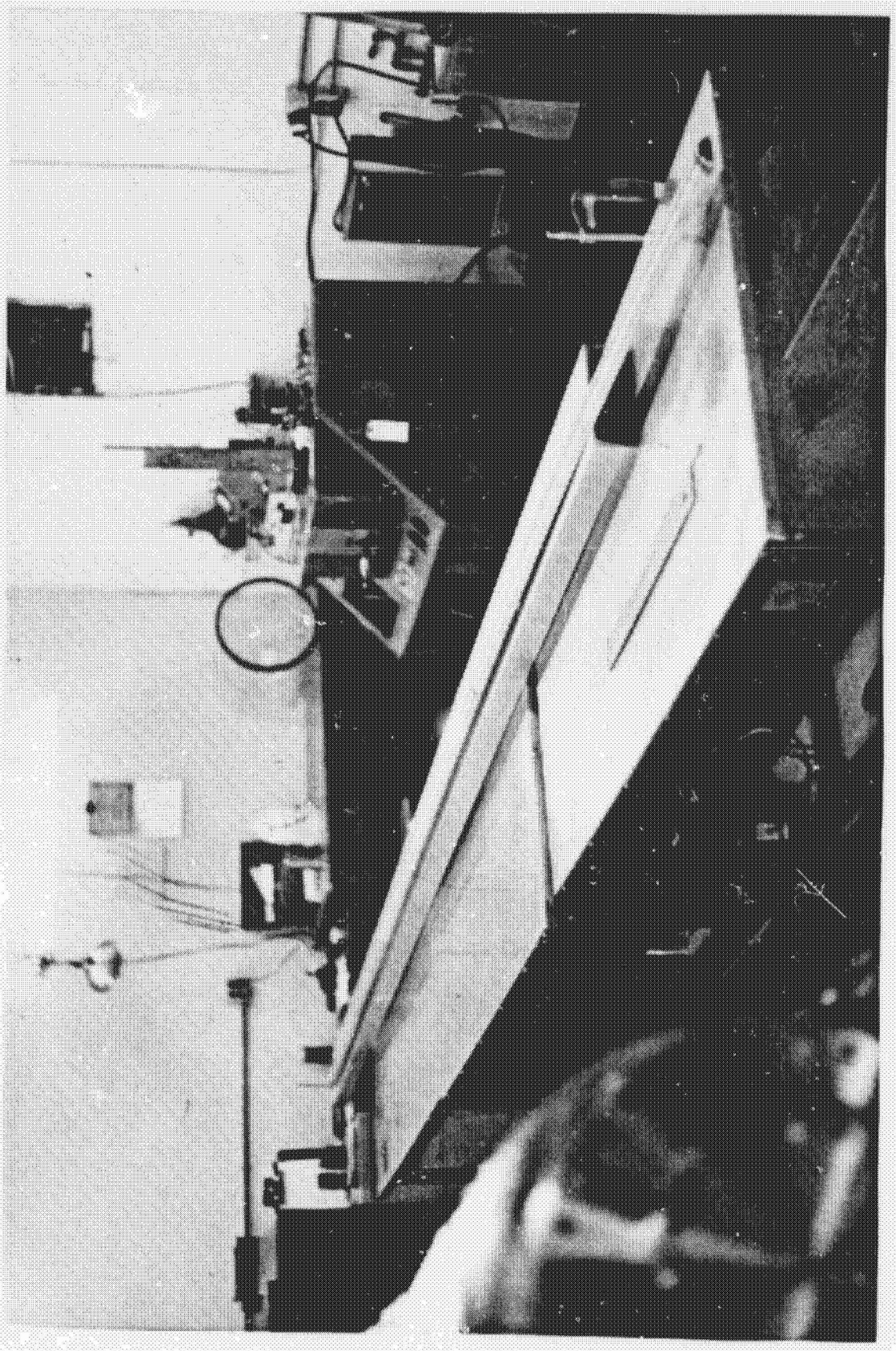

Fig. 16. As Received Titanium Heat Pipe Envelope

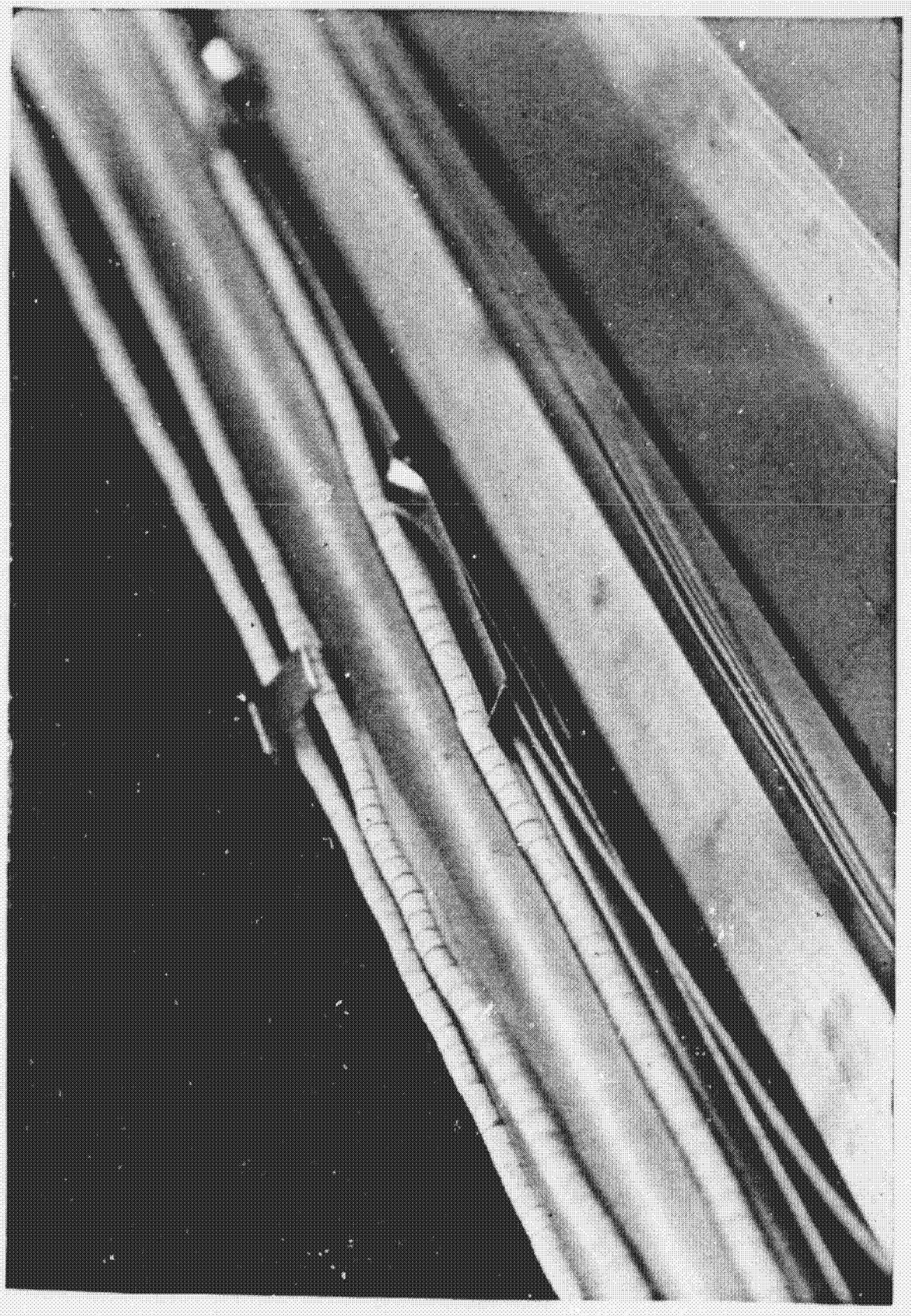

Fig. 17. S.S. Spring Clips Bolding Trace Heaters and Thermocouples

Figure 18 shows the distillation set up as originally configured. However, since the steel swagelock fitting tests leaked, an elbow and seal-off parts were machined out of titanium. Figure 19 shows the titanium parts fitted to the heat pipe along with the distillation pot.

To assure that a final seal-off of the heat pipe could be made satisfactory, several tests seal-offs were made on the titanium-titanium joint. Figure 20 shows the joint parts prior to, an after, a test seal-off.

4.4 Heat Pipe Arteries

Prior to final assembly of the titanium elbow and seal-off tube to the heat pipe, discussions with LANL revealed that the arteries in the heat pipe were "closed" on both ends. Experience has shown that if the arteries are selfpriming, then it is a good practice to leave the condenser end of the arteries open. Accordingly, the condenser end cap was cut off, the arteries opened and the end cap rewelded on. Figure 21 shows the open end of the heat pipe with an artery just visible in the corner.

4.5 Potassium Loading and Distillation

Following the rewelding of the end cap on the condenser, the titanium elbow and seal-off tube were welded to the heat pipe. This weld was done (as seen in Figure 22) in a glove bag, to reduce contamination. After welding, the heat pipe was leak checked, placed in the test rack, fitted with thermocouples and trace heaters, and placed in the vacuum system. Figure 23 is the test rack assembly and heat pipe prior to insertion into the vacuum system.

The distillation pot and potassium capsules were placed in a dry box and purged until the oxygen concentration was less than 1 ppm as visually monitored by the absence of an oxide film on liquid potassium.

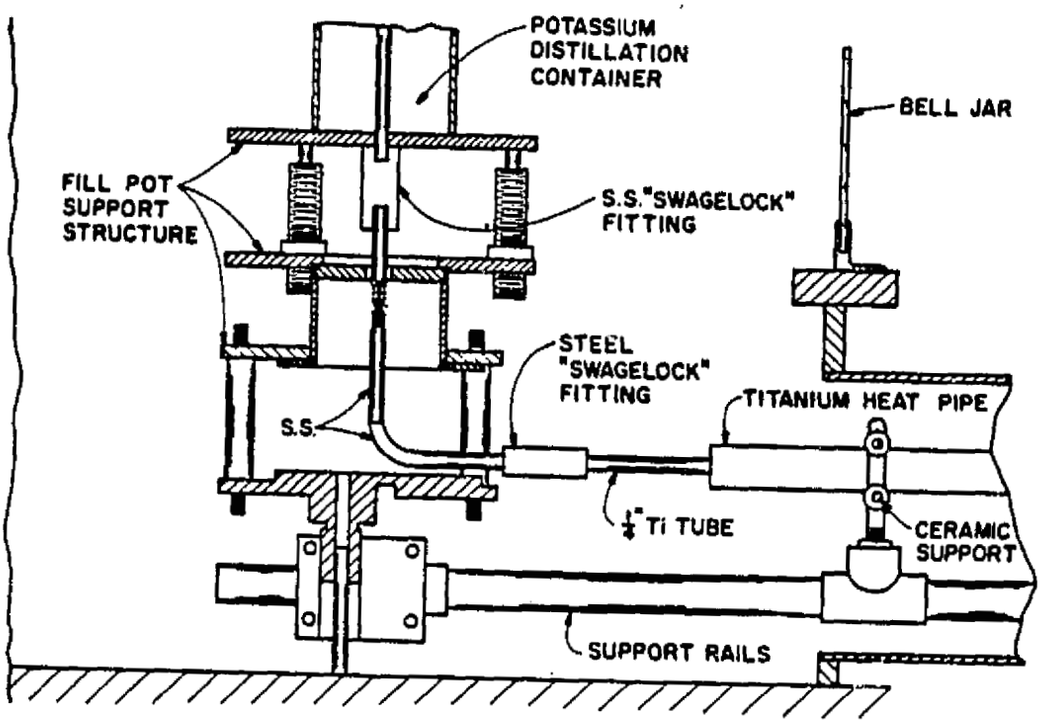

Fig. 18. Initial Distillation Set Up

Fig. 19. Titanium Elbow and Seal-off Parts And S.S. Distillation Pot

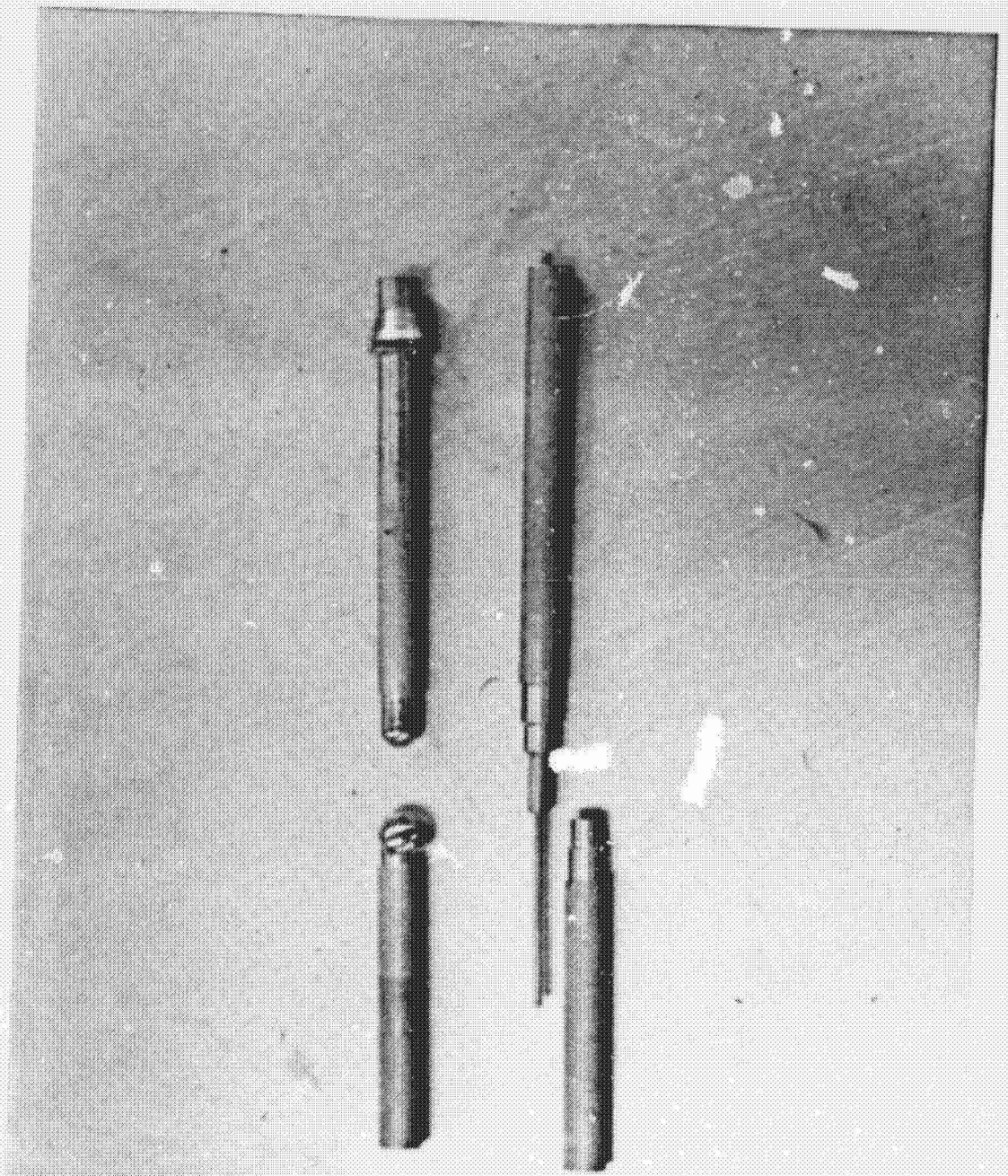

Fig. 20. Titanium Seal-off Test Parts

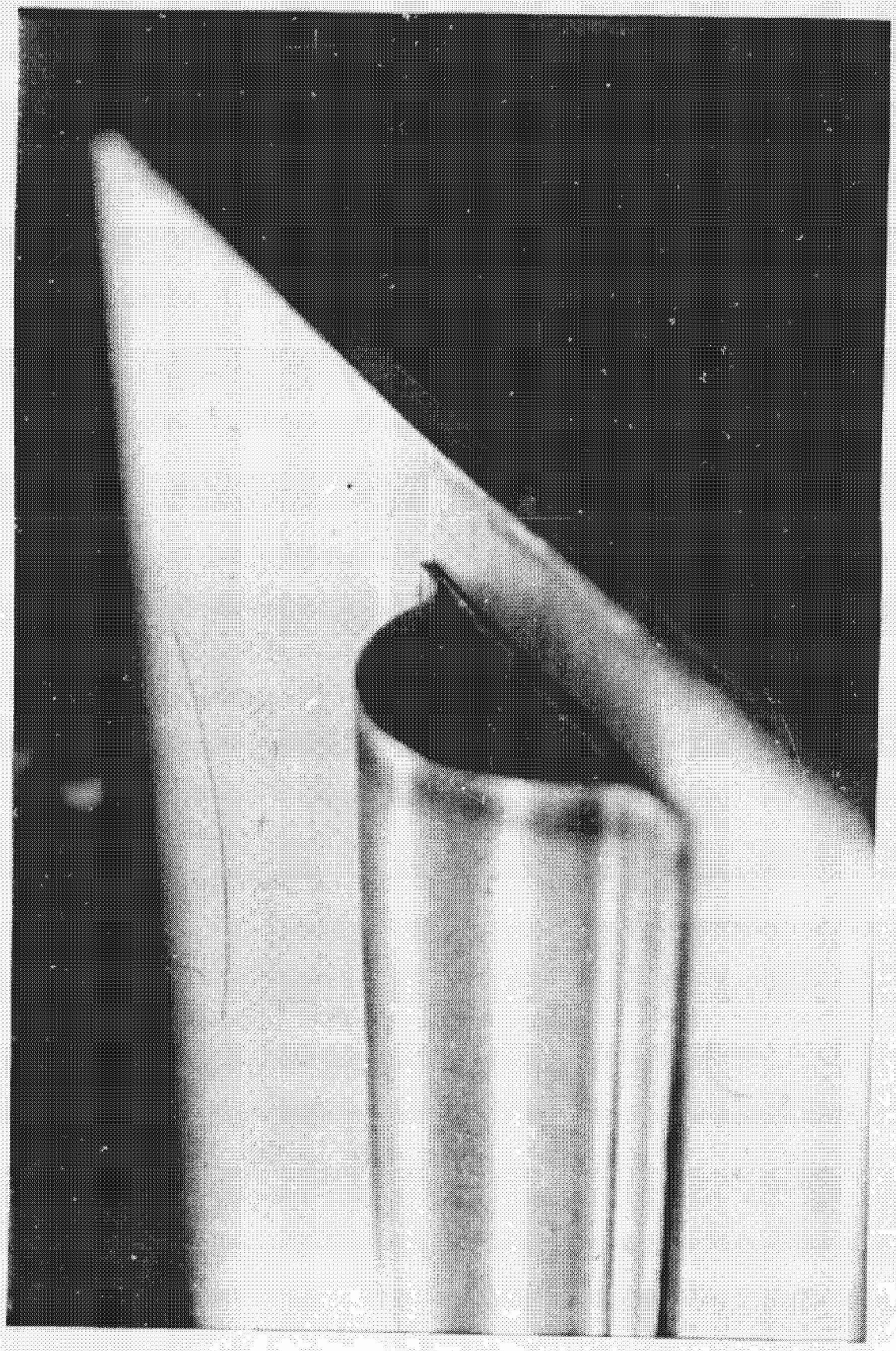

Fig. 21. Condenser End of Titanium Heat Pipe Showing Artery

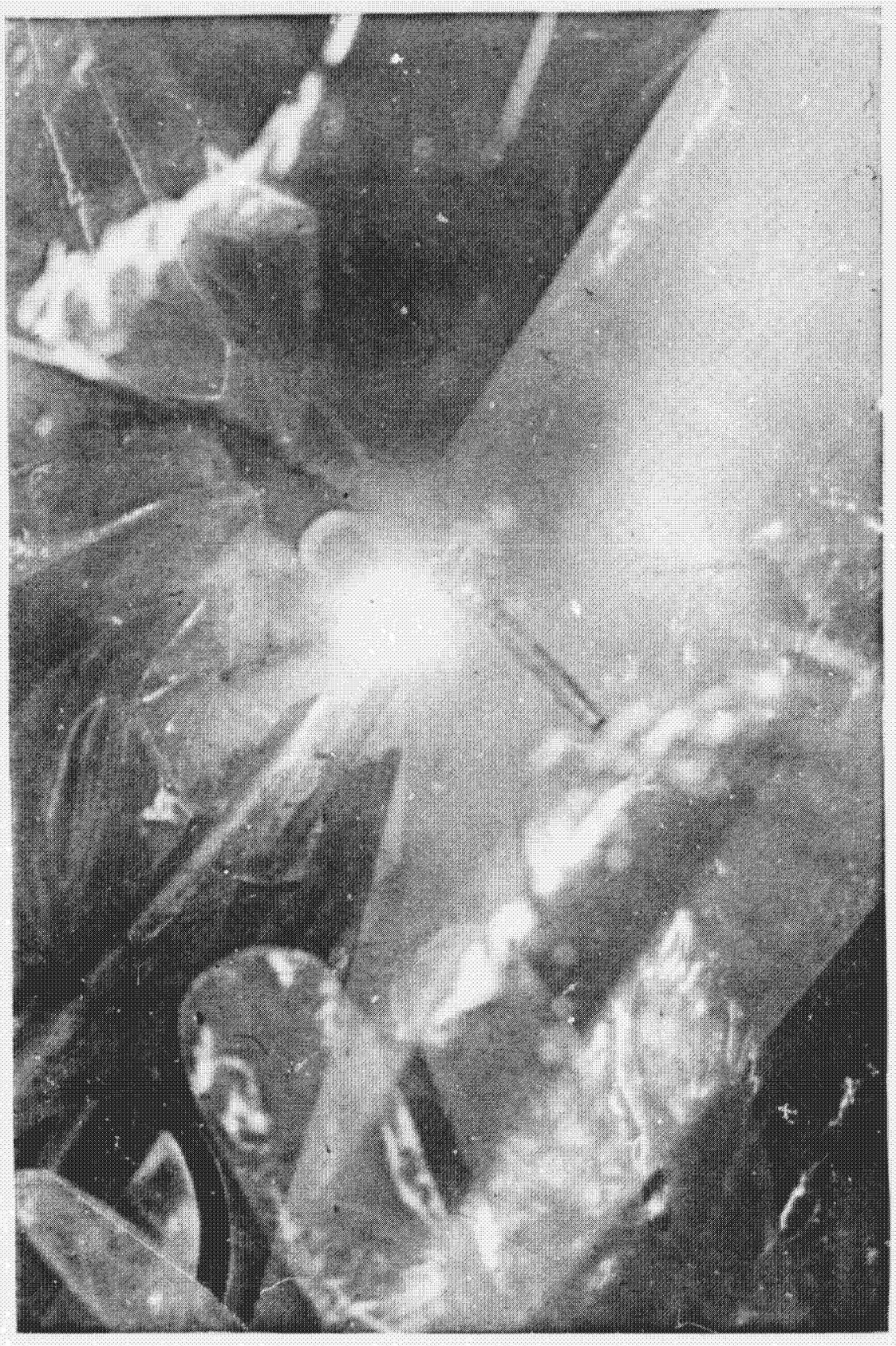

Fig. 22. Welding Of Titanium In Glove Bag

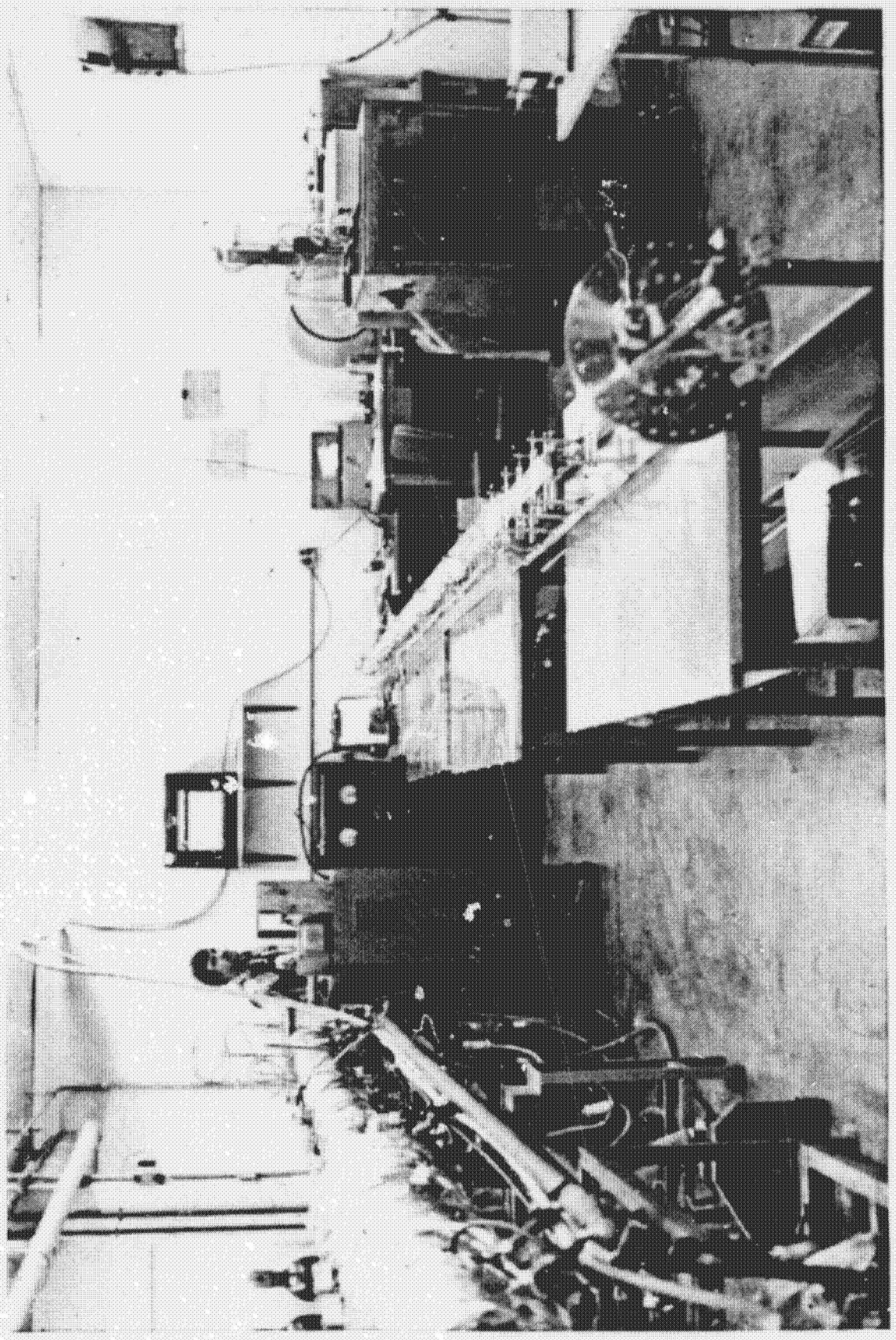

Fig. 23. Titanium Heat Pipe Ready for Loading

Figure 24 shows the loading of potassium into the distillation pot, which also had hafnium and zirconium getters in it. Following the introduction of the potassium, the pot was sealed using a nickel gasketed "Conflat" flange.

The distillation pot was removed from the glove box and placed in position over the heat pipe and the entire system evacuated. The pressure in the system was maintained below 5×10^{-5} Torr as heat was applied, first to the heat pipe to bake it out and second to the distillation pot to outgas it.

With everything hot and the pressure at 1×10^{-5} Torr, the temperature of the distillation pot was turned up to a maximum of 730 C, as shown in Figure 25. Figure 26 shows the distillation pot with a "cold top" indicating that the distillation was complete. Following initial testing of the heat pipe to assure proper wetting and fill, the seal tube was closed as seen in Figure 27.

4.6 Test Results - 60 cm Coil

Using the RF coil shown in Figure 14, which was 60 cm long, the radiator heat pipe was tested to its performance limit against gravity and with gravity assist. Figure 28 shows the temperature profile at 522 watts for the heat pipe operating against a 0.25 degree gravity tilt. Figure 29 shows the temperature profile at 826 watts, with a 0.23 degree gravity assist tilt.

The stated power levels were measured by calorimeter means, recording the power in the calorimeter with the RF off and the trace heaters on, and then measuring the power in the calorimeter with the RF and trace heaters on at the stated conditions. The 522 watts against gravity corresponds to 1.4 watts/cm^2. An evaporator length of 300 cm would be required to achieve 2600 watts without burnout; and at

Fig. 24. Loading of Potassium Iuto Distillation

Fig. 25. Distillation Pot At 730 C

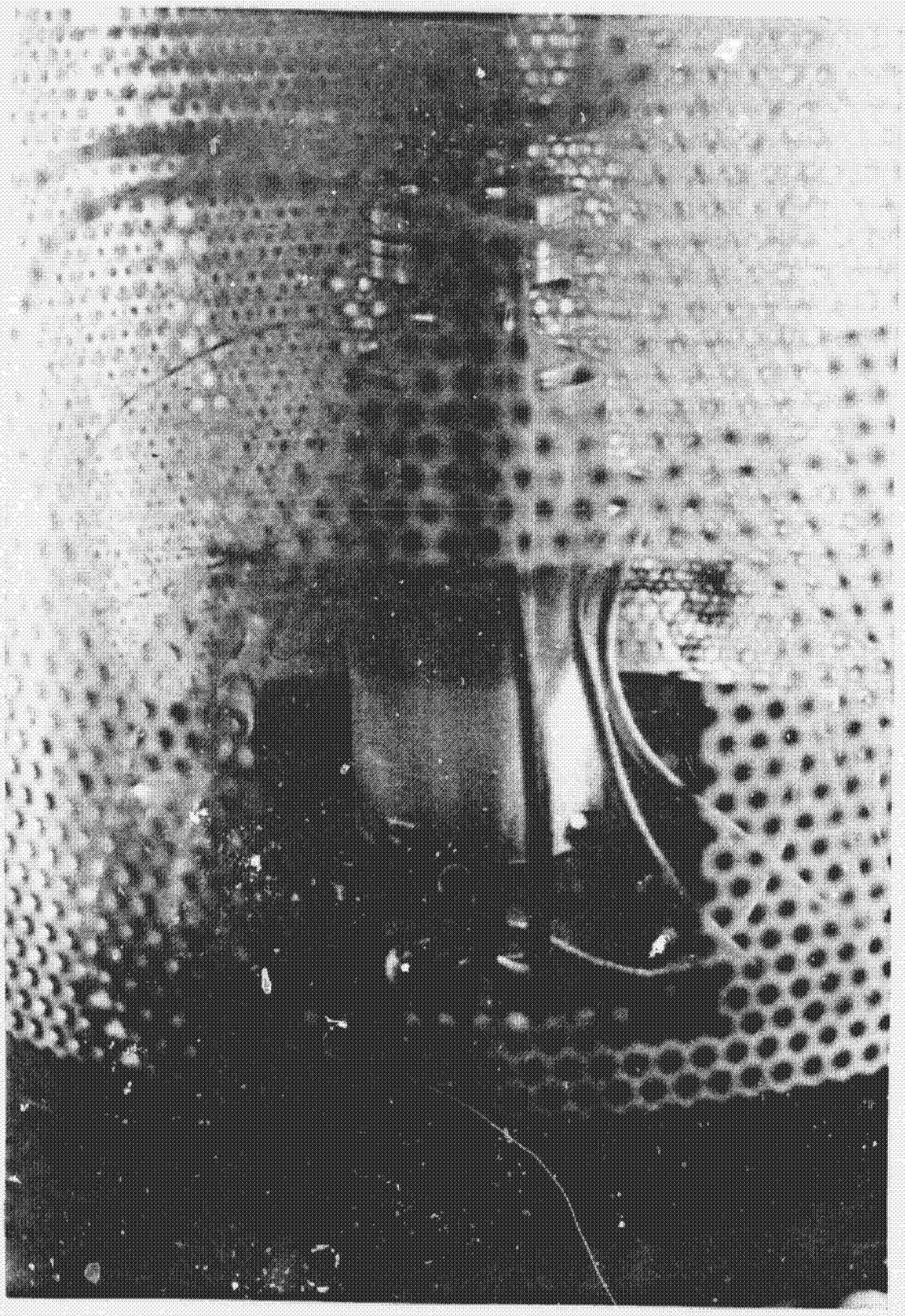

Fig. 26. Distillation Pot After Potassium Left

Fig. 27. Scaling Off The Heat Pipe.

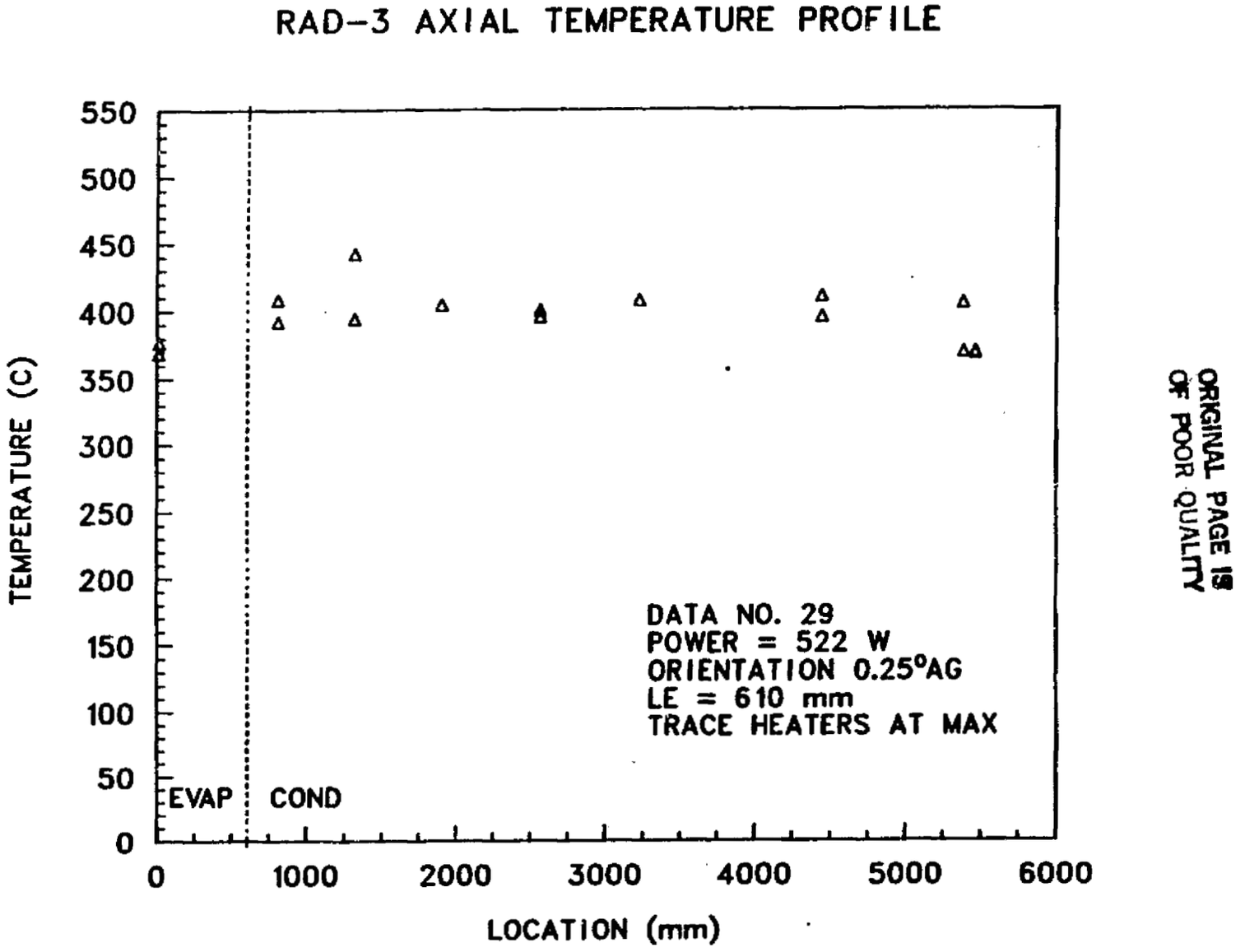

Fig. 28. RAD 3 Temperature Profile At 552 W Against 0.25 Degree Gravity Tilt
Courtesy, Steve Girrens, LANL

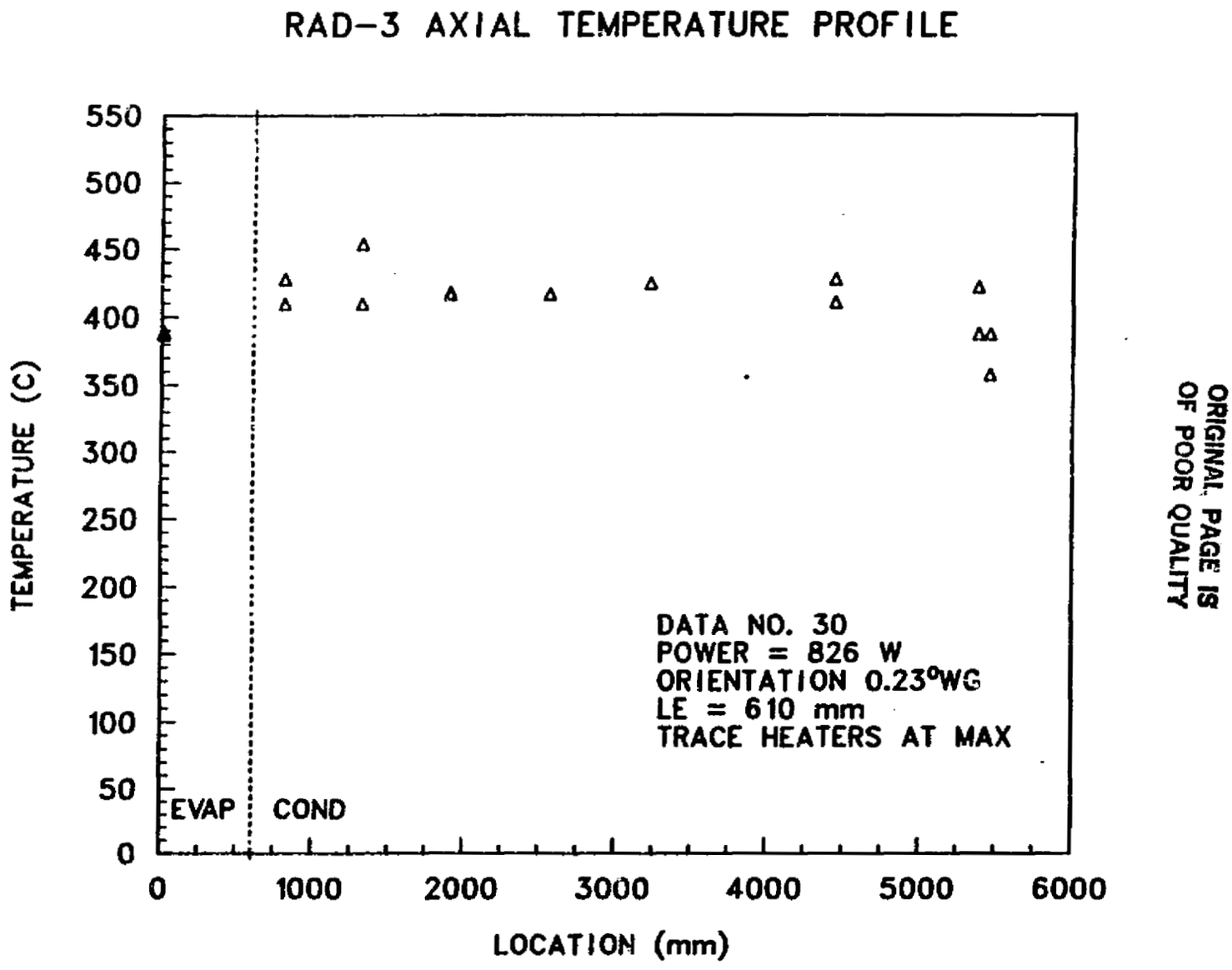

Fig. 29. RAD 3 Temperature Profile AT 826 W
With 0.23 Degree Gravity Assist
Courtesy, Steve Girrens, LANL

2.2 W/cm^2 a length of 190 cm would be required. The test chamber, as built, could only accommodate a 137 cm long evaporator and still be able to observe the surface. Accordingly, a 137 cm long coil was fabricated.

4.7 Test Results - 137 cm Coil

Considerable data was taken with the 137 cm long coil, and is summarized here. Additional data is found in Appendix B. Figure 30 is a plot of the start up temperature profiles for the heat pipe. It is interesting to note that the 228 and 440 watt power levels were taken at 0.25 degrees and 0.3 degrees tilt against gravity. Figure 31 shows the evaporator sonic limit of the heat pipe at start up powers, and Figure 32 shows the departure from the expected wicking limit due to the poor performance of the shot-blasted evaporator wick.

Figure 33 shows the temperature profile at 590 watts with an against-gravity tilt of 0.52 degrees. This curve is almost an exact duplicate of the curve in Figure 8, which is for the 60 cm evaporator, with an against gravity tilt of 0.25 degrees. The good agreement between the curves of Figures 33 and 28 for two different test conditions show the accuracy of the test method to be within a 13% range. Figure 34 shows the temperature profile at 1.86 kw with a 1.35° gravity assist. This was the maximum power transferred by the heat pipe and corresponds to 2.2 watts/cm^2, which is the same value as observed with the 60 cm coil.

The data points, which represent the maximum power level for the heat pipe, were determined by the onset of hot spots in the evaporator for the particular operating condition. Photographs of the evaporator hot spots were taken, but the intensity of the slides did not permit reproduction. Figure 35 is a view of the evaporator after the heat pipe was removed from the test station, showing a warping of the flat evaporator as a result of the hot spots.

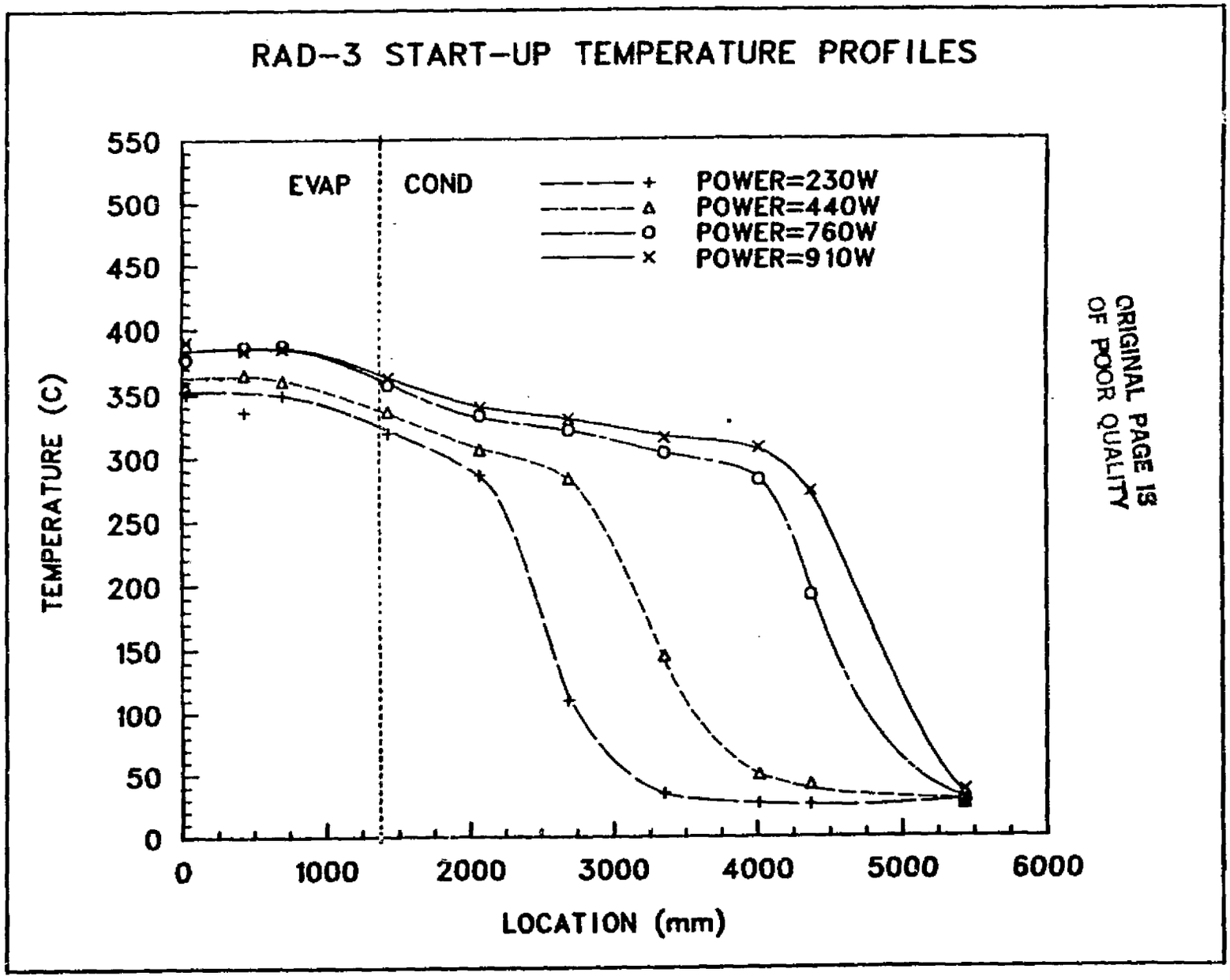

Fig. 30. RAD 3 Start Up Temperature Profiles
Courtesy, Steve Girrens, LANL

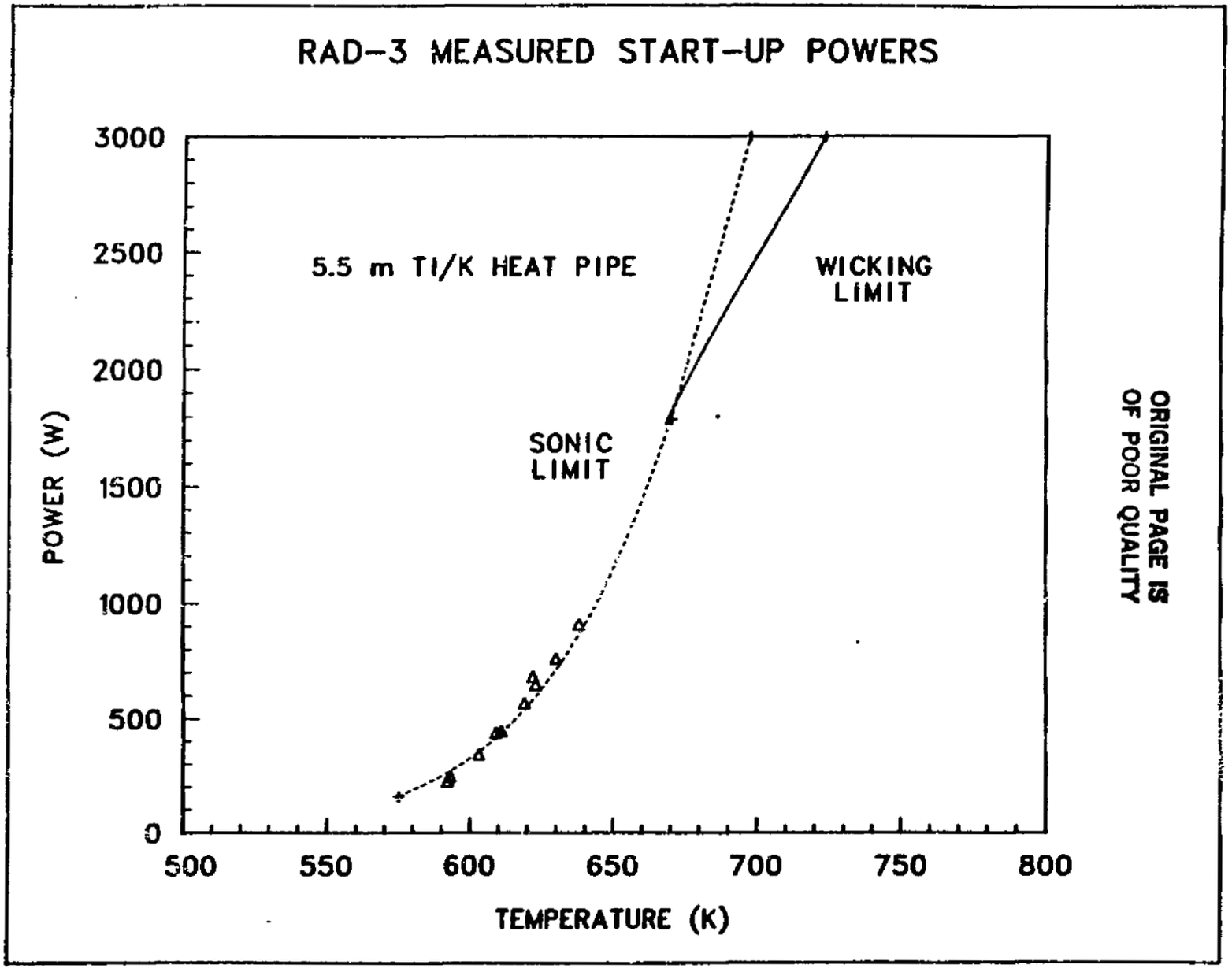

Fig. 31. RAD 3 Evaporator Sonic Limit Curve
Courtesy, Steve Girrens, LANL

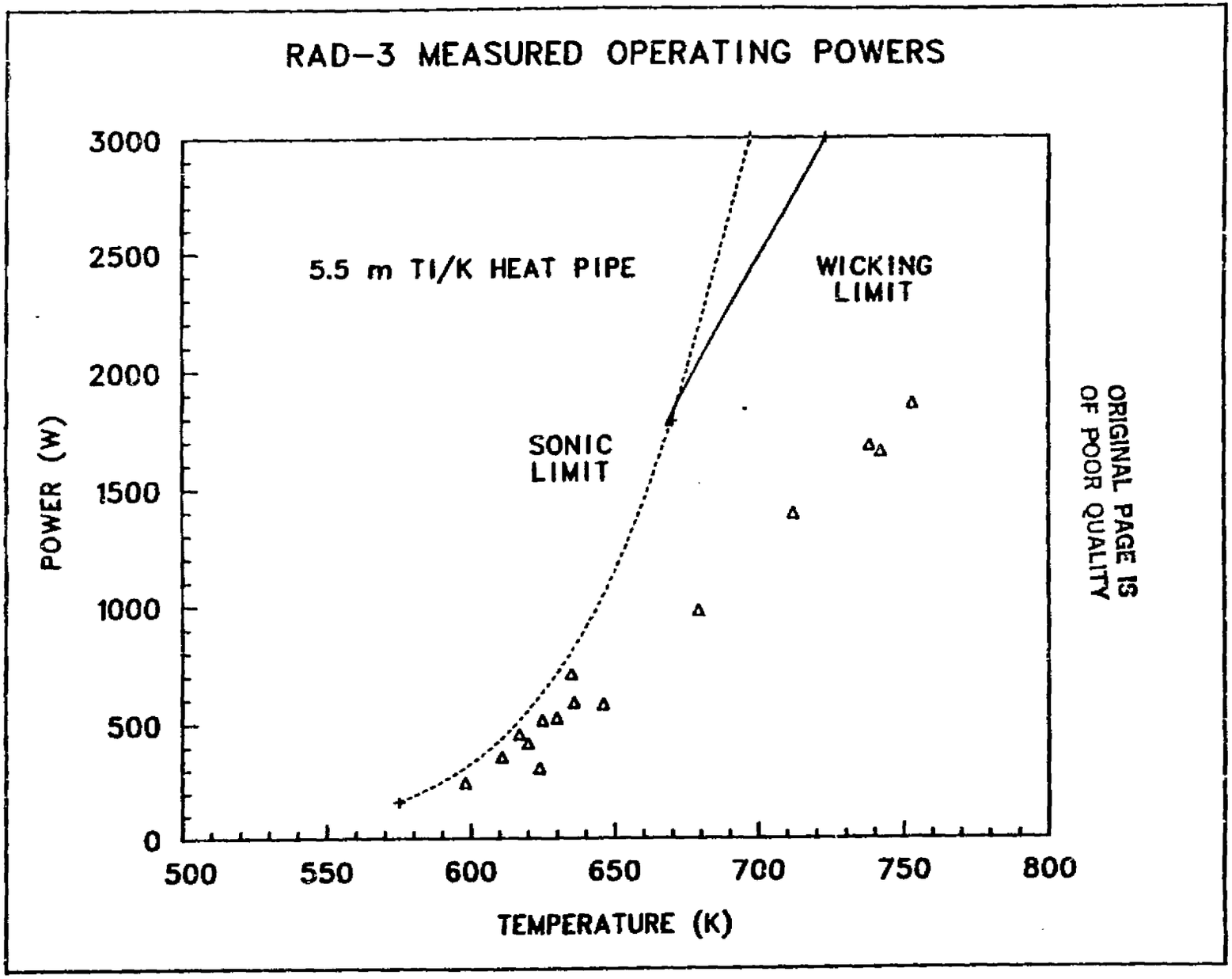

Fig. 32. RAD 3 Wicking Limit Curve
Courtesy, Steve Girrens, LANL

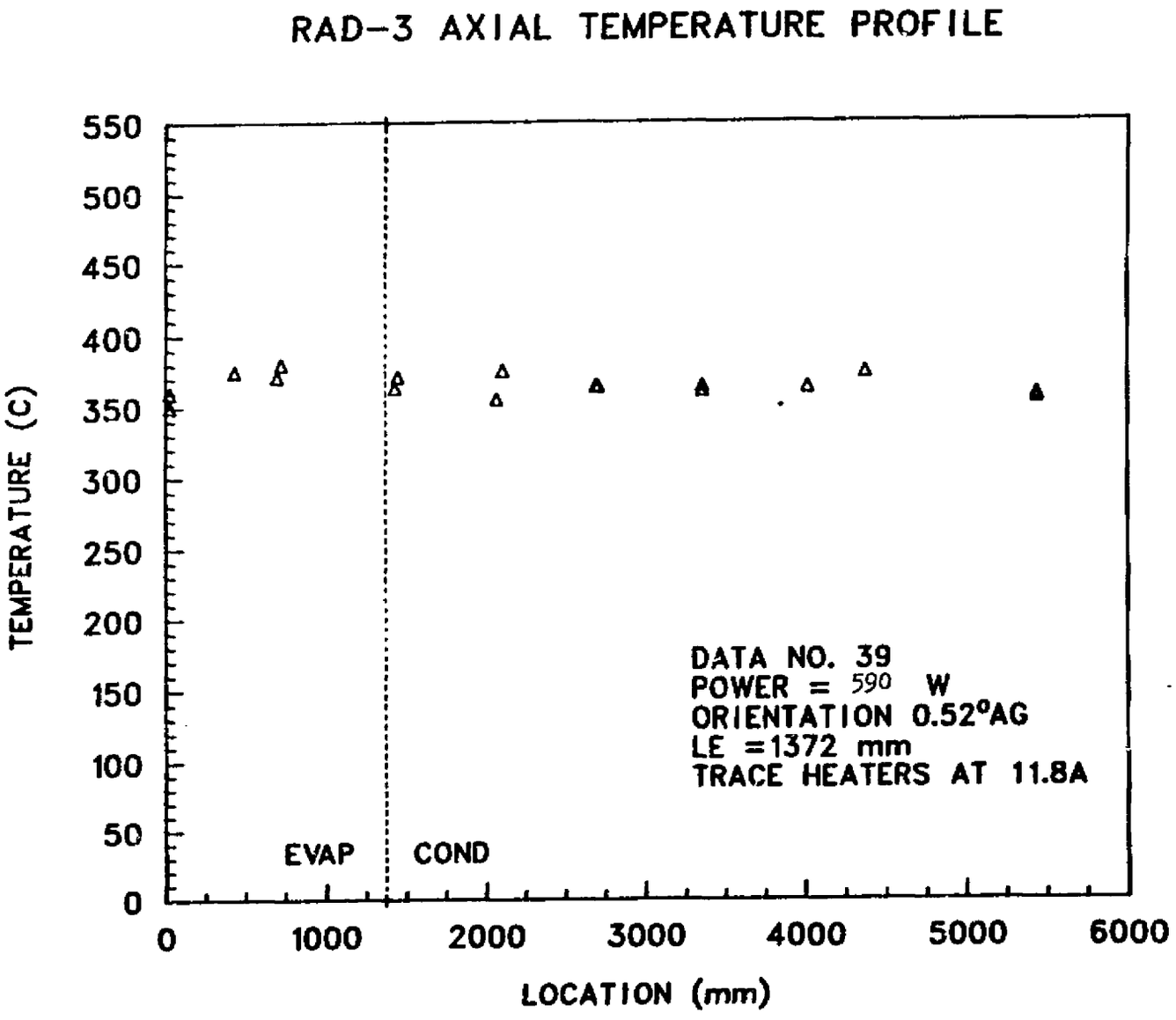

Fig. 33. RAD 3 Temperature Profile at 590 Watts Against a 0.52° Gravity Tilt
Courtesy, Steve Girrens, LANL

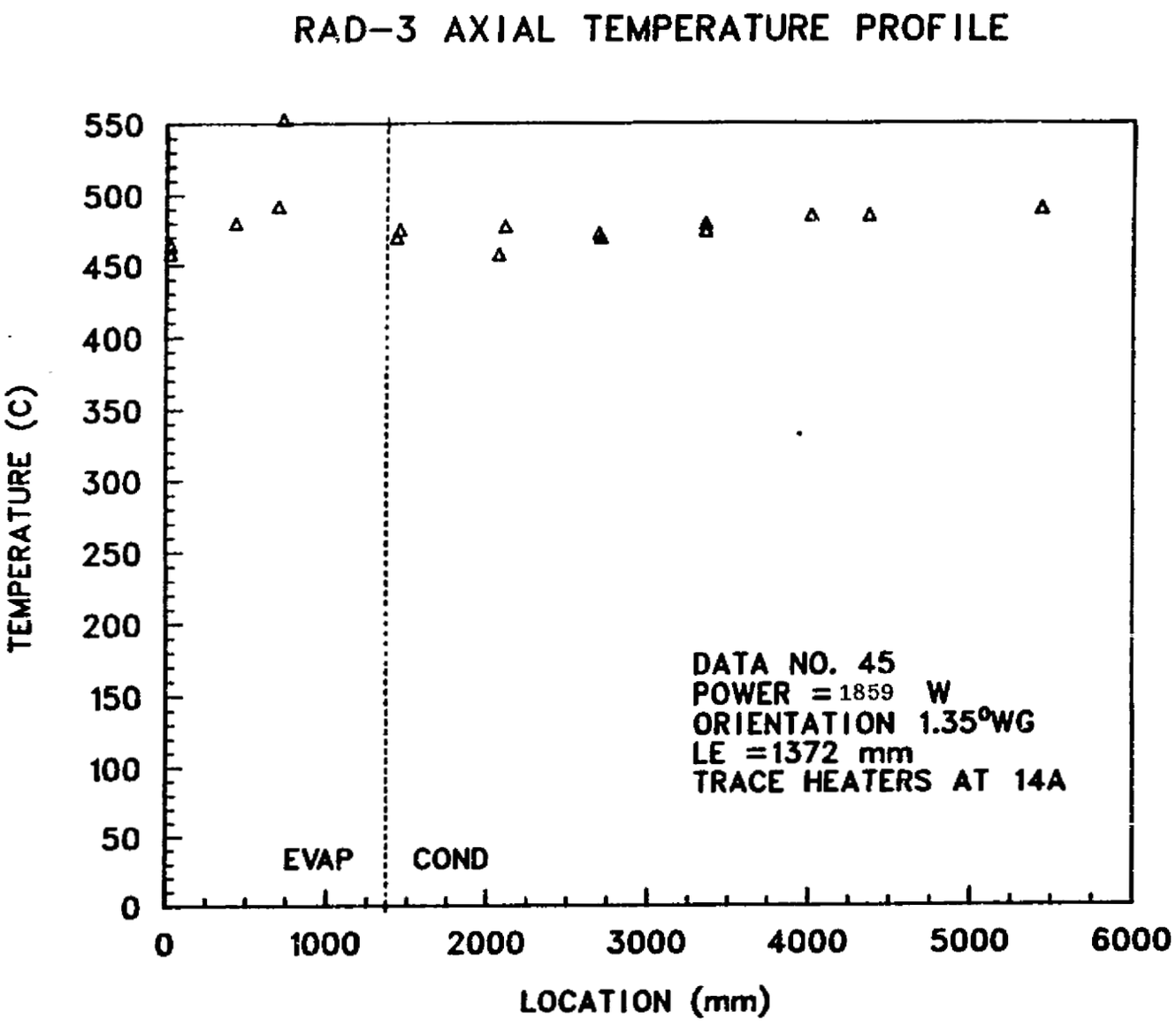

Fig. 34. RAD 3 Temperature Profile at Max Power of 1.86 KW
Courtesy, Steve Girrens, LANL

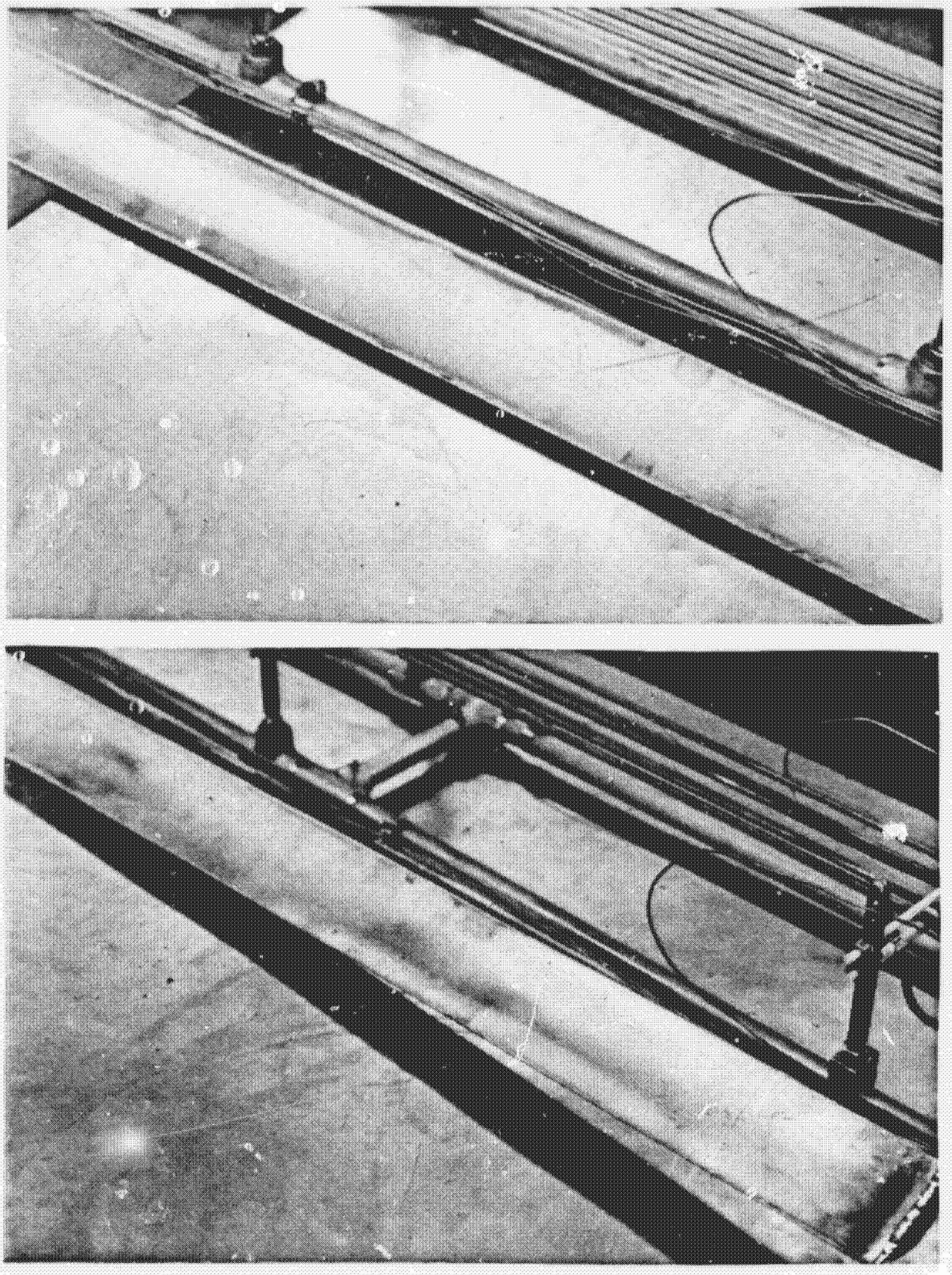

Fig. 35. Warping of Evaporator

5. CONCLUSIONS AND RECOMMENDATIONS

Heat Pipe Performance

- Liquid metal heat pipes with large diameter-to-length ratios can be designed to meet the power requirements of large scale high temperature spacecraft radiators.

- Arterial wicked liquid metal heat pipes of circular and semi-circular crossection with length to diameter equivalent ratios of 220:1 and 350:1 respectively, have shown no adverse operational effects resulting from start up with the working fluid frozen throughout the heat pipe, or from prolonged operation with a portion of the working fluid frozen in the condenser.

Circular Crossection

- Non-bonded screen/artery wicks can support an evaporator heat flux of 22 W/cm^2. Evaporator wick-to-wall bonding methods to increase the evaporator heat flux limits should be pursued and include:
  - The use of sintered powdered metal evaporator wicks.
  - The use of a lower thermal expansion heat pipe envelope material thus enabling the use of an oxidized or ceramic coated SS thermally expanded mandrel to bond a layer of screen to the evaporator wall.
  - The development of a ceramic coated flexible bladder which is pressurized at bonding temperature, thus permitting the use of SS heat pipe envelopes.
- Heat pipes with minimum mass based on a minimum wall thickness of 0.025 cm and consistent with the envelope material's column buckling strength should be designed, fabricated and tested.

Semicircular Crossection

- Single layer screen arteries, perform as designed, (within the limits of their distribution wick).

- Evaporator distribution wicks obtained by shot blasting the inner surface of the heat pipe envelope are limited in their ability to distribute the working fluid over a large area.

- Linear heat fluxes of 3.2 W-cm/cm^2 and 5.1 W-cm/cm^2 were achieved for artery operation against and with gravity respectively. These heat fluxes are 1.4 W/cm^2 x 2.29 cm and 2.2 W/cm^2 x 2.29 cm where the half distance between adjacent arteries is 2.29 cm.

- Increased performance of the shot blasted distribution wick could be achieved by increasing the depth of penetration and size distribution of the shot particles and/or increasing the number of arteries servicing the wick, thus reducing lateral flow resistance.

- Alternate methods to increase the performance of the semi-circular crossection heat pipe include:

    - Sintered powder metal wicks.
    - Bonded screen wicks.

Heat Pipe Processing

- The distillation of the working fluid into a clean, well out-gassed and heated heat pipe, followed by operating the heat pipe at design temperature and the insitu seal off of the heat pipe, produces a liquid metal heat pipe which shows excellent wetting and rewetting of the wick structure by the working fluid.

- The use of a male/female connection between the distillation pot

and heat pipe, which also serves as the vacuum port and seal off site, permits separate handling of the heat pipe and distillation pot. This separation allows for all welding to be done before the liquid metal is introduced into the distillation pot and does not require the use of mechanical fittings on the heat pipe side of the seal off. Mechanical fittings on the distillation pot side, when used for convenience, can tolerate a small vacuum leak because both sides of the system are evacuated.

- Fluid filling methods commensurate with volume production of heat pipes should be investigated. Possible methods in addition to distillation include direct injection of the fluid and the use of rupturable fluid capsules. The first approach includes direct injection of purified working fluid into a pre-outgassed evacuated heat pipe with subsequent seal off. It might be necessary to operate the heat pipe at temperature prior to seal off. The second approach includes the development of a thin walled zirconium and/or hafnium canister which is prefilled with purified working fluid, and is inserted into the heat pipe prior to the last end cap weld. Following outgassing of the heat pipe the canister would be ruptured by heating to a prescribed temperature. The canister then would remain in the heat pipe and act as a getter. Subsequent operation and seal off would follow.

Computer Modeling

- Thermacore computer program A37 was shown to have better agreement with low temperature sodium heat pipes then HTPIPE. This stems from the use of different thermophysical data for sodium and the use of improved calculation rationale in A37.

- A37 is currently limited to temperature profile predictions for

the cases where the end of the condenser has reached the temperature equivalent to or greater than a working fluid vapor pressure of approximately 0.1 Torr.

- Improved modeling could be achieved by the inclusion of:
  - Variable heat input to the evaporator.
  - Heat loss in the "adiabatic" zone.
  - Transonic vapor flow modeling at the entrance to the condenser.
  - Improved vapor flow modeling for the condenser in the viscous and transition to inertial flow regimes and their effects on pressure recovery.
  - Improved thermophysical property data for working fluids from room temperature to the critical temperature.

Improved computer modeling is necessary for implementation of system studies for space power systems like NEP, SPAR and SP-100. The current DOE sponsored SP-100 system and NASA/DOD sponsored TASP program have high temperature molybdenum alloy heat pipes radiating to the hot side of thermoelectric generators. These heat pipes, while capable of transferring the required power with a sufficient safety margin at design temperature, must also be capable of transferring sufficient thermal power on start up to enable the thermoelectrics to come up to temperature. That is, the system must "boot strap" itself up to operating conditions.

Analysis of these heat pipe start up conditions will require A37 predictions in the low temperature range, thus the need for improved computer modeling. Also to achieve full system implications, the thermoelectrics must be modeled as the heat sink to which the heat pipe is radiating. This will include their thermal capacity, transients

and radiation to space. This modeling could be included in A37 or could be part of a system program which includes the improved A37.

Based on the above conclusions and comments the following recommendation are made.

A multiphase Technology Development Program should be undertaken to establish the heat pipe as a viable heat transfer tool for use in space nuclear power subsystems. This effort should begin with the development of a comprehensive computer program which models the heat pipe from room temperature to operating temperature as a function of its interaction with the heat source and heat sink. Computer program A37 should be expanded to make this possible.

As part of this computer modeling, heat pipes representative of those being modeled should be designed, fabricated, and tested under conditions simulating system start up and operating conditions. The results of these tests should be used to verify the computer modeling and/or adjustments made so good correlation is achieved between experimental data and predicted heat pipe performance.

A second and parallel effort should be undertaken to investigate the effect several parameters have on the life of a heat pipe envelope-working fluid combination. The parameters of interest include fluid, envelope and wick impurity levels, fabrication and processing techniques, operating temperature, radial and axial heat fluxes and fluid circulation rates. A matrix of tests should be designed and carried out and the results of these tests should be used to develop a life expectancy model which can then be used for selecting the proper heat pipe for a given application.

As system design studies progress and a particular system is selected, the heat pipes for that system should be designed using the above computer

modeling and life expectancy data, followed by the fabrication and testing of prototypes.

7. NEW TECHNOLOGY

Title:	Heat Pipe Computer Modeling
Inventors:	Donald M. Ernst G. Yale Eastman Susan M. Cunningham
Initial Disclosure:	Progress Report #1 - JPL Contract 955935 December, 1980, Section 2.1
Subquarter Disclosures:	Progress Reports - JPL Contract 955935 #2 January 1981 - Section 2.2 #3 February 1981 - Section 2.2 #4 March 1981 - Section 2.2 #5 April 1981 - Section 2.2 #6 May 1981 - Section 2.2
Current Disclosures:	Final Report - JPL Contract 955935 September, 1982, Section 3 Pages 17-32

7. NEW TECHNOLOGY

Title:	Improved Evaporator Wick
Inventors:	Donald M. Ernst G. Yale Eastman
Initial Disclosure:	Progress Report #3 - JPL Contract 955935 February, 1981 - Section 2.1
Current Disclosure:	Final Report JPL Contract 955935 September 198 ection 2.3 Pages 14-16, Figure 8

6. REFERENCES

1. Heat Pipe Heat Rejection System and Demonstration Model for the Nuclear Propulsion (NEP) Spacecraft, Final Report, JPL Contract 955100, Donald M. Ernst, Thermacore, Inc., Lancaster, PA.

2. Heat Pipe Computer Program (HTPIPE) Users Manual, Prenger, Jr., F.E., Los Alamos National Laboratory, Los Alamos, NM.

3. LA-3941-MS, Quarterly Status Report on the Space Electric R & D Program for the Period Ending April 30, 1968, May 26, 1968.

4. Busse, C.A., Theory of the Ultimate Heat Transfer Limit of Cylindrical Heat Pipes, Int. J. Heat and Mass Transfer, Vol. 16, pp 169-186.

5. Personal Communication, Coyne Prenger, LANL.

6. Laminar Pipe Flow with Injection and Suction Through a Porous Wall, Yuan, S.E. and Finkelstein, A.B., Transaction of the ASME, May 1956, pp. 719-724.

7. Ernst, D.M., Evaluation of Theoretical Heat Pipe Performance, Thermionic Energy Commission Specialists Conference, Palo Alto, CA, Oct. 1967.

8. APPENDIX A

PROGRAM A37 1: 3 P.M. 8/24/82

NEED INSTRUCTIONS (Y/N) --- ?Y

DIMS(IN OR CM), ANG(DEG), TEMP(DEG C), POWER(WATTS)

FLUID CODE	TEMP (C)		
1 AMMONIA	-78	TO	100
2 EMTHANOL	-20	TO	150
3 ETHANOL	10	TO	165
4 WATER	5	TO	360
5 DOWTHERM A	150	TO	400
6 MERCURY	250	TO	450
7 CESIUM	375	TO	825
8 RUBIDIUM	200	TO	725
9 POTASSIUM	400	TO	900
10 SODIUM	450	TO	1100
11 LITHIUM	800	TO	1800
12 LASL SODIU			
13 LASL LITHI			
14 ACETONE	-23	TO	202
15 BENZENE			
16 TOLUENE			
17 FREON 11	20	TO	140
18 FREON 12	-40	TO	50
19 FREON 13	-110	TO	20
20 FREON 13B1	-40	TO	50
21 FREON 21	-40	TO	50
22 FREON 22	-40	TO	50
23 FREON 113	-30	TO	50
24 FREON 114	-70	TO	100
25 FREON 502	-40	TO	50

WICKS: 0 = WICKLESS
1 = 150X270 NI
2 = 200X400 NI
3 = ELMET325 MO
4 = AMAX-B
5 = FM1006
6 = FM1008
7 = FM1205

OR 99 TO INPUT SPECIAL WICK CHARACTERISTICS

OR MESH NUMBERS LISTED BELOW:

MESH #	WIRE DIAM.(INCHES)	MESH #	WIRE DIAM.(INCHES)
20	.016	30	.013
40	.010	50	.009
60	.0075	80	.0055
100	.0045	120	.0037
140	.0029	170	.0024
200	.0021	230	.0018
270	.0016	325	.0014
400	.0012		

WALL & WICK MATERIALS:
1 = ALUMINUM
2 = COPPER
3 = 304 STAINLESS
4 = HASTELLOY-X
5 = NICKEL
6 = MOLYBDENUM
7 = NIOBIUM
8 = COPPER-NICKEL
9 = ADMIRALTY BRASS
10 = LOW CARBON STEEL

A37 CONTAINS THE FOLLOWING FILES:

FILE	DATE	DESCRIPTION
ANL-2	3/30/82	ARGONNE PIPE 2.375 IN DIA 28 IN LONG
AHP-2	2/ 5/82	ARTICULATED NH3 HP AL/SS ART
JPL-2	5/24/82	JPL-2 FINAL REPORT

```
WANT EXISTING DATA DISPLAYED (Y/N) --- ?Y

JPL-2 FINAL REPORT
```



```
INITIAL CONDITIONS:  MEASUREMENTS IN CENTIMETERS

LINE 0        GRAVITY MULTIPLIER = 1          LOCATION = EARTH

LINE 1        E-LENGTH        A-LENGTH        C-LENGTH
                28              0               407             CM

LINE 2        FLUID           WETTING ANGLE   EVAP TEMP       MAX DEL-T
                12              0               662  DEG C      500  DEG C

LINE 3        EVAP  O.D.      ADB  O.D.       COND  O.D.
                2.667                           2.667           CM

              WALL THICKNESS                  EVAP GRAVITY ANGLE
                .287 CM                         0 DEG

LINE 4        INITIAL POWER   STOPOFF POWER
                2000            2366.37         WATTS

LINE 5        EVAP            ADB             COND
                2                               2               WRAPS
                200                             200             MESH

LINE 6        EVAP WIRE       ADB WIRE        COND WIRE       STD DIAM?
                Y                               Y

LINE 7        WALL MATL = 3                   WICK MATL = 3

LINE 8        # BENDS =  0

LINE 10        2 ARTERIES      2 WORKING       .39  CM ARTERY O.D.

LINE 11        2 WRAPS         200  MESH ARTERY

LINE 12        Y              ARTERY MESH IS OF STD DIAMETER

LINE 13        1              ADIABATIC VAPOR FLOW IN ADB SECTION

LINE 14        1              EVAP SONIC EQ. USES .474 BUSSE ISOTHERMAL

LINE 15        EVAP            ADB             COND
                4               1               32              SEGMENTS

LINE 16       EMISSIVITY = .263                COND AREA FACTOR = 100  %

              CONDENSER RADIATES TO SPACE

LINE 17       HEAT SINK # 1  ALONG CONDENSER

BEGINS AT       404 CM        ENDS AT         405 CM          FROM A-C
X-SECTNL AREA   7.56 CM2      LENGTH          7.62 CM
HEAT SINK MATL = 3            COOL END OF HEAT SINK = 50 DEG C


CHANGE WHICH LINE (99 TO RUN, STOP TO QUIT) --- ?99
```

```
BEGINNING A37INC CALCULATIONS NOW ...
AT A STOPOFF POWER OF 2366.37   WATTS, DELTA-T = 22.6724   DEG C
CONTINUE TO ULTIMATE POWER (Y/N) --- ?Y
RESULTS WITHOUT INTEGRATING:
 5100   WATTS CAUSES ------ EVAP CAPILLARY LIMIT, DPV > DPL
                           1 STOPOFF      2 EQUILIBRIUM  3 NON-LIMITED
TRANSFER POWER (WATTS)       2366.37        3355.82        5000
RADIATED POWER (WATTS)       3554.86        3355.14        2658.29
TOTAL DELTA-T  (DEG C)       22.6721        38.3899        109.86
(8)

WANT TO CALCULATE BY INTEGRATING (Y/N) --- ?Y
AT A STOPOFF POWER OF 2366.37   WATTS, DELTA-T = 20.3936   DEG C
CONTINUE TO ULTIMATE POWER (Y/N) --- ?Y
RESULTS OF INTEGRATING      4              1             32 SEGMENTS:
 5400   WATTS CAUSES ------ EVAP SONIC LIMIT
                           4 STOPOFF      5 EQUILIBRIUM  6 NON-LIMITED
TRANSFER POWER (WATTS)       2366.37        3477.65        5300
RADIATED POWER (WATTS)       3572.93        3476.93        2804.97
TOTAL DELTA-T  (DEG C)       20.394         35.155         85.616
(8)

WANT TO SEE ANY SEGMENT BY SEGMENT DETAILS (Y/N) --- ?Y
WHICH INTEGRATED POWER (4, 5 OR 6) --- ?4
ENTER YYY, YNY, ETC. TO SEE DETAILS OF E, A, C --- ?YYY
```

3477.65 WATTS OVER 4 SEGMENTS 7 CM LONG IN EVAPORATOR

SEG	TEMP IN	DEL-T	VAPR IN	DEL-V	DPI	DPV	Q7	Q1	Q2
1	639.501	0.394	61310	352	319	32	0	869	434
2	639.107	1.171	60958	1036	963	73	869	869	1304
3	637.937	2.016	59921	1750	1629	120	1738	869	2173
4	635.920	2.988	58171	2514	2342	171	2608	869	3042
***	632.932	6.569	55657	5653	5255	398	3477	3477	

3477.65 WATTS OVER 32 SEGMENTS 12.7188 CM LONG IN CONDENSER

SEG	TEMP IN	DEL-T	VAPR IN	DEL-V	DPI	DPV	Q7	Q1	Q(1)	Q2
1	632.932	0.506	55657	416	-69	485	3477	106	0	3424
2	632.426	0.481	55240	393	-69	462	3371	106	0	3318
3	631.945	0.456	54847	370	-69	439	3265	105	0	3212
4	631.489	0.430	54476	347	-69	417	3159	105	0	3106
5	631.060	0.404	54129	324	-70	395	3053	105	0	3000
6	630.656	0.378	53804	302	-70	373	2947	105	0	2895
7	630.278	0.353	53501	280	-70	351	2842	105	0	2789
8	629.925	0.327	53221	259	-70	330	2737	104	0	2684
9	629.598	0.302	52961	238	-71	309	2632	104	0	2579
10	629.297	0.276	52723	217	-71	288	2527	104	0	2475
11	629.020	0.251	52506	197	-71	268	2422	104	0	2370
12	628.769	0.119	52308	93	-71	164	2318	104	0	2266
13	628.650	0.110	52215	85	-71	157	2213	104	0	2161
14	628.540	0.100	52130	78	-71	149	2109	104	0	2057
15	628.440	0.091	52051	70	-71	142	2005	104	0	1952
16	628.349	0.081	51981	63	-71	135	1900	104	0	1848
17	628.268	0.072	51918	55	-72	127	1796	104	0	1744
18	628.197	0.062	51862	48	-72	120	1692	104	0	1640
19	628.135	0.052	51814	40	-72	112	1587	104	0	1535
20	628.083	0.042	51773	32	-72	104	1483	104	0	1431
21	628.040	0.033	51741	25	-72	97	1379	104	0	1327
22	628.008	0.023	51715	17	-72	89	1275	104	0	1223
23	627.985	0.013	51697	10	-72	82	1171	104	0	1119
24	627.972	0.003	51687	2	-72	74	1067	104	0	1015
25	627.969	-0.007	51685	-5	-72	66	963	104	0	911
26	627.975	-0.017	51690	-12	-72	59	858	104	0	806
27	627.992	-0.026	51703	-20	-72	51	754	104	0	702
28	628.018	-0.036	51724	-28	-72	43	650	104	0	598
29	628.055	-0.046	51752	-35	-72	36	546	104	0	494
30	628.101	-0.056	51788	-43	-72	28	442	104	0	390
31	628.157	-0.066	51831	-51	-72	20	338	104	0	286
32	628.222	-0.196	51882	-152	-161	8	233	104	129	117
***	628.418	4.514	52035	3622	-2377	5996	0	3347	129	

WANT TO SEE ANY SEGMENT BY SEGMENT DETAILS (Y/N) --- ?N

WANT TO SEE ANY DETAILS (Y/N) --- ?Y

PRINT RUN CONDITIONS (Y/N) --- ?Y

```
RUN CONDITIONS:  FOR A37                                  1:17 P.M.      8/24/82

FILE NAME - JPL-2        JPL-2 FINAL REPORT

LOCATION = EARTH

SONIC LIMIT IN THE EVAPORATOR IS BASED ON ISOTHERMAL (BUSSE) VAPOR FLOW

ARTERY HEAT PIPE
                                                                  GRAVITY ANGLES
FLUID      = LASL SODIU WETTING ANGLE =     0.00 DEG      EVAP    0.00 DEG
EVAP TEMP =  662        MAX DELTA-T    =     500 DEG C
WALL MATL = 304SS                                         COND    0.00 DEG
WICK MATL = 304SS

EVAP  LENGTH   28.0000 IN   28.0000 CM  EVAP O.D.  2.6670 IN  2.6670 CM
COND  LENGTH  407.0000 IN  407.0000 CM  COND O.D.  2.6670 IN  2.6670 CM
TOTAL LENGTH  435.0000 IN  435.0000 CM

WALL THKNESS    0.2870 IN    0.2870 CM

                --- WICK THICKNESS --- WRAPS     WICK  MESH WIRE DIAM
EVAP WICK       0.0093 IN    0.0237 CM   2   200 MESH     STANDARD
COND WICK       0.0093 IN    0.0237 CM   2   200 MESH     STANDARD

ARTERIES        0.0093 IN    0.0237 CM   2   200 MESH     STANDARD

ARTERY O.D.     0.1535 IN    0.3900 CM   2 ARTERIES  ( 2 WORKING)

ARTERY SPACING  0.8850 IN    2.2478 CM  IN EVAP
ARTERY SPACING  0.8850 IN    2.2478 CM  IN COND

   4 SEGMENTS IN EVAP      1 SEGMENTS IN ADB     32 SEGMENTS IN COND

HEAT SINK NO.  1 IS MADE OF 304SS        WITH COOL END TEMP OF  50 DEG C
BEGINS AT     159.0550 IN  404.0000 CM  FROM A-C
ENDS AT       159.4490 IN  405.0000 CM  FROM A-C
CROSS-SECTN     7.5600 IN2   7.5600 CM2
LENGTH          7.6200 IN    7.6200 CM

PIPE WALL EMISSIVITY = .263   COND AREA FACTOR = 100  %

CONDENSER RADIATES TO SPACE


SELECT DETAILS & ORDER TO PRINT (1,456,25,ETC. OR 0=NONE) --- ?5

WHICH DETAILS (A=ALL, N=NONE, T=TEMPERATURES ONLY) --- ?A
```

5 INTEGRATED DETAILS FOR THERMAL EQUILIBRIUM POWER OF 3477.65 WATTS

PE	PE-A	PA-C	PC	
61311	55657	55657	52038	DYNES/CM2

	EVAP	ADB	COND	
DPV VISCOUS	398	0	5997	DYNES/CM2
DPV INERTIAL	5255		-2377	DYNES/CM2
DPL MESH (CIR)	1433		99	DYNES/CM2
DPL ARTERY	45	0	676	DYNES/CM2
DPC	43132	43320	43320	DYNES/CM2
DPG	0	0	0	DYNES/CM2
DPD	0	0	-1617	DYNES/CM2
TOTL CAPILLARY	37121	0	41703	DYNES/CM2
TOTL DPV + DPL	7131	0	4395	DYNES/CM2
LEFTOVER CAP	29990	37309	37309	DYNES/CM2

EVAP TEMP	COND TEMP	DELTA-T	
662	626.845	35.155	DEG C

TE	TE-A	TA-C	TC	
639.501	632.932	632.932	628.422	DEG C

DELTA-T VALUES:

EVAP WALL	EVAP WICK	EVAPORATION	
20.7989	.999188	.700684	DEG C

VAPOR (E)	VAPOR (A)	VAPOR (C)	
6.56909	0	4.50977	DEG C

CONDENSATION	COND WICK	COND WALL	
.482042E-01	.683445E-01	1.46029	DEG C

LOCATION	MACH #	SONIC LIMIT	ENTRAINMENT	
EVAP	.224952	6342	13500	WATTS
E-A	.224952	6342		WATTS
ADB	.224952	6342	0	WATTS
A-C	.224952	15460		WATTS
COND			17300	WATTS

	EVAP	COND	AXIAL (AT EVAP)	
POWER DENSITY	15	1	623	WATTS/CM2

E A REY #	A A REY #	C A REY #	E R REY #	C R REY #
2779	0	107	22	3

COLD FLUID CHARGE	215.03 GRAMS	144.51 CM3
ARTERIES	56.56 GRAMS	
MESH WRAP	157.68 GRAMS	
PIPE WALL/ENDCAPS	7425.05 GRAMS	
TOTAL MASS	7854.32 GRAMS	

9. APPENDIX B

FILL AND TESTING OF RAD-3 (5.5m Ti/K) RADIATOR HEAT PIPE

by
S. P. Girrens

BACKGROUND AND DESCRIPTION

RAD-3 is the first titanium radiator experimental heat pipe built to actual design length. The heat pipe was constructed to verify performance of a 360 stringer heat pipe design radiator with the following design characteristics:

Beginning of mission power/heat pipe	2.65 kW by 360 pipes
End of mission power/heat pipe	2.97 kW by 321 pipes
Length	5.17 m
Total cross-sectional area	588 mm^2
Flat side (armor) thickness	0.60 mm
Curved side thickness	0.60 mm

RAD-3 has a semi-circular cross-section of radius 2.0 cm. The flat section is 6.2 cm wide. The pipe has two, single layer 50 mesh Ti screen arteries each 12 mm^2 in cross-section. The arteries were open on the fill tube end. The entire inner surface was shot-blasted for the distribution wicking system. The length dimensions are as follows:

Heat pipe:	5.47 m
Fill tube:	0.24 m
Total:	5.71 m

The screen arteries for this pipe were formed over a mandrel and then spot welded to the flat section before welding the flat and curved sections together in order to control artery dimension. Curved section wall thickness is 0.056 cm (0.022") and the flat section thickness is 0.07 cm (0.028"). The 5.5 m curved section was assembled by butt-welding three approximately 2 m long sections together. The screen arteries and flat section are continuous lengths. The approximate cross-sectional area available for vapor flow is 6.3 cm^2.

On February 6, 1981 it was agreed that Thermacore, Inc., principal investigator Don Ernst, would fill and test RAD-3 under JPL contract* A test plan

*EDITORS NOTE: JPL SUB CONTRACT 955935

and procedures was established between Thermacore and Los Alamos in March. The titanium heat pipe container was also shipped to Thermacore in Lancaster, Pennsylvania in March.

TEST OBJECTIVES

The test objectives established for RAD-3 included the following:

1. fill and wet-in with arteries (flat side) down orientation;
2. successful start-up;
3. operation at 500°C in vacuum at low power (run at maximum uncoated power) and measure axial ΔT's;
4. operation at 500°C in a low pressure atmosphere (run inert gas atmosphere to increase heat transfer) at maximum uncoated power and measure axial ΔT's;
5. vary evaporator area and/or input heat flux to obtain dry out limits on shot blast distribution wick.

HEAT PIPE FILL

Calculations made on the amount of potassium required to fill RAD-3 resulted in an estimate of 250 cc or 213 g at room temperature. Therefore, it was decided to load the fill pot with 260 g of potassium for transfer by distillation into the pipe.

Actual fill operations began on Monday, October 19, 1981. The system had been outgassing all weekend at 200 C. Potassium was taken to 200 C the night before to initiate molten outgassing stage. At 817 slowly started increasing pot temperature from 250 to 650 C. At 1050 began to observe potassium moving through snivvy by both current fluctuation in snivvy and visual observation. From 1130 to 1345 pot was maintained at 650 C. At 1345 pot temperature was increased to 710 C and maintained until 1615. At 1615 the pot temperature was again increased to 730 C and maintained until 1655. As can be seen in the temperature chart in Appendix 1, at 1655 TC's 21 and 22 crossed over indicating that the potassium distillation was complete. Approximate total transfer time was 6 hours.

WET-IN AND ARTERY FILL:

Heat was supplied to the heat pipe by two devices, (1) the trace heaters (Nichrome wire insulated with ceramic beads) which were lying along the

arteries were confirmed to be functioning excellently in that several times the input power was increased, allowing a hot spot to develop, and then reduced to observe distribution wick recovery. The largest heat pipe power obtained for the 60 cm evaporator was 826 W with gravity assist and the temperature profile is shown in Fig. 5. In order to prepare for heat pipe seal or burn-off the trace heaters were turned off. Figures 6-8 are temperature profiles of the pipe operating with gravity and the trace heaters off. The heat pipe was successfully sealed at the end of the day.

After the events of the 23rd, we came to the conclusion that the shot-blasted distribution wick would not support the input heat flux of 7 W/cm^2 required to operate the heat pipe at 500 C against gravity. It was also calculated, based on a maximum input flux of 1.4 W/cm^2, that an evaporator of length 230 cm was required to operate the heat pipe against gravity at 500 C. Based on these observations, we decided to construct a new rf coil 137 cm long in order to get more power into the pipe. The new coil length of 137 cm was selected because this was the length of vacuum chamber which was constructed with sufficient viewing ports allowing visible observation of hot spots. The new coil configuration selected was a 3-turn, 3/16 in. copper tubing, 1/8 in. gaps between tubes, mitered corners design. The trace heaters would continue to be used in order to artificially increase heat pipe operating temperature.

Work on the new coil was performed during the weekend. Other work included cleaning the bell jar of the distillation apparatus and and filling residue, relocating the heat pipe on the support structure to facilitate easier tank tilting which also put the heat pipe completely into the calorimeter jacketed area.

Upon disassembling the distillation pot, no potassium was evident therefore confirming transfer of all 260 g of potassium into the pipe. Observations of the heat pipe showed slight material distortions in areas where hot spots occurred and a concave inward shape of the flat section indicating a vacuum tight fill tube seal. System modifications were completed Monday, October 26 and the pipe and new rf coil were reassembled into the vacuum test chamber. The trace heaters were turned on to 10A and a pressure of 4×10^{-5} torr was soon attained in the chamber. The tank and pipe orientation was .52° with gravity to facilitate artery fill and wet-in of the new evaporator section.

length of the heat pipe on the curved section, and (2) a four-turn rf coil (constructed of 0.64 cm wide flat traveling-wave tube) which was oriented opposite the flat section at one end of the heat pipe simulating the heat source for the evaporator. The rf coil was 60 cm in length.

Tuesday and Wednesday, October 20 and 21, were spent performing wet-in and artery fill operations. Throughout these operations, the trace heaters were maintained between 11-12A. An axial temperature profile of the heat pipe with only the trace heaters providing heat input at 11A is shown in Fig. 1. As the rf coil power was increased, hot spots would develop at various locations in the evaporator. The first hot spot occurred 6-11 cm from the end of the evaporator along the edge of the pipe next to artery #1. (Since there are two arteries, they will be distirguished by referring to them as artery #1 or #2 with artery #2 being located on the heat pipe side adjacent the side vacuum tank viewing ports.) The orientation of the pipe at this time was a 1.0^{o} tilt gravity assist (evaporator lower than condenser), and the rf current was 65A. In an effort to increase overall heat pipe temperature for wet-in, it was felt that increasing the gravity assist by lowering the vacuum tank would allow higher rf powers. This process of lowering the tank and then increasing rf power was continued to a point where the orientation was 2.5^{o} gravity assist at an rf current of 115A. The highest wet-in temperatures were attained at this point and an axial profile illustrating these temperatures is shown in Fig. 2.

Since the pipe was taken to a relatively good wet-in temperature by lowering the vacuum tank, it was next decided to fill the arteries. The orientation selected for artery fill was a slight gravity assist angle of 0.31^{o}. To fill the arteries, the rf coil would be turned on only occasionally while the trace heaters would be on continually. Thus, the trace heaters would drive potassium by evaporation to the evaporator section and intermittent rf power would redistribute the working fluid. After performing this operation for about 6 h , the heat pipe was brought up to horizontal to verify artery operation. At an RF current of 80A a hot spot again developed by artery #1 at the same location described earlier. The heat pipe was again returned to the 0.31^{o} down orientation for refill of arteries. After 2.5 h of rewet the pipe was raised to horizontal at an rf current of 70A. This time a hot spot was observed to start in the center of the flat at the end of the evaporator and move towards the arteries and towards the beginning of the evaporator.

This phenomena suggested that the arteries were filling but then becoming drained due to some type of dry-out. It was established that the best artery fill orientation for the remaining of the experiment would be the 0.31^{o} down orientation and trace heaters on 12A.

HEAT PIPE TESTING

Actual heat pipe testing began Thursday, October 22. During the previous night, the pipe was maintained in the 0.31^{o} down orientation with trace heat only at 12A. A calorimeter measurement was taken to get a datum for how much heat the trace heaters were inputing into the system. Once the datum was established, increases in measured amounts of heat during rf operation would indicate heat pipe power. The primary objective of the day was to determine if the arteries were filled and operating. To perform this test, the rf coil was turned on to 70A which was measured to be 720 W. The heat pipe was then raised to a horizontal orientation. Almost as soon as the tank was raised, the heat pipe would develop localized hot spots, indicated by an orange glow in the titanium container, which would continue to grow or get brighter until rf power was shut off. This operation of raising the pipe at 70A rf was performed twice. It was also determined that a minimum of 2 h was required to refill the arteries after allowing a local artery hot spot to occur. Even though we felt the arteries were working, the events of the day were not conclusive for confirming artery operation.

On the 23rd, a new procedure for determining artery operation was performed. First, the trace heaters were turned up to their maximum allowable current of 15A. After allowing time for the system to stabilize, temperatures and calorimeter measurements were made and illustrated in Fig. 3. The rf was then turned on to 55A. Next, the tank was raised to a $.25^{o}$ against gravity orientation. The heat pipe was operating with no visible hot spots. The rf power was then increased in 5A increments and after each increase allowed to stabilize. At 70A a hot spot developed in the middle of the evaporator flat, approximately 25 cm from the end of the heat pipe. Upon turning the rf power back down to the 55A level, the hot spot would disappear indicating heat pipe recovery. After allowing the system to stabilize at the 65A rf power level, temperature and power measurements were made and shown in Fig. 4. The heat pipe was transporting 522 W against gravity. Apparently, the distribution wick had reached a dry-out limit at about 1.4 W/cm^2 input heat flux. The

Testing resumed Tuesday the 27th with the trace heaters being turned up to 11.8A and a stabilized temperature and calorimeter measurement obtained for a datum condition. Figures 9-12 contain temperature profiles and power levels for the longer evaporator condition operating against gravity. Figure 13 shows the temperature profile and power level obtained while the heat pipe was actually being tilted to operate against gravity. Upon increasing the rf coil power to 75A a hot spot developed in the center of the flat evaporator section 71 cm from the end of the pipe. This location is 11 cm into the new evaporator region. When the rf power was reduced the heat pipe distribution system recovered and the hot spot disappeared. When the rf power was again increased, the hot spot returned at 60A which was lower than the previously attained 67A. The vacuum chamber was then tilted to allow the heat pipe to operate with gravity. The trace heaters were also turned up to 14A to attain higher temperatures. Figures 14 and 15 illustrate the powers and temperatures reached after the first day of testing the longer evaporator configuration.

On Wednesday, the day again started by obtaining a datum trace heat power at 11.8A. The temperature profile for this datum condition is shown in Fig. 16. The rf was then turned on to 55A and the pipe was tilted to operate at 0.5^{o} against gravity. Figures 17 and 18 are the temperatures and powers obtained in this orientation. What is of interest is that the data presented in Fig. 18 is, within acceptable measurement error, a reproduction of the data presented in Fig. 12 taken one day earlier. Upon increasing the rf to 85A, a hot spot developed again in the center of the flat evaporator section approximately 71-81 cm from the end of the heat pipe and slowly spread both towards the arteries and axially along the pipe. The hot spot was also confirmed by #1 thermocouple which indicated a 80 C temperature increase 72 cm from the end of the heat pipe in the evaporator section. The hot spot could be eliminated and reproduced by decreasing and then increasing the rf power again indicating distribution wick recovery and artery operation. The highest heat pipe power measured before dry-out was 888 W which computes to an input flux of 1.1 W/cm^2 which is lower than the previously measured and computed 1.4 W/cm^2 from the 60 cm evaporator tests. Having established heat pipe operation against gravity it was next decided to test for maximum power and temperatures utilizing gravity assist to reduce distribution wick dry-out problems. The pipe was tilted down to a 1.35^{o} gravity assist orientation and the trace heaters were turned up to 14A. As the rf power was increased, the entire

evaporator began to turn orange in color. Since the evaporator was apparently increasing in temperature uniformly it was assumed that excess potassium, free flowing down the flat section, was aiding evaporative fluid distribution. Figures 19-21 show temperature profiles and powers attained during this testing phase. Figure 20 contains data taken for the maximum power, 2383 W, transported by the heat pipe. Testing during the remainder of the day involved turning off the trace heaters and manipulating the rf input to obtain a few power shut down temperature profiles. These data are presented in Figs. 22-24.

The final day and morning of testing, October 29 and 30, were spent obtaining temperature start-up profiles for both against and with gravity orientations. The data taken during this testing phase is presented in Figs. 25-34. Figure 28 shows the temperature profile measured when the heat pipe transported the highest power recorded of 1003W while operating against gravity. Figure 29 shows the data recorded for an actual rf power-up while the heat pipe was orientated against gravity.

DISCUSSION OF TEST RESULTS

The primary problem encountered testing RAD-3 was the low limiting values for heat flux into the flat evaporator section of the pipe. Because of this distribution wick dry-out limit the trace heaters were used to effectively reduce the condenser radiative heat rejection flux in order to allow the condenser to reach axially uniform temperature profiles. The dry-out problem was also reduced by allowing the heat pipe to operate in a gravity assist orientation thus utilizing the free flowing excess liquid to attain higher evaporative fluxes.

Another problem arose in that the thermocouples near the rf coil would occassionally pick up rf and give observable erroneous temperature measurements. This is evident by comparing temperature profile data with the rf off to data with the rf on.

The start-up profiles are interesting in that while the heat pipe is beginning to operate at low powers, the working fluid contained in the arteries towards the end of the condenser remains at ambient temperatures.

Computer calculations using the HTPIPE code were performed on the RAD-3 heat pipe configuration. Due to the irregular shape of RAD-3, cross-sectional artery and vapor shape dimensions were difficult to obtain. In order to make analytical performance calculations, the artery radii were assumed at 0.19 cm

and the vapor passage area at 6.3 cm^2. As is shown in Figs. 35 and 36, a first comparison of the computed predictions with the measured results indicated a performance discrepancy in that measured powers exceeded even the sonic limit. This was due to the fact that since the entire heat pipe was contained inside the water jacketed vacuum tank, heat rejected from the evaporator was also included in the calorimeter measured power. The operating powers computed by the theoretical analysis predict the maximum amount of heat which the pipe is able to transport through the evaporator-condenser interface. Therefore, in order to compare the experimental data with the performance analysis, calculations were made to determine the amount of heat rejected in the evaporator and then the measured power was reduced by the computed result. Two methods were used to determine the reduced operating powers. When the trace heaters were on, the measured power was reduced by the ratio of evaporator radiating area to total radiating area since the entire heat pipe was operating at nearly isothermal temperatures. The power reduction area ratio was calculated to be 0.22. The start-up and trace heaters off power measurements were reduced by calculating the radiative heat rejected in the evaporator by utilizing an average evaporator temperature and then subtracting this power from the calorimeter measured power. This different power reduction method was used for the start-up and trace heaters off operating conditions because as is evident in the temperature profiles, large axial temperature variations in the condenser section make the area ratio method infeasible. Table I contains a listing of the measured powers and the calculated reduced powers for all the 137 cm evaporator data. Figures 37-39 illustrate the excellent correlation obtained between the analytical predictions and the reduced operating power data. Appendix II contains a listing of the input and results obtained from the HTPIPE computer calculations. As is evident in Figs. 37 and 38, a good performance representation of data was obtained covering a wide temperature operating range of 180 C. The maximum power obtained was 1.86 kW at an evaporator exit temperature of 480 C. The average condenser temperature at this power level was 487 C. This data point, 63% of design power, was a significant result when considering the heat input dry-out limitation. The attainment of design power was not expected for these experiments because of the uncoated condition (that is, a high emissivity coating is required on the condenser exterior for the testing of performance limits) of the heat pipe. Figure 39 shows that the start-up capability of the heat pipe is very stable and predictable in the low power range.

SUMMARY

The testing of RAD-3 should be regarded as a successful step in the development of very long, light-weight, high-temperature heat pipes for space applications. Significant experimental procedures and results obtained include the following accomplishments.

1. Successful filling and wet-in procedures developed for very long, thin-walled heat pipe structures.
2. Successful start-up of very long arterial liquid metal heat pipes demonstrated.
3. Needed data obtained on radiator heat pipe operation at fractional power levels.
4. 590 W of heat transported against gravity, demonstrating successful artery operation.
5. 1860 W of heat transported at 487 C in gravity-assist mode, demonstrating overall capability of the pipe.
6. A low input heat flux dry-out limit of 1.1-1.4 W/cm^2 for the shot-blasted distribution wick showing the necessity for wire screen supplementation in the evaporator section of the heat pipe.
7. Excellent correlation between analytical predicted performance and actual test data.

No further testing of RAD-3 is budgeted at this time.

TABLE I

COMPARISON OF MEASURED AND REDUCED OPERATING POWERS FOR 137 CM EVAPORATOR DATA

Data Number	Evaporator Exit Temperature (C)	Measured Power (W)	Reduced Power (W)
35	325	316	246
36	347	534	417
37	344	584	456
38	357	673	525
39	363	756	590
40	406	1258	981
41	439	1786	1393
43	351	396	309
44	373	748	583
45	469	2122	1655
46	480	2383	1859
47	465	2156	1682
48	338	745	359
49	352	944	515
50	362	1171	713
51	320	606	246
52	330	730	344
53	336	844	440
54	346	1003	568
55	338	851	447
56	350	1091	648
57	357	1230	763
58	349	1116	684
59	365	1389	910
60	319	591	228

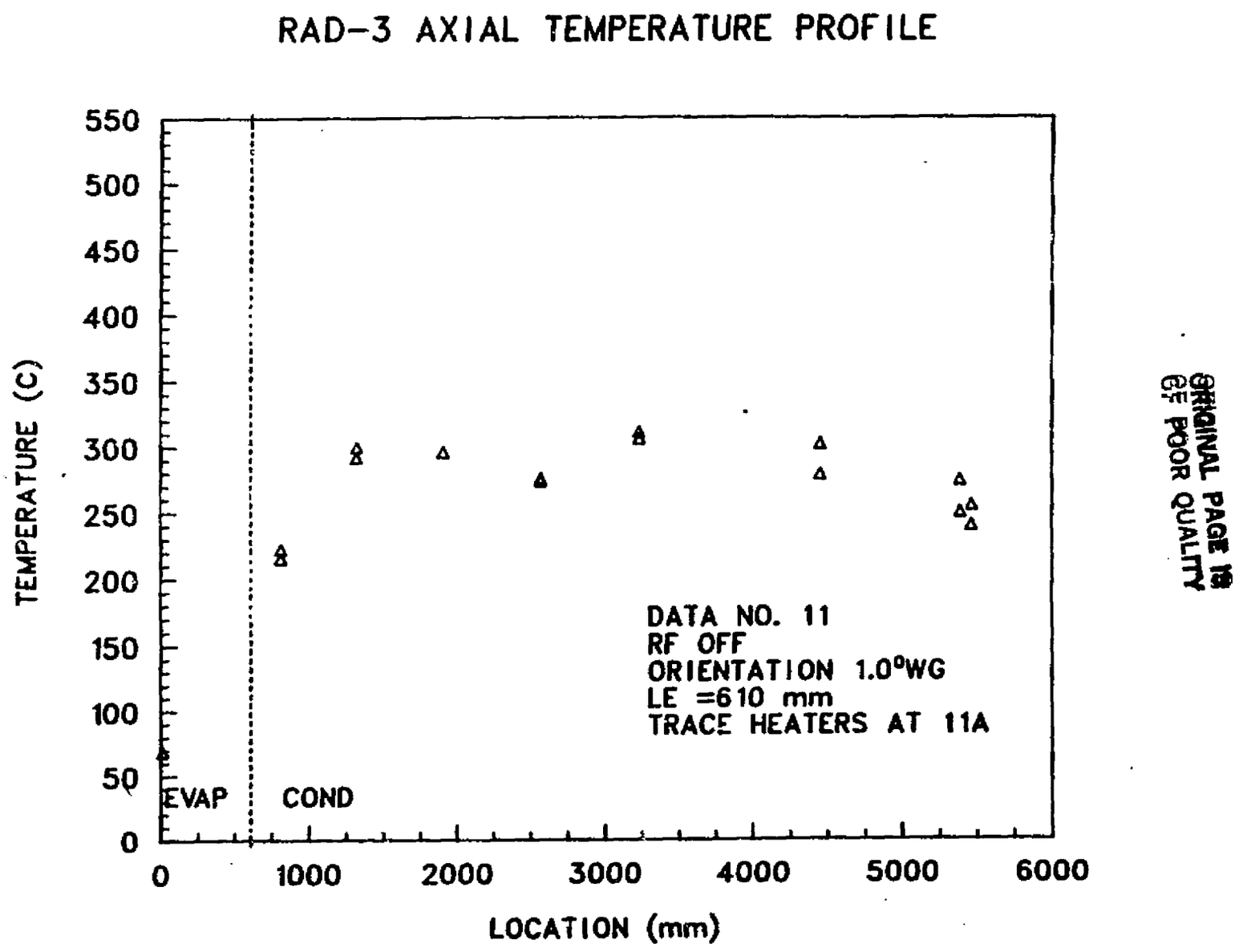

Fig. 1. Wet-in temperature profile with trace heat only.

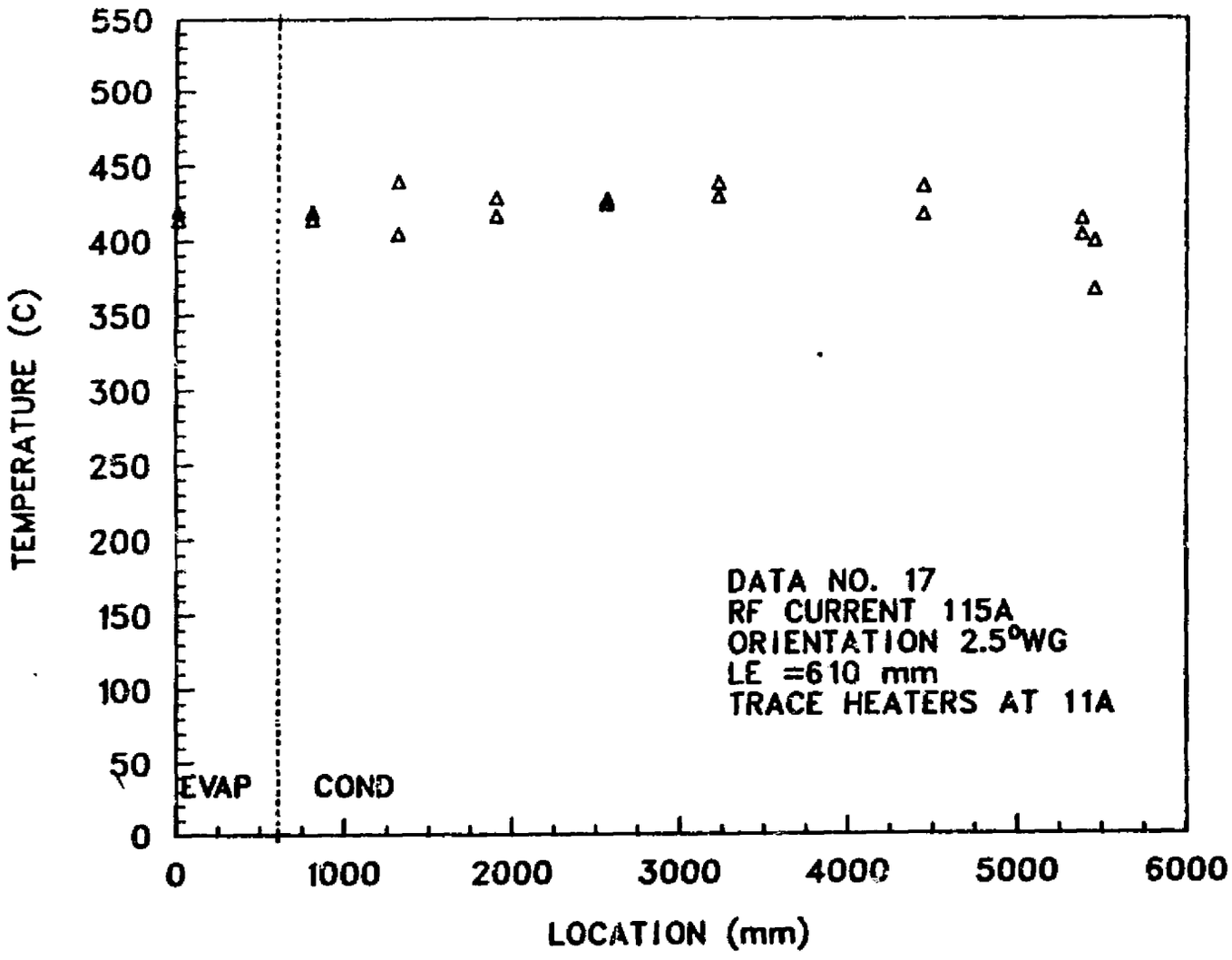

Fig. 2. Temperature profile at highest wet-in temperature condition.

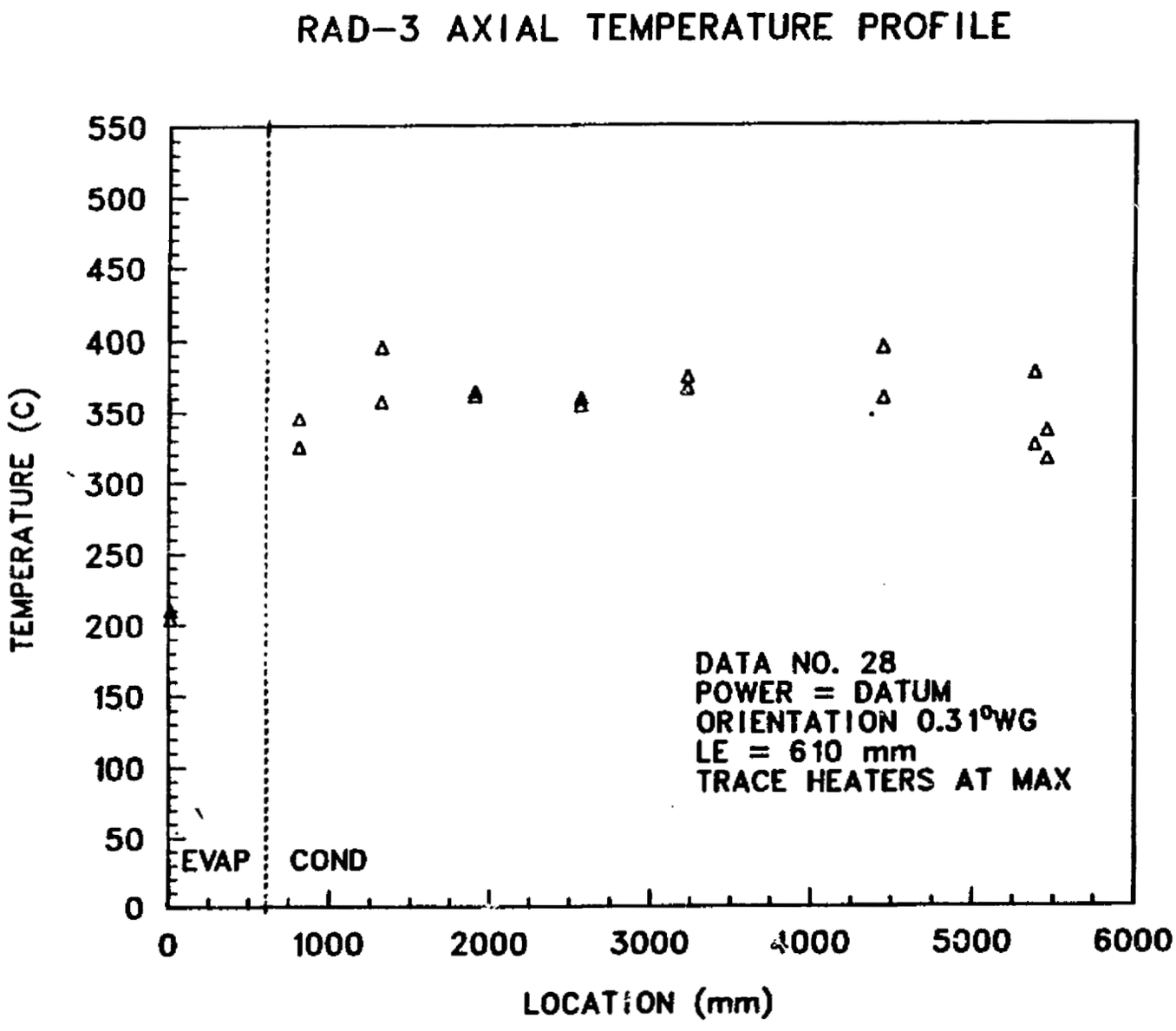

Fig. 3. Datum temperature profile for trace heaters at maximum.

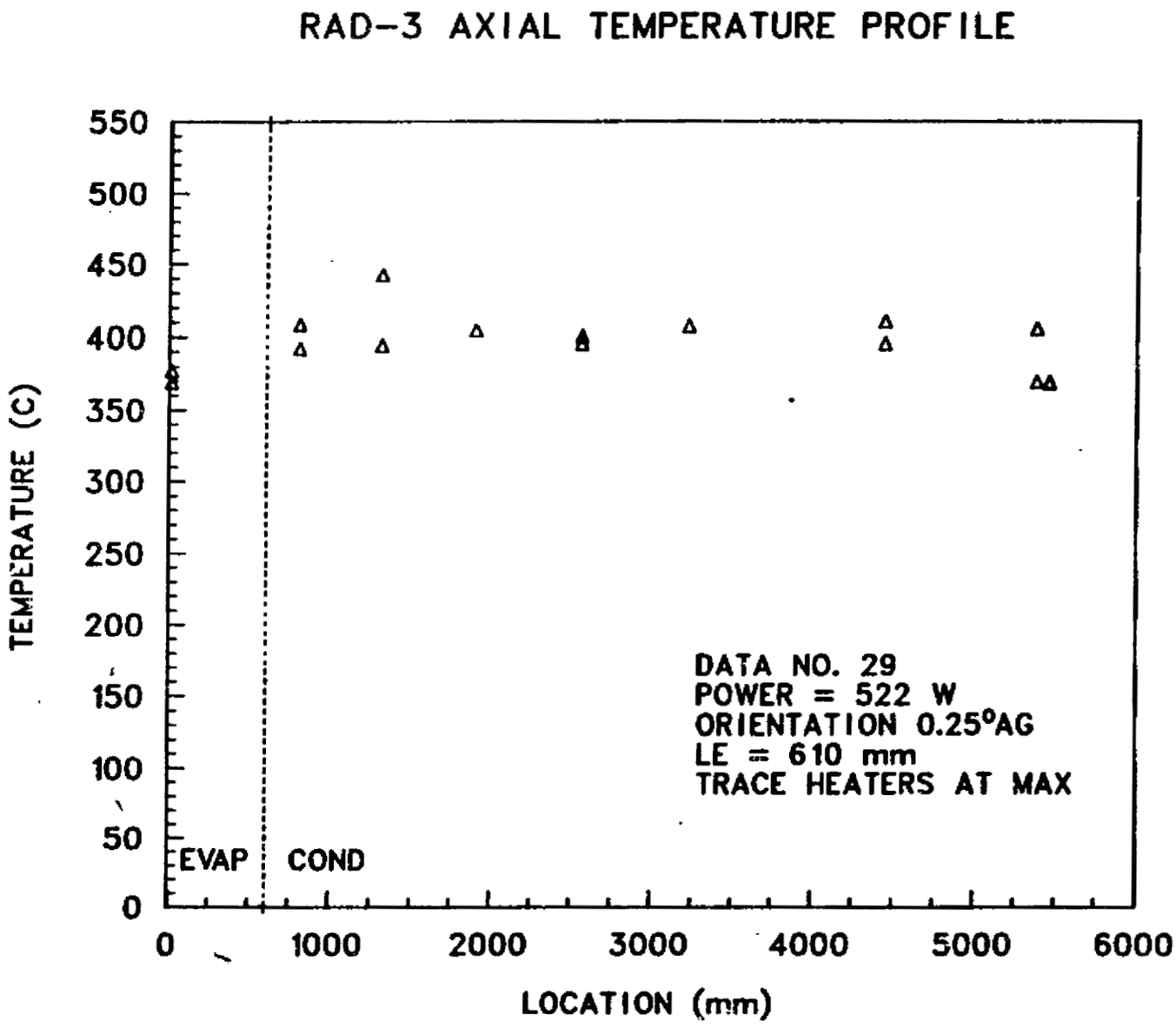

Fig. 4. Temperature profile for data record number 29.

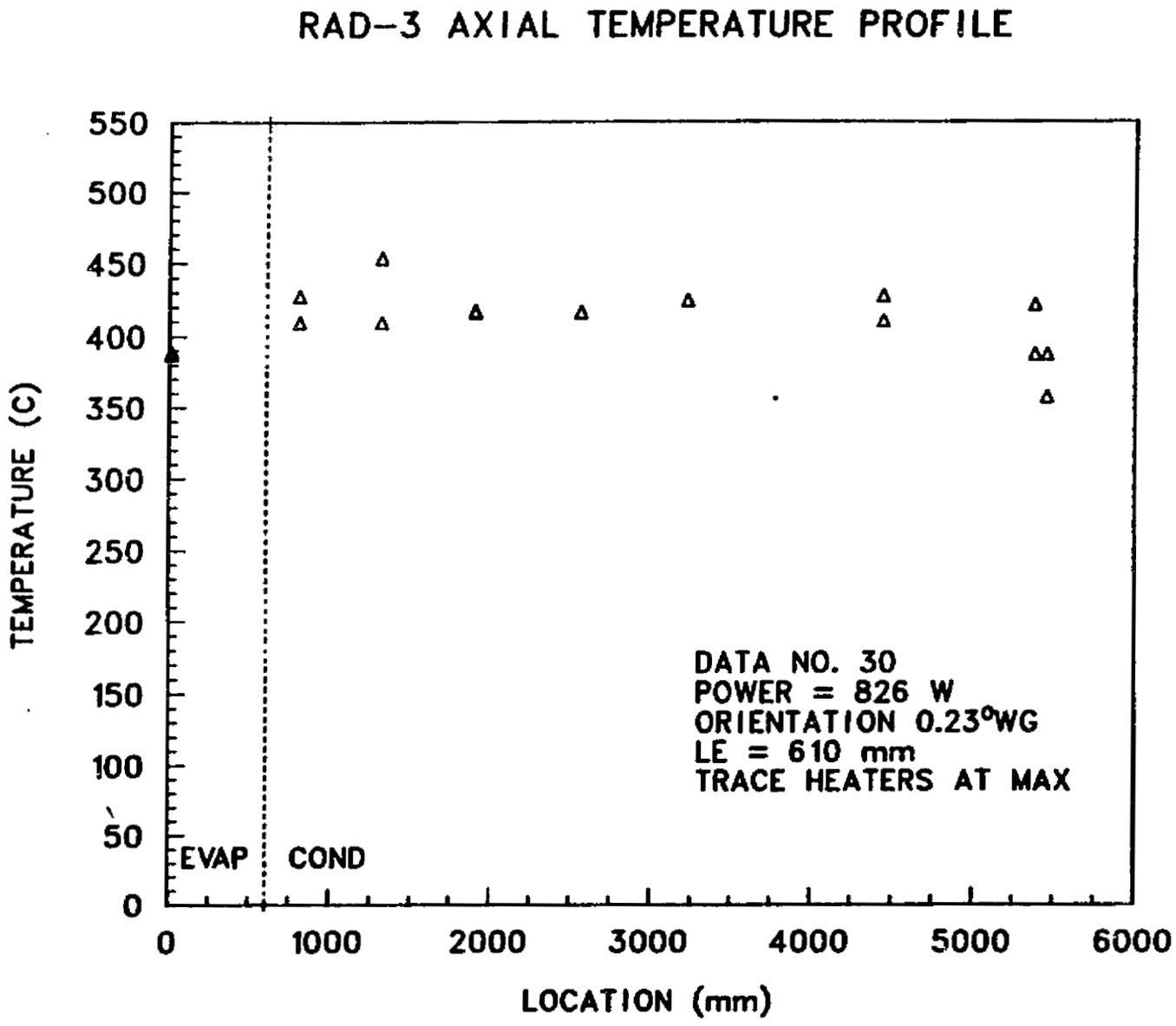

Fig. 5. Temperature profile for data record number 30.

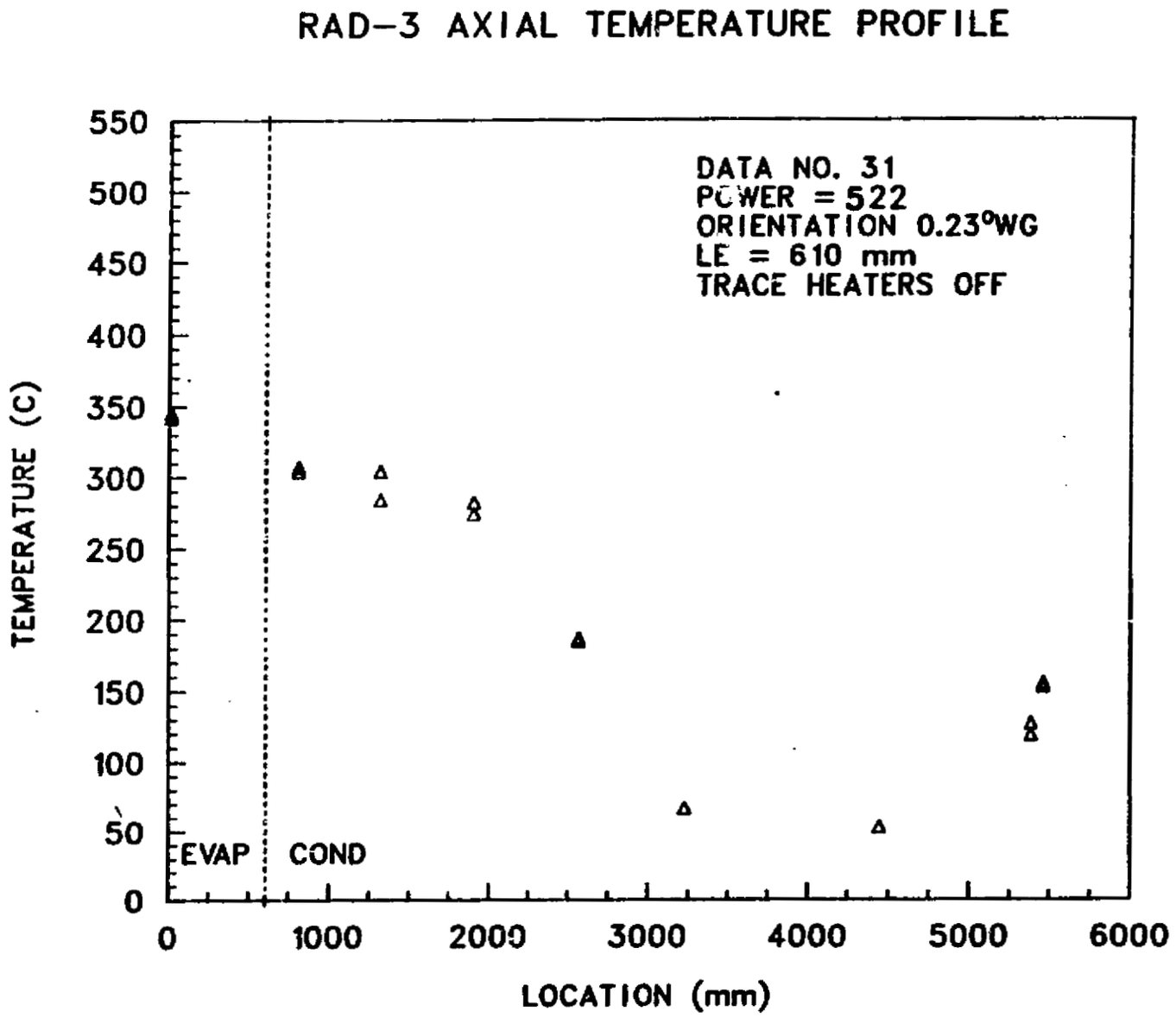

Fig. 6. Temperature profile for data record number 31.

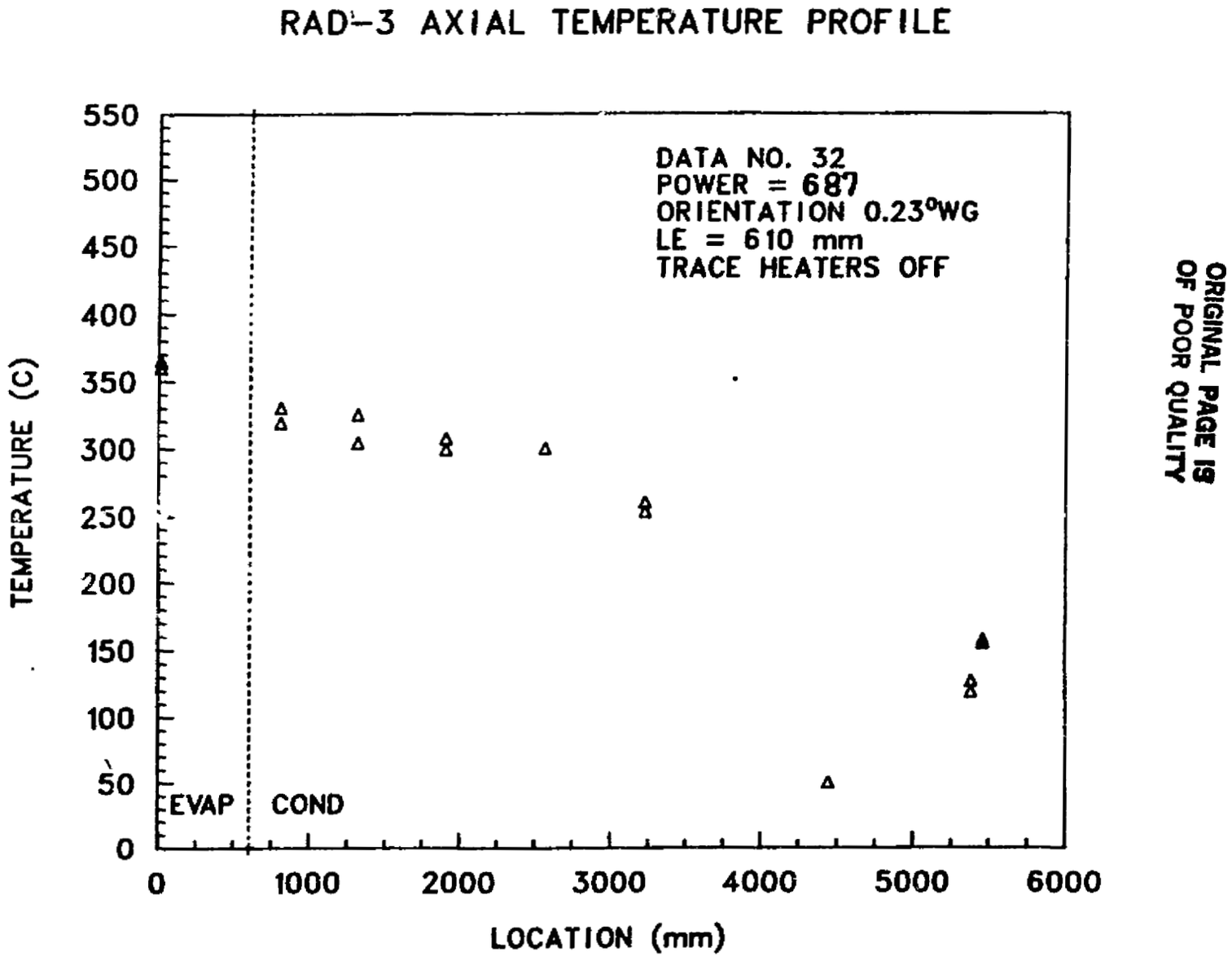

Fig. 7. Temperature profile for data record number 32.

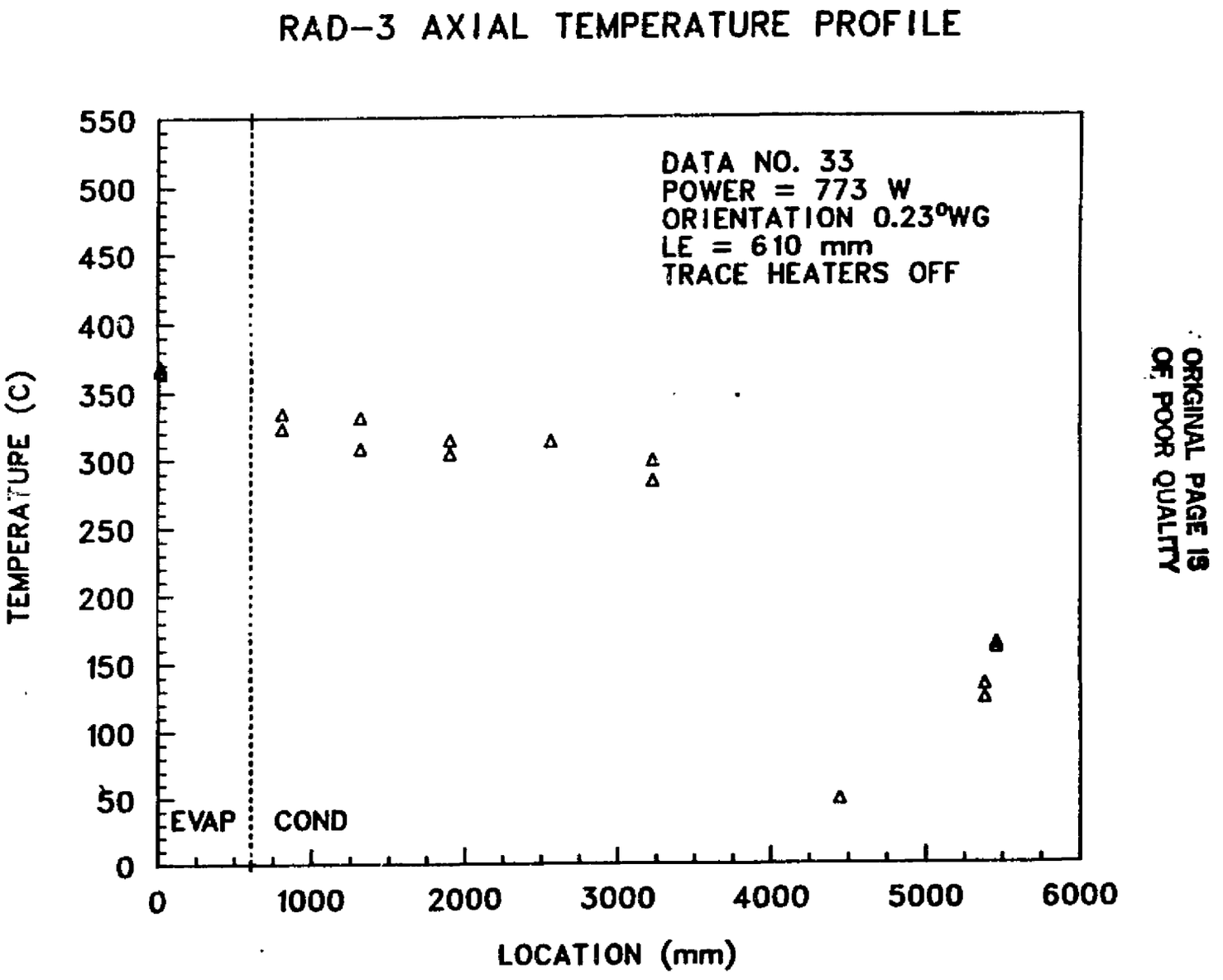

Fig. 8. Temperature profile for data record number 33.

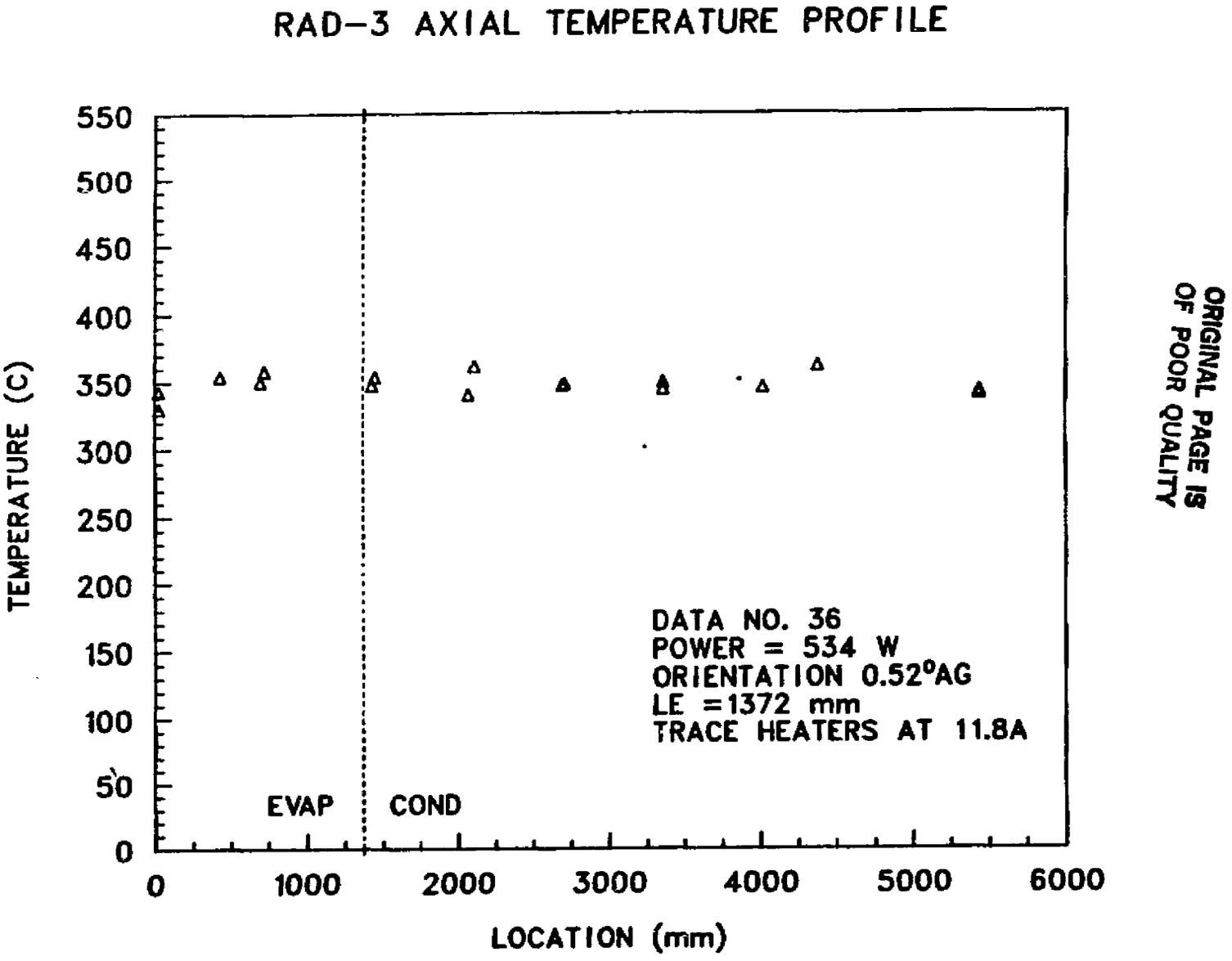

Fig. 9. Temperature profile for data record number 36.

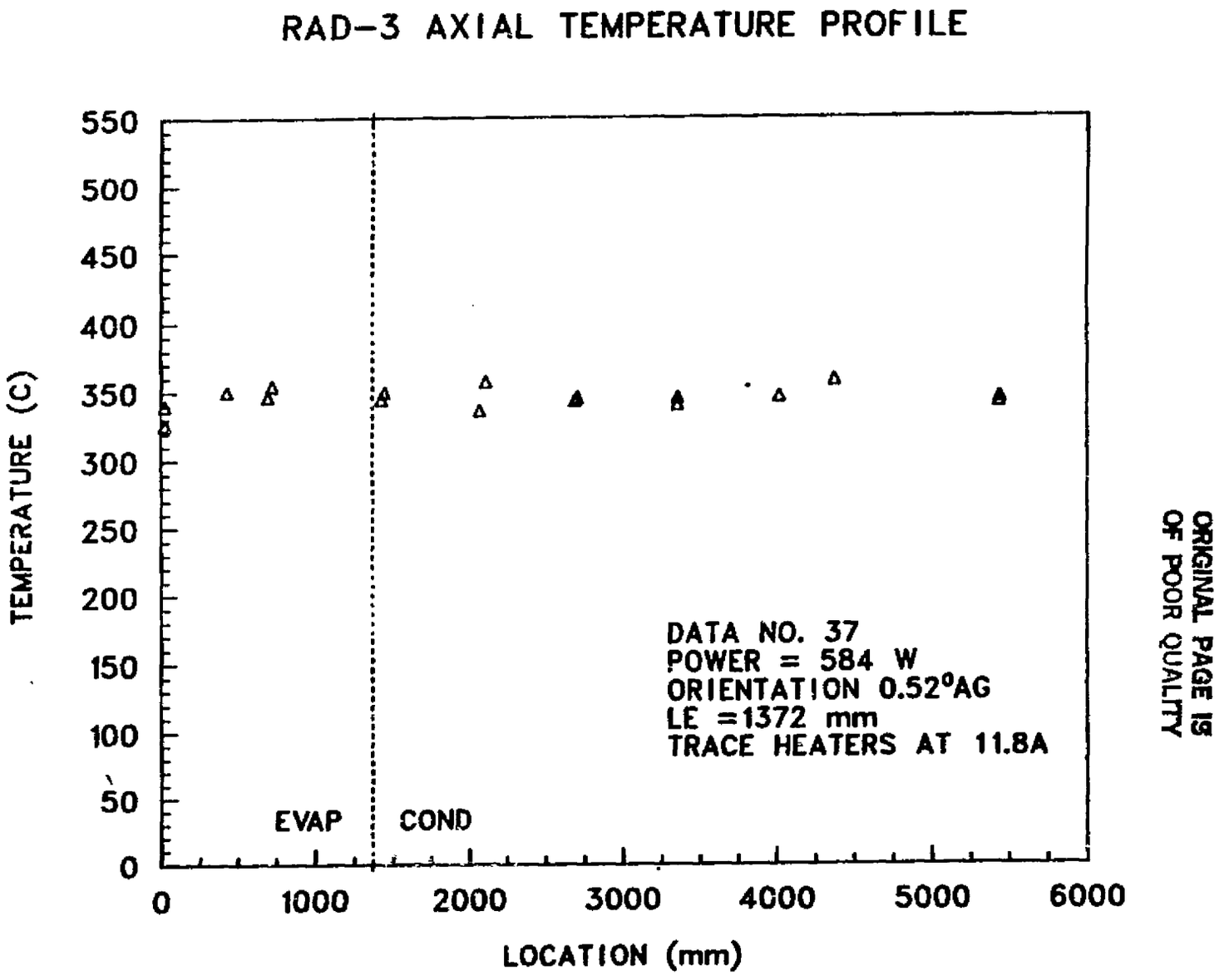

Fig. 10. Temperature profile for data record number 37.

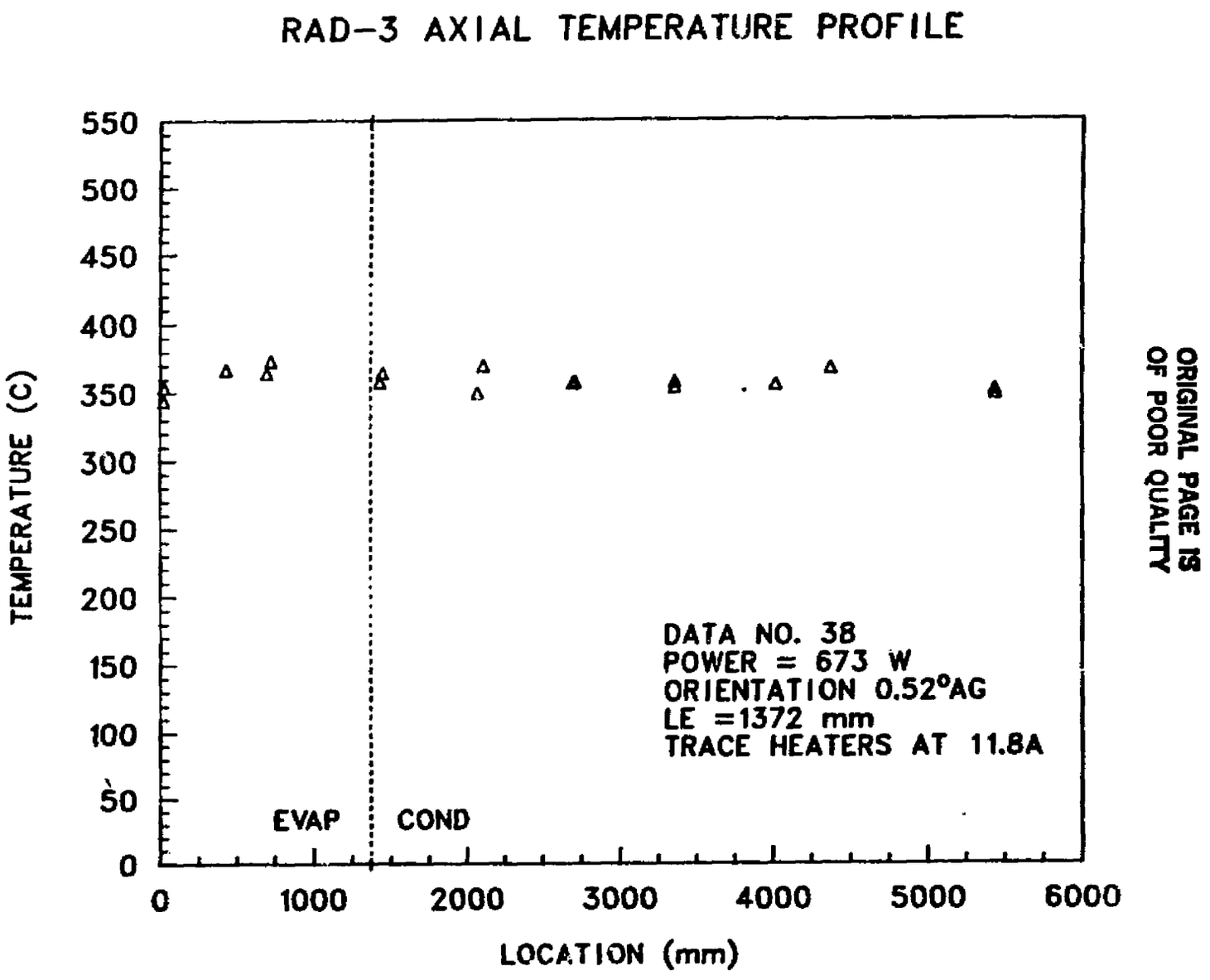

Fig. 11. Temperature profile for data record number 38.

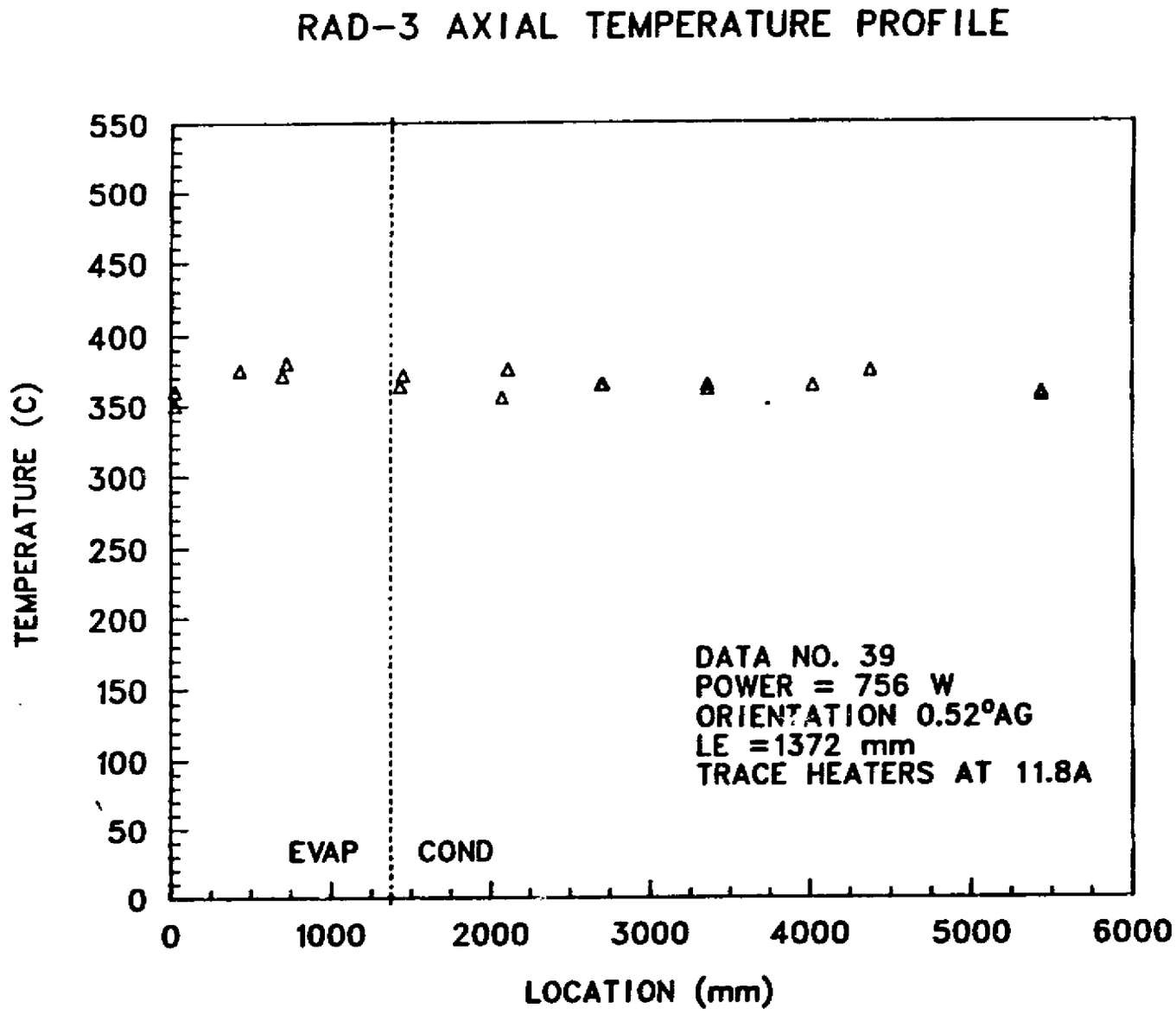

Fig. 12. Temperature profile for data record number 39.

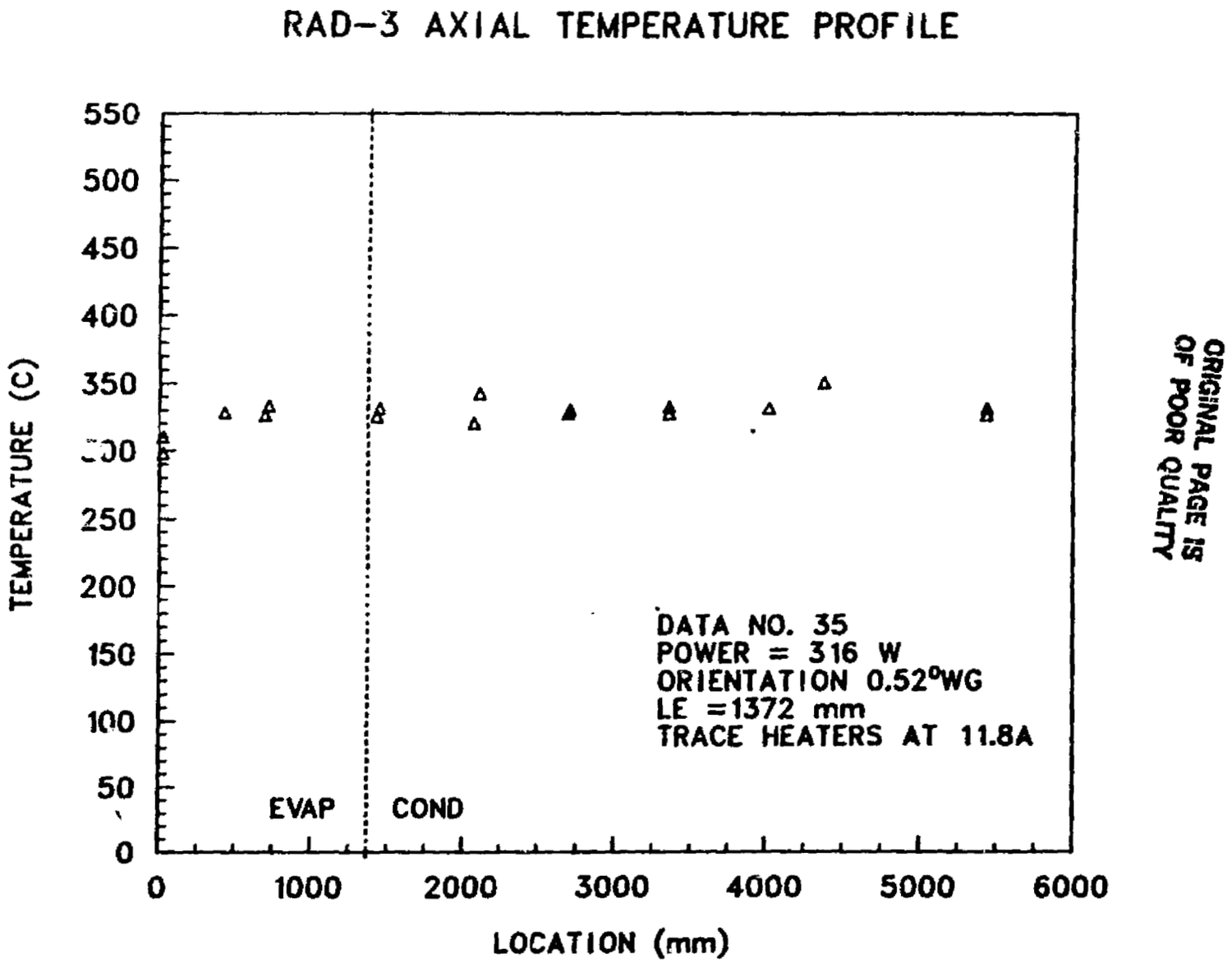

Fig. 13. Temperature profile for data record number 35.

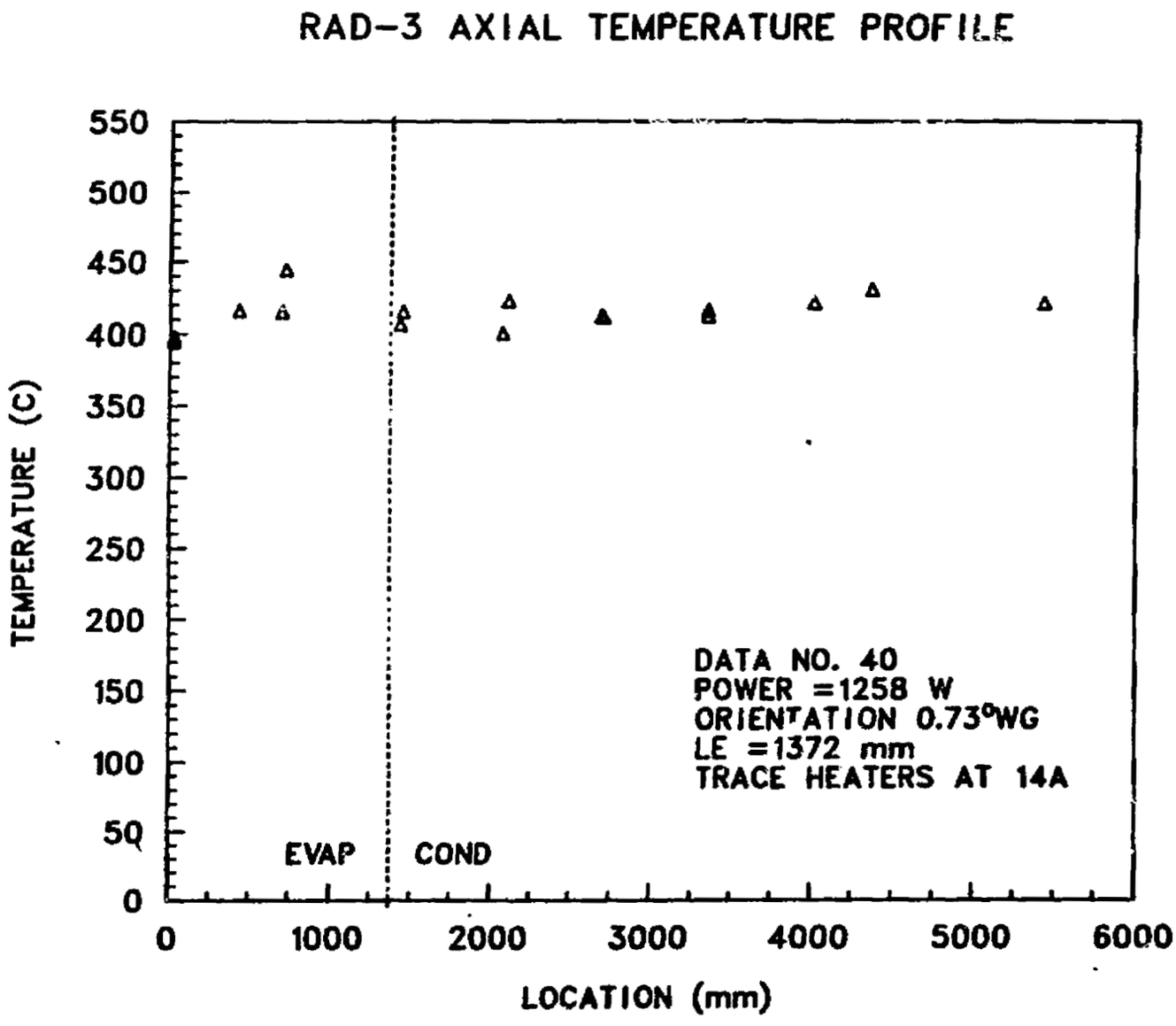

Fig. 14. Temperature profile for data record number 40.

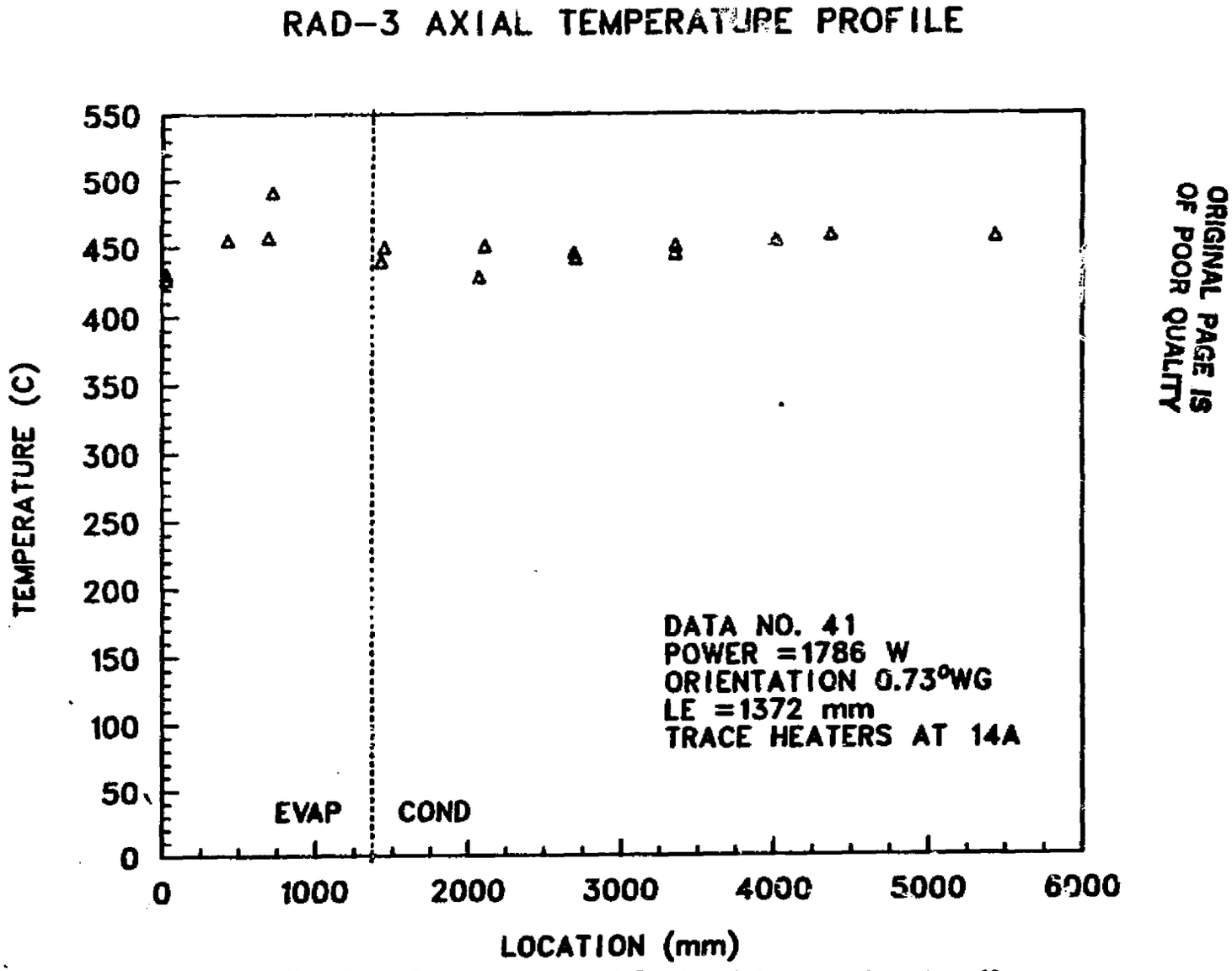

Fig. 15. Temperature profile for data record number 41.

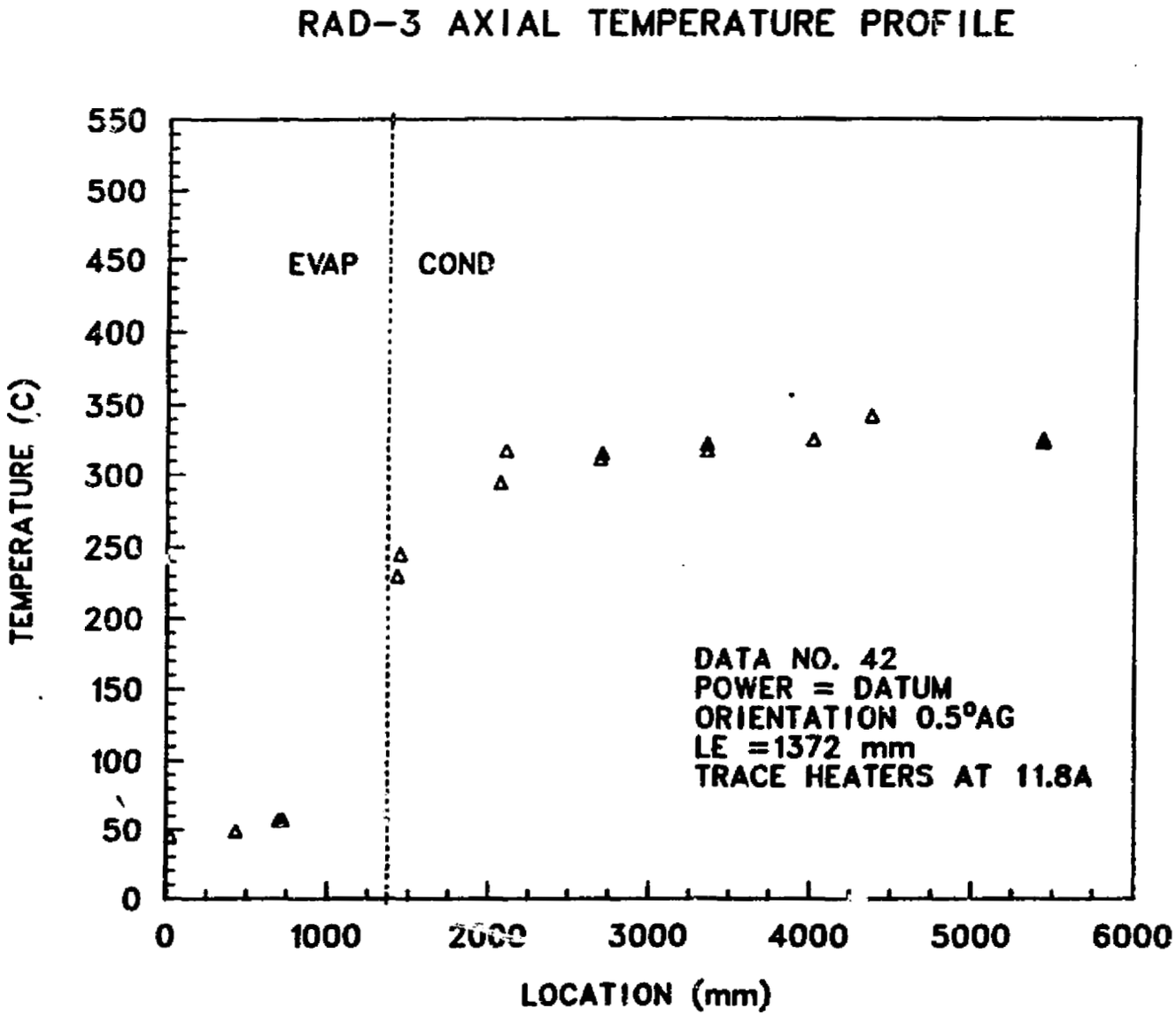

Fig. 16. Datum: temperature profile for trace heaters at 11.8 A.

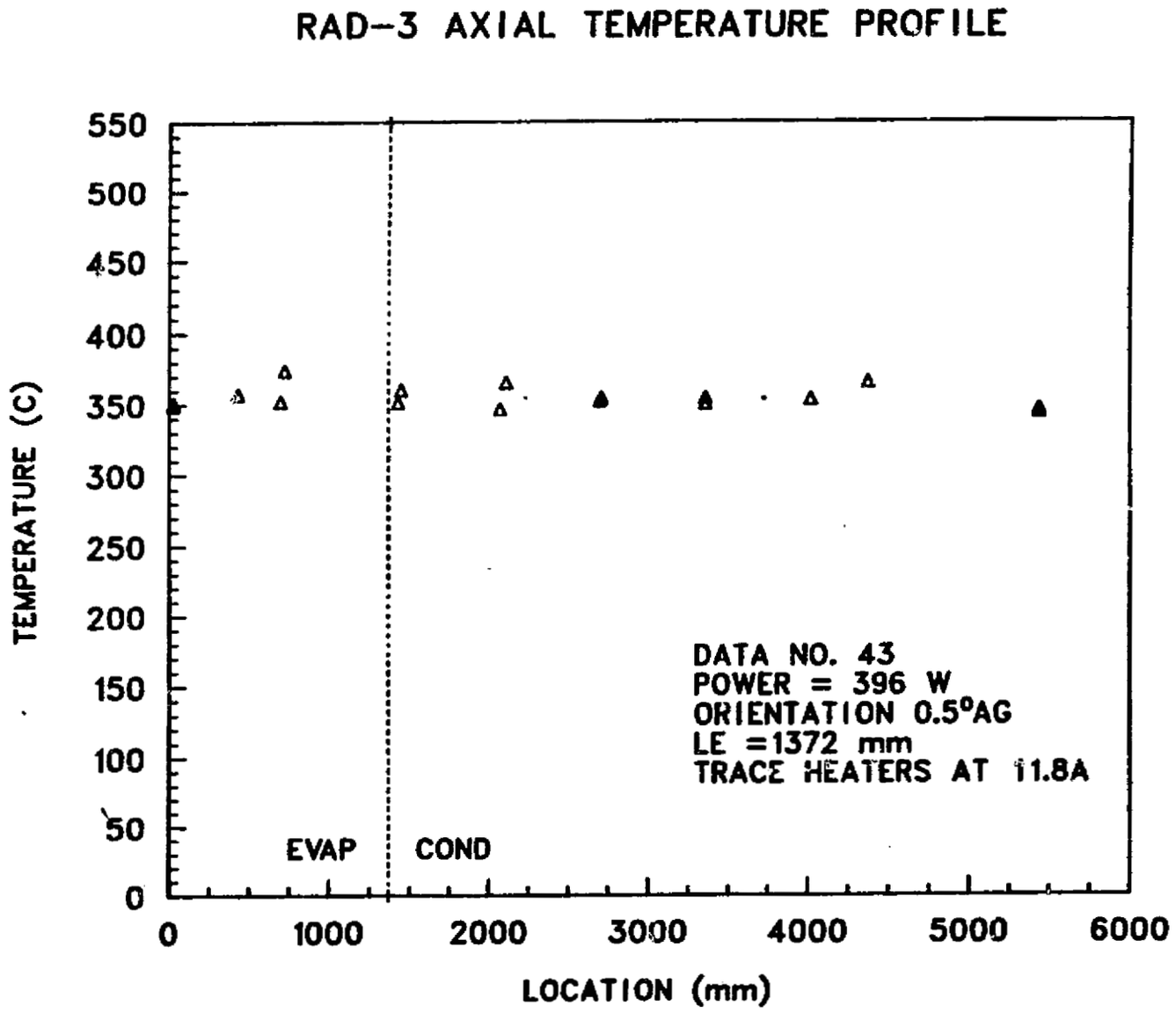

Fig. 17. Temperature profile for data record number 43.

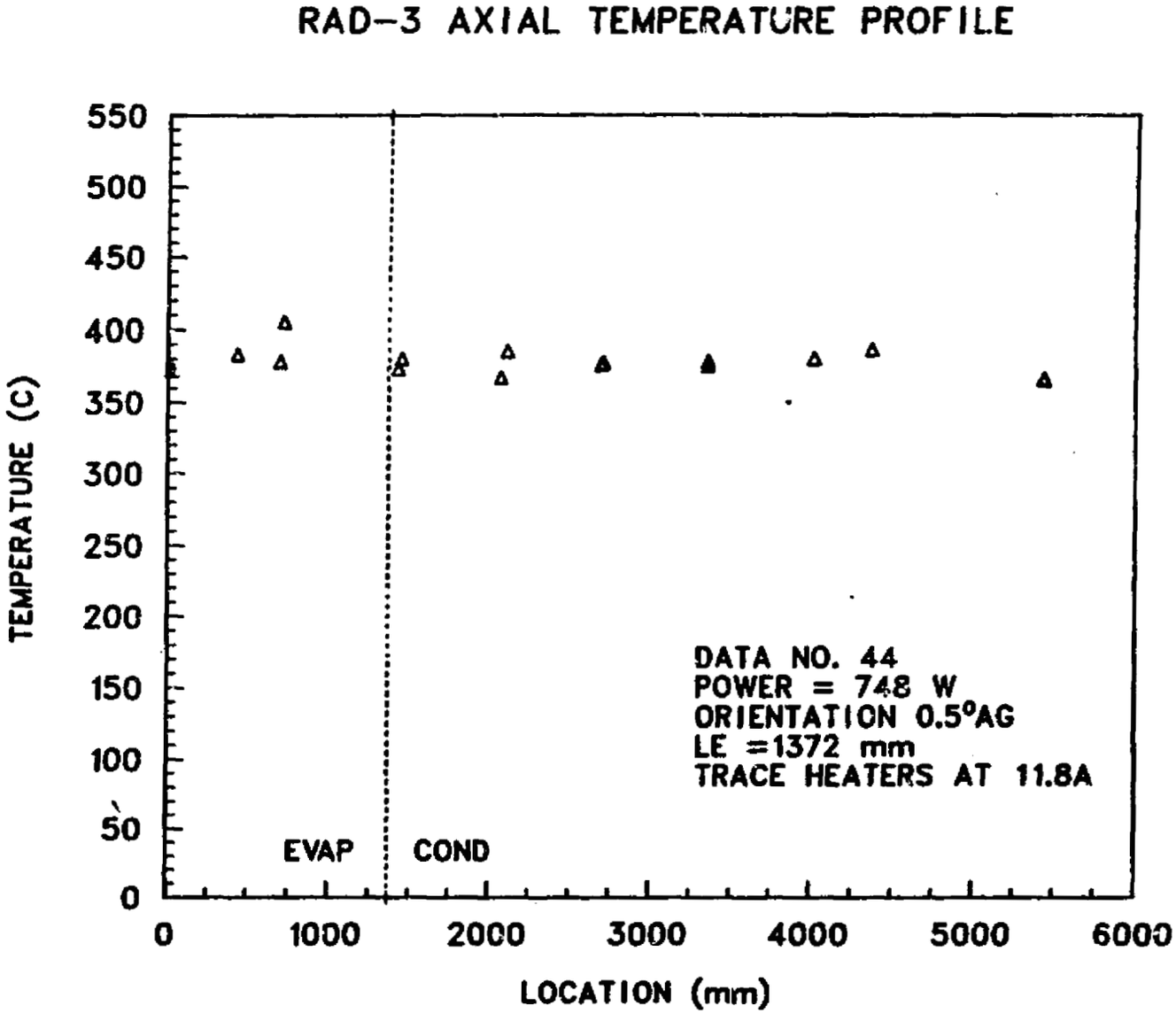

Fig. 18. Temperature profile for data record number 44.

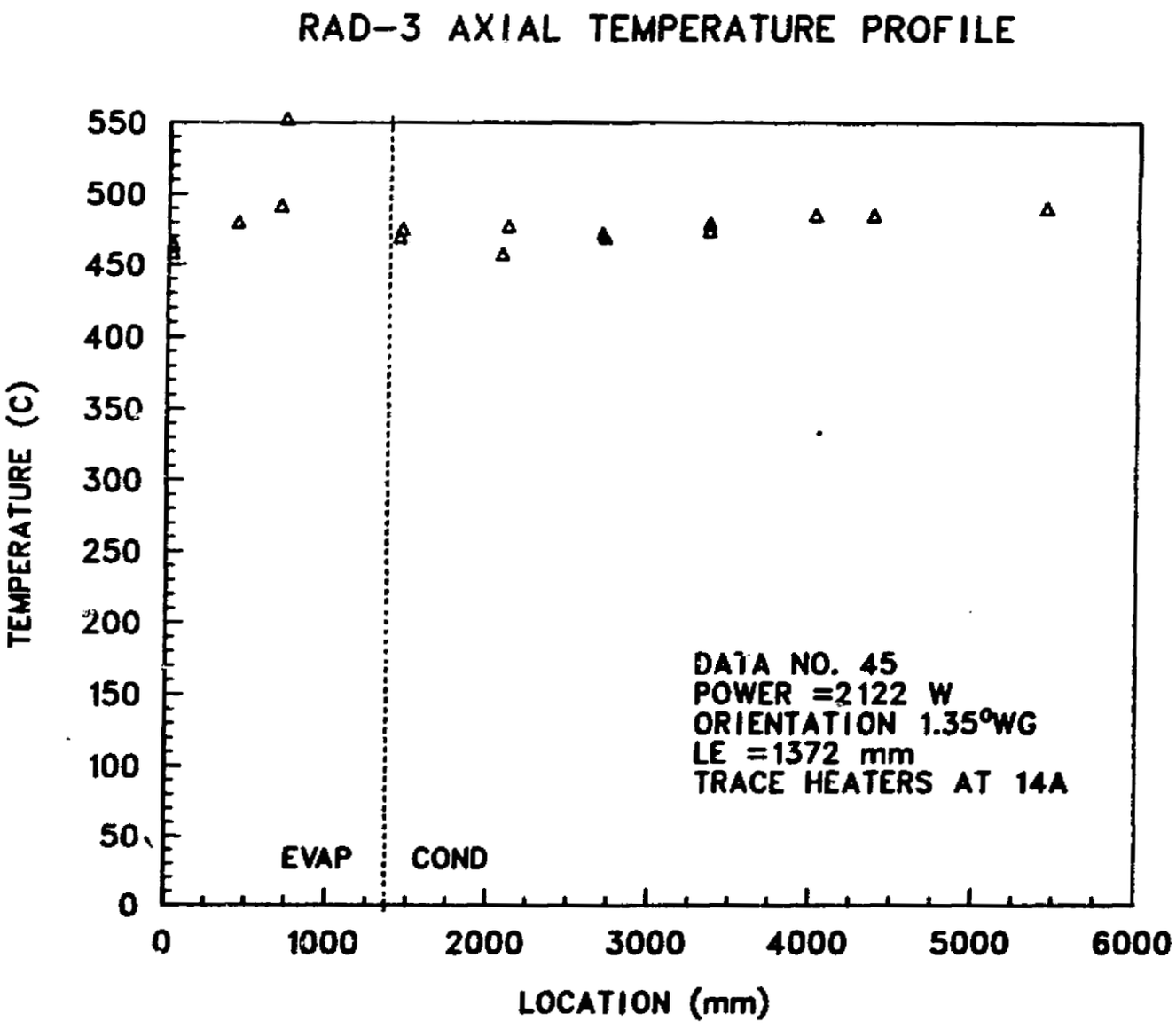

Fig. 19. Temperature profile for data record number 45.

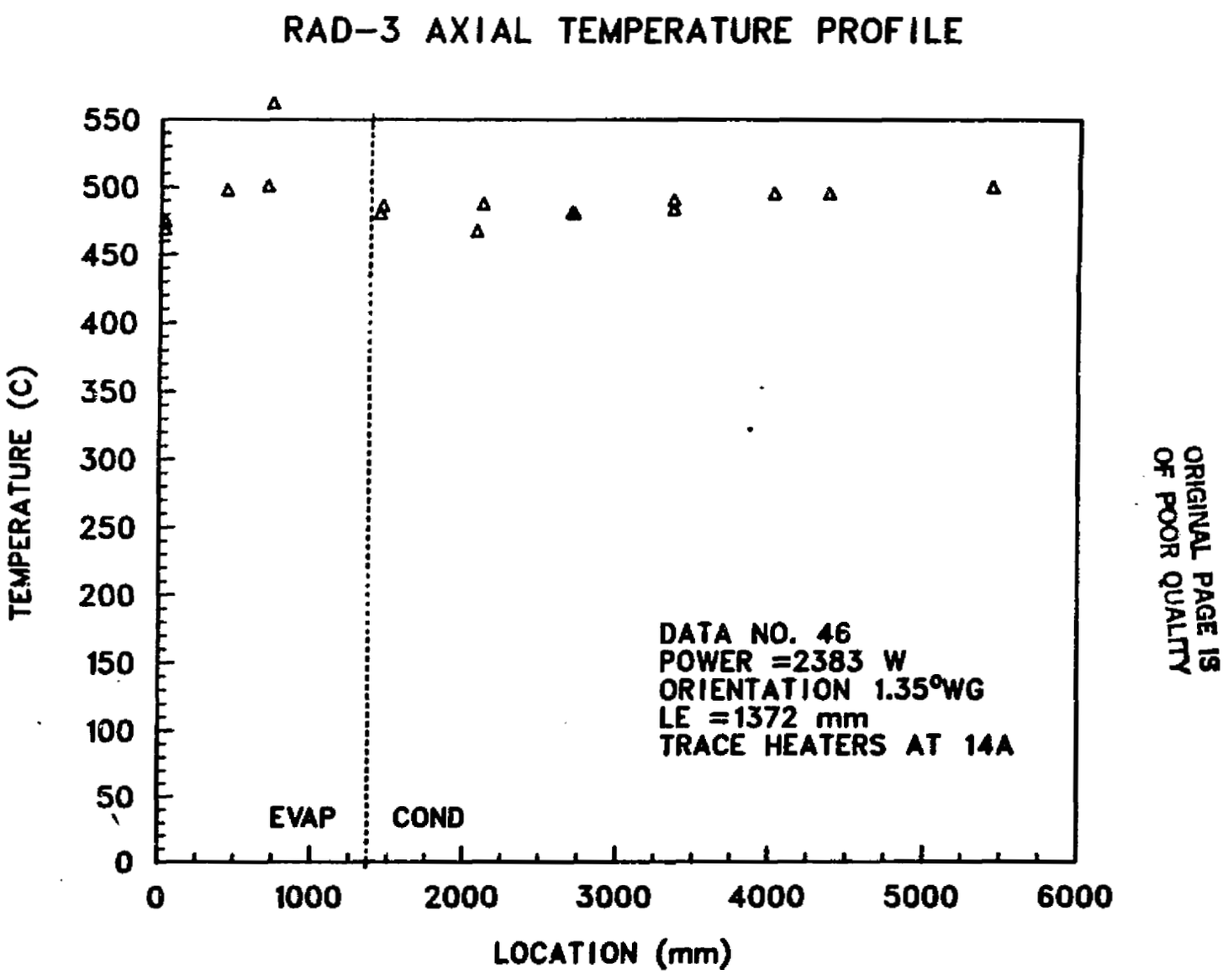

Fig. 20. Temperature profile for data record number 46.

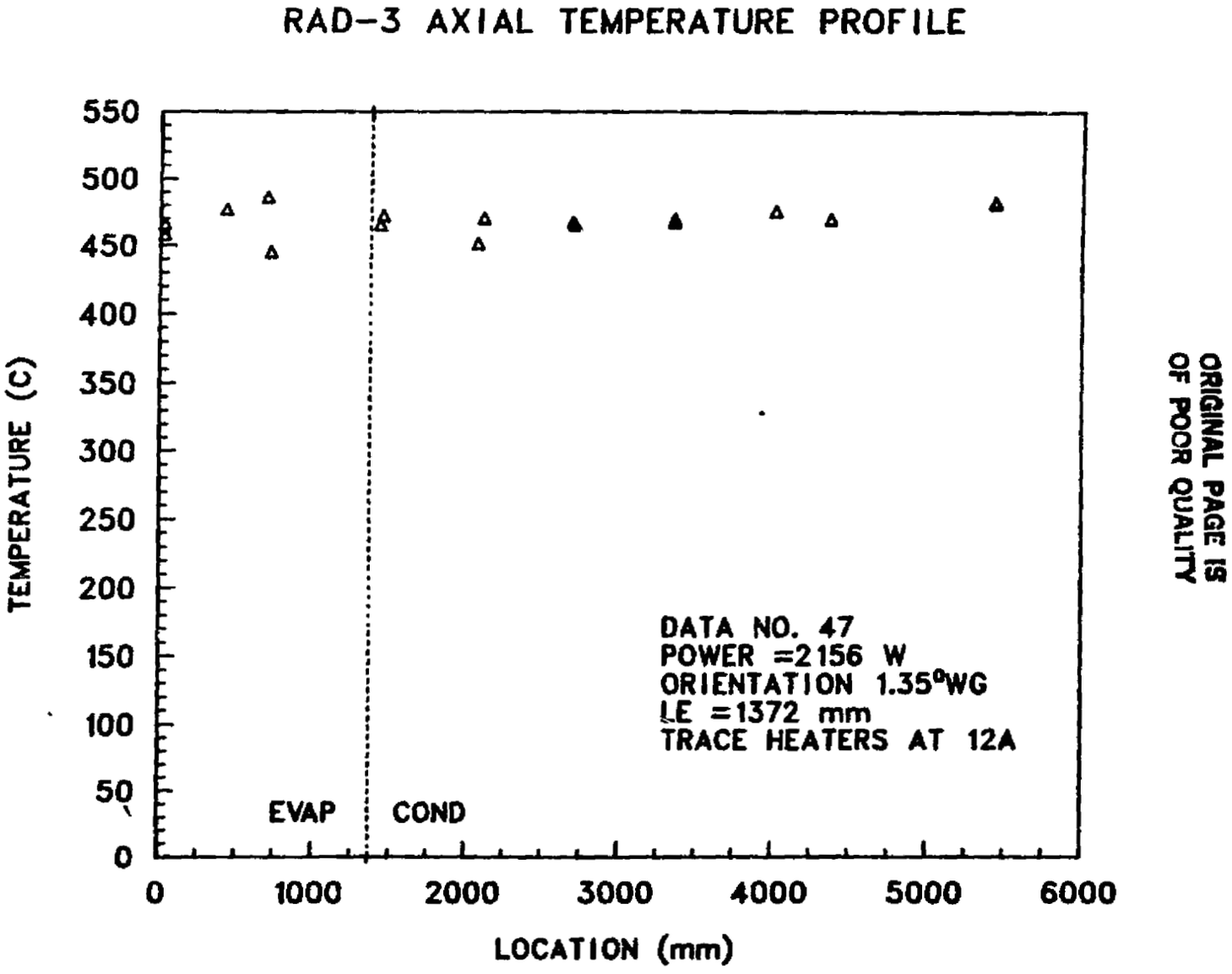

Fig. 21. Temperature profile for data record number 47.

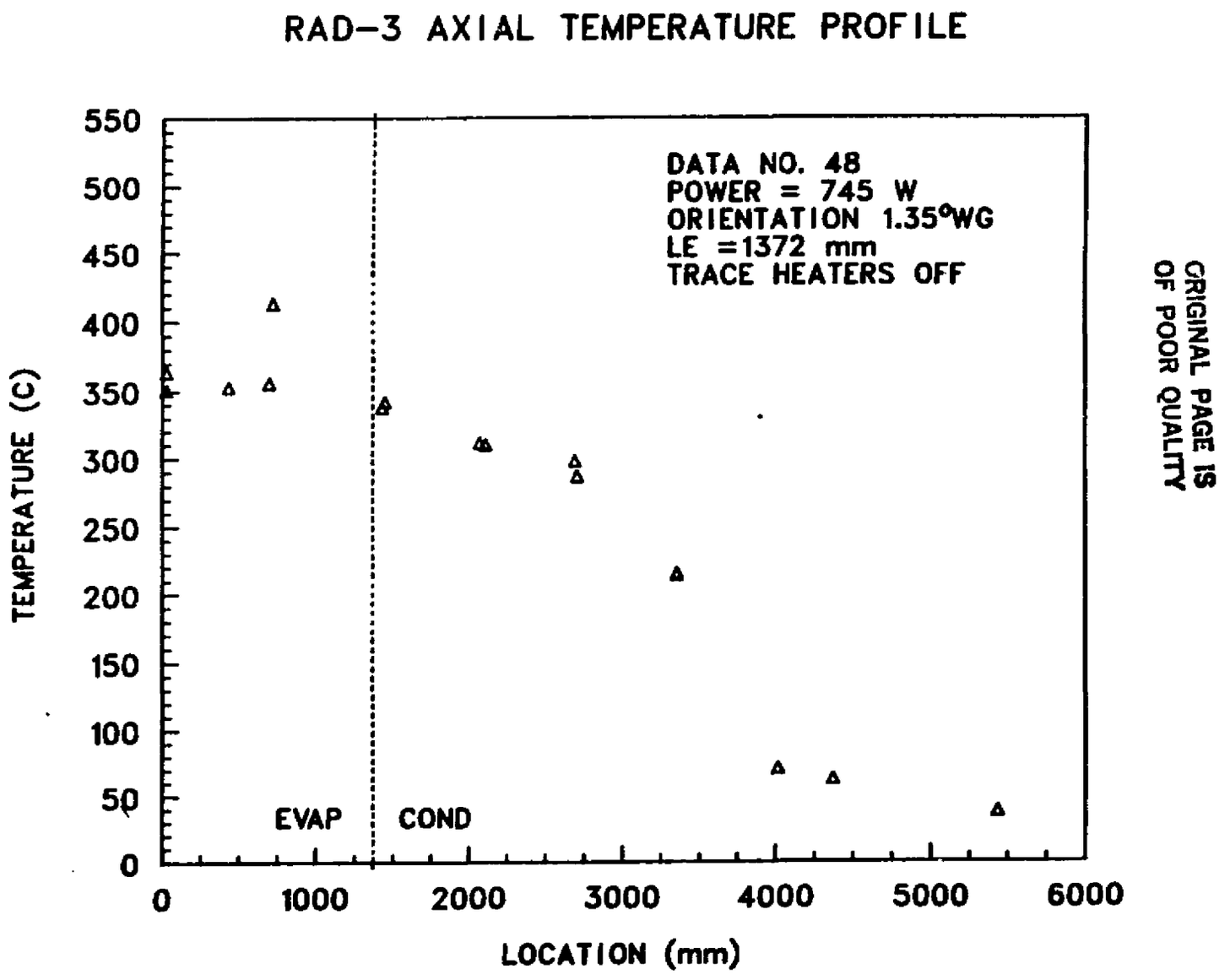

Fig. 22. Temperature profile for data record number 48.

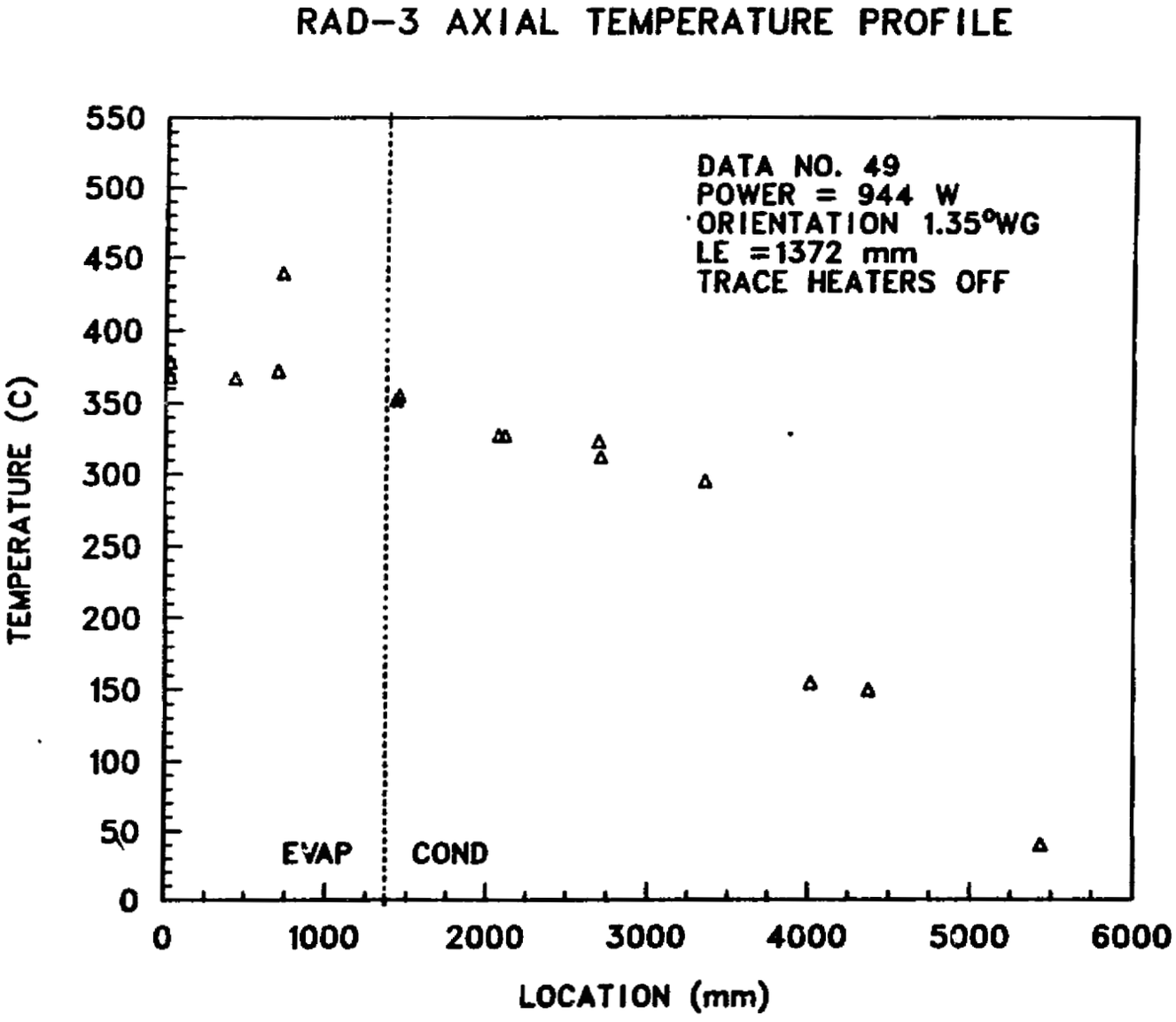

Fig. 23. Temperature profile for data record number 49.

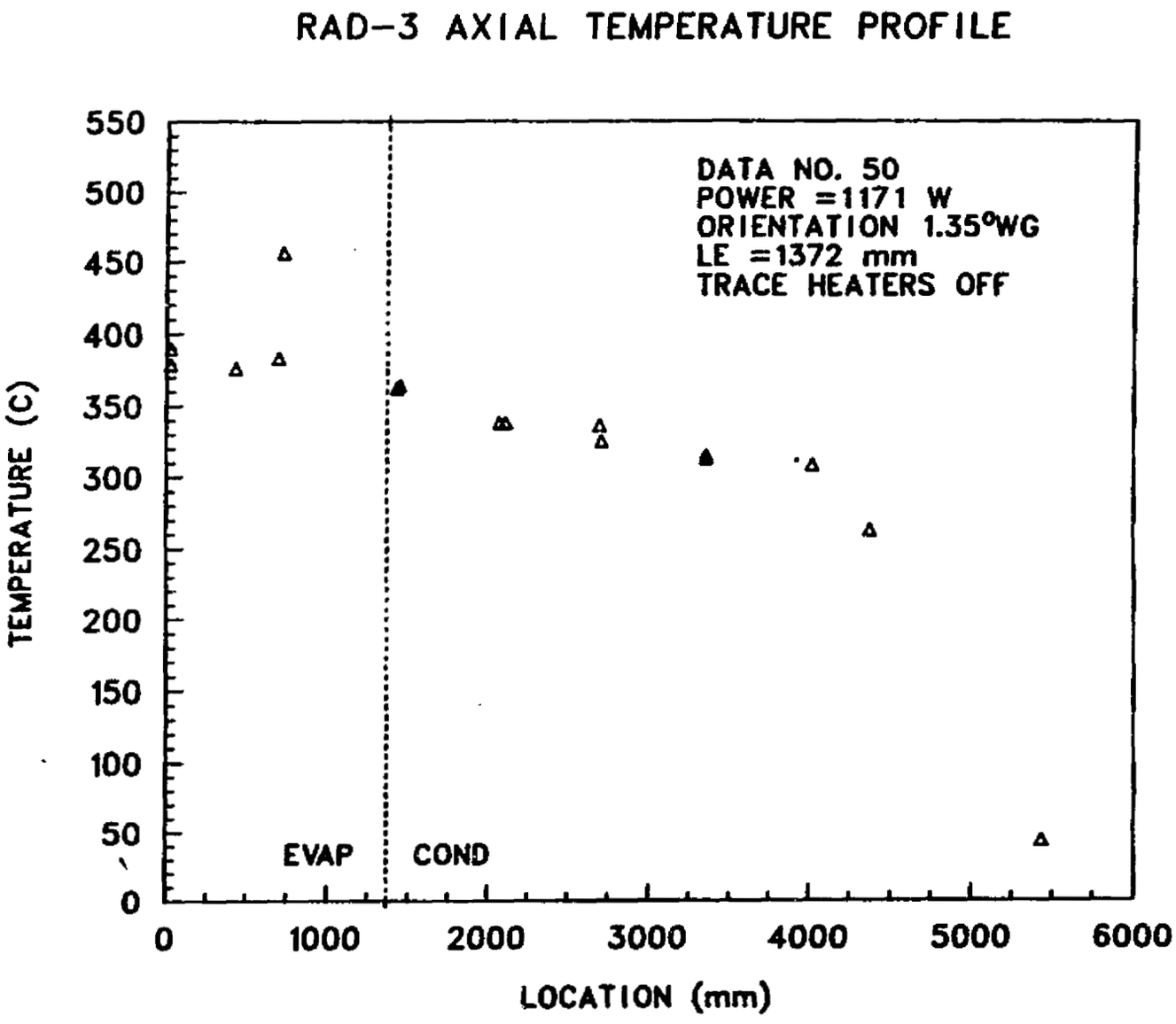

Fig. 24. Temperature profile for data record number 50.

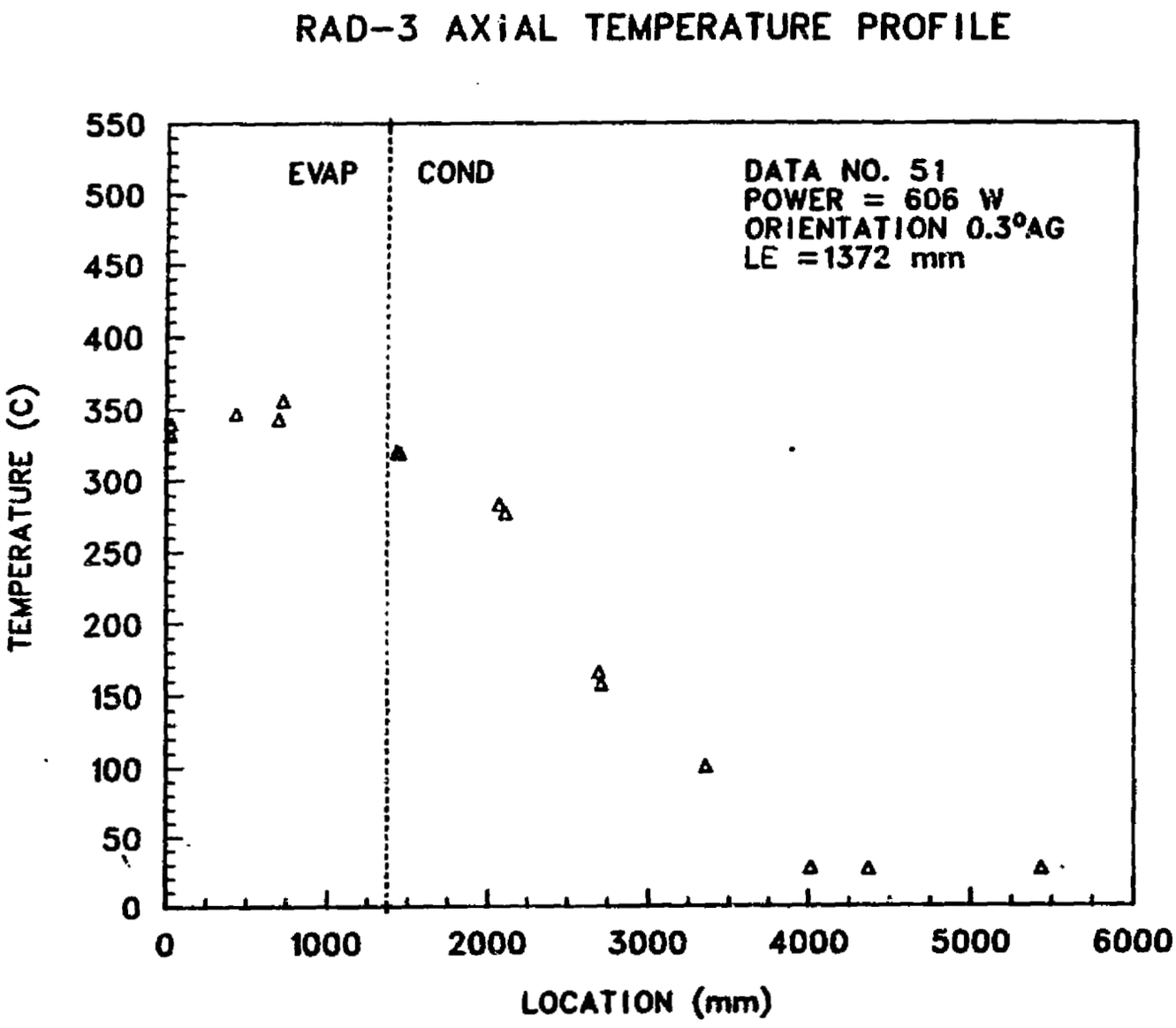

Fig. 25. Start-up temperature profile for data record 51.

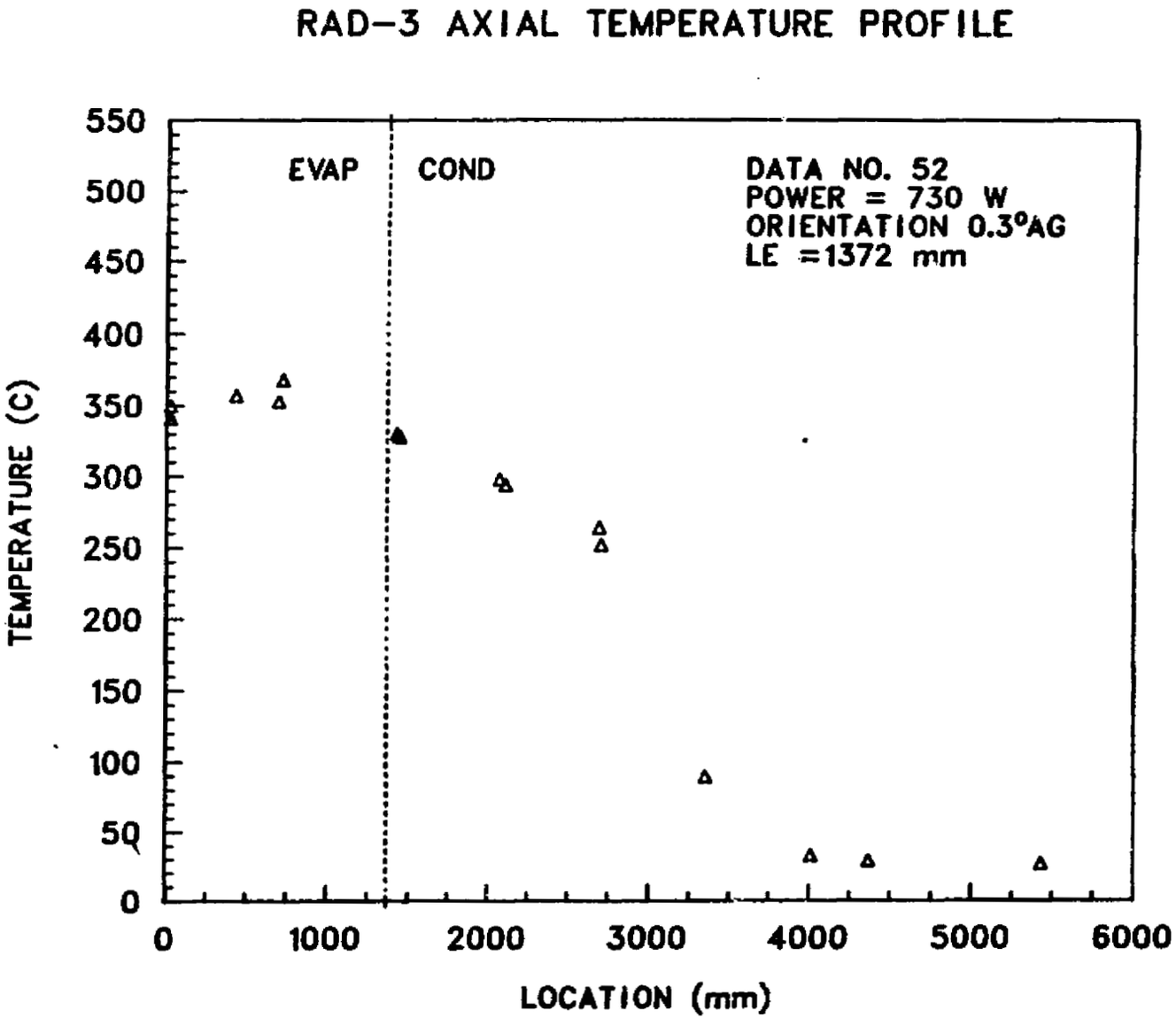

Fig. 26. Start-up temperature profile for data record number 52.

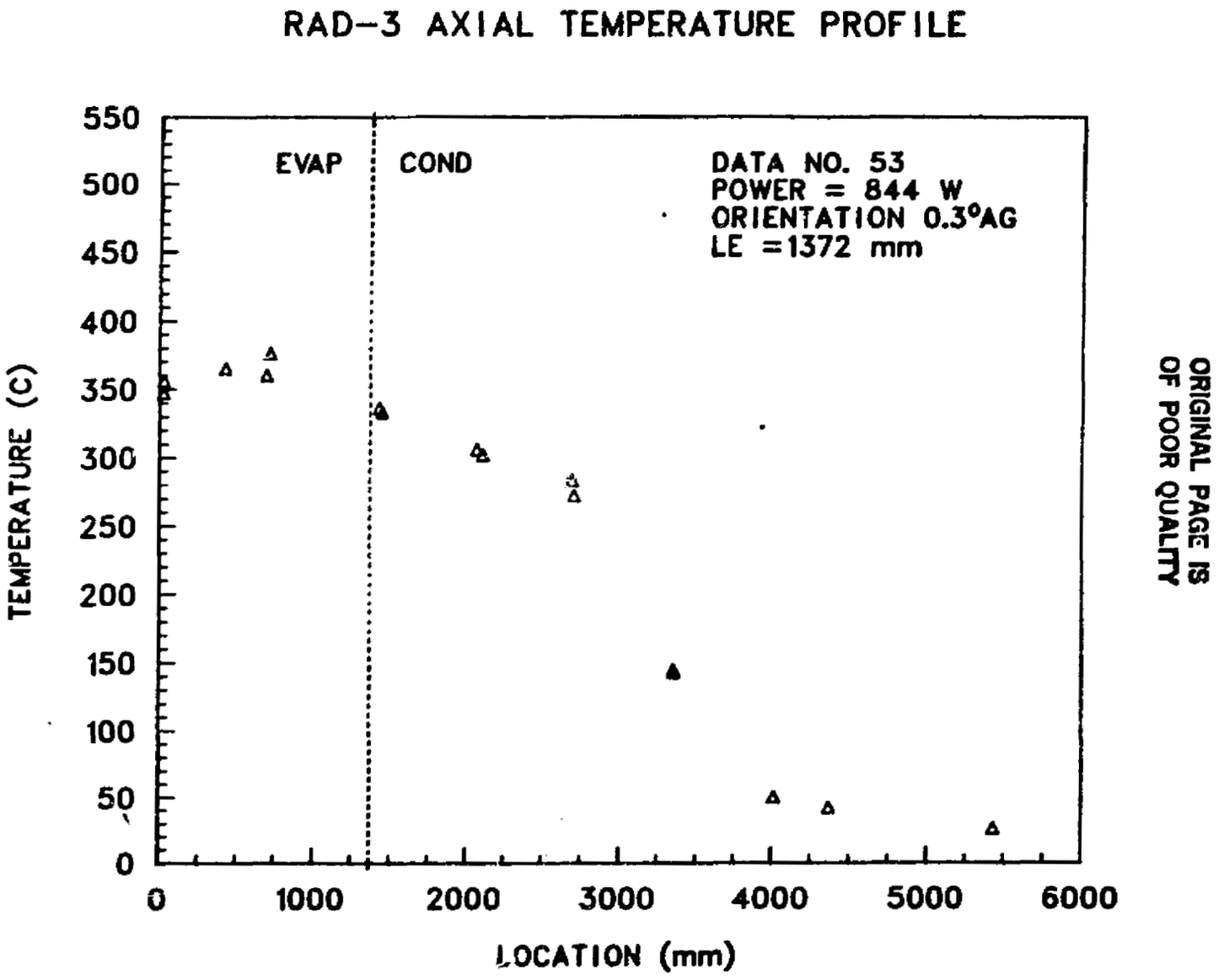

Fig. 27. Start-up temperature profile for data record 53.

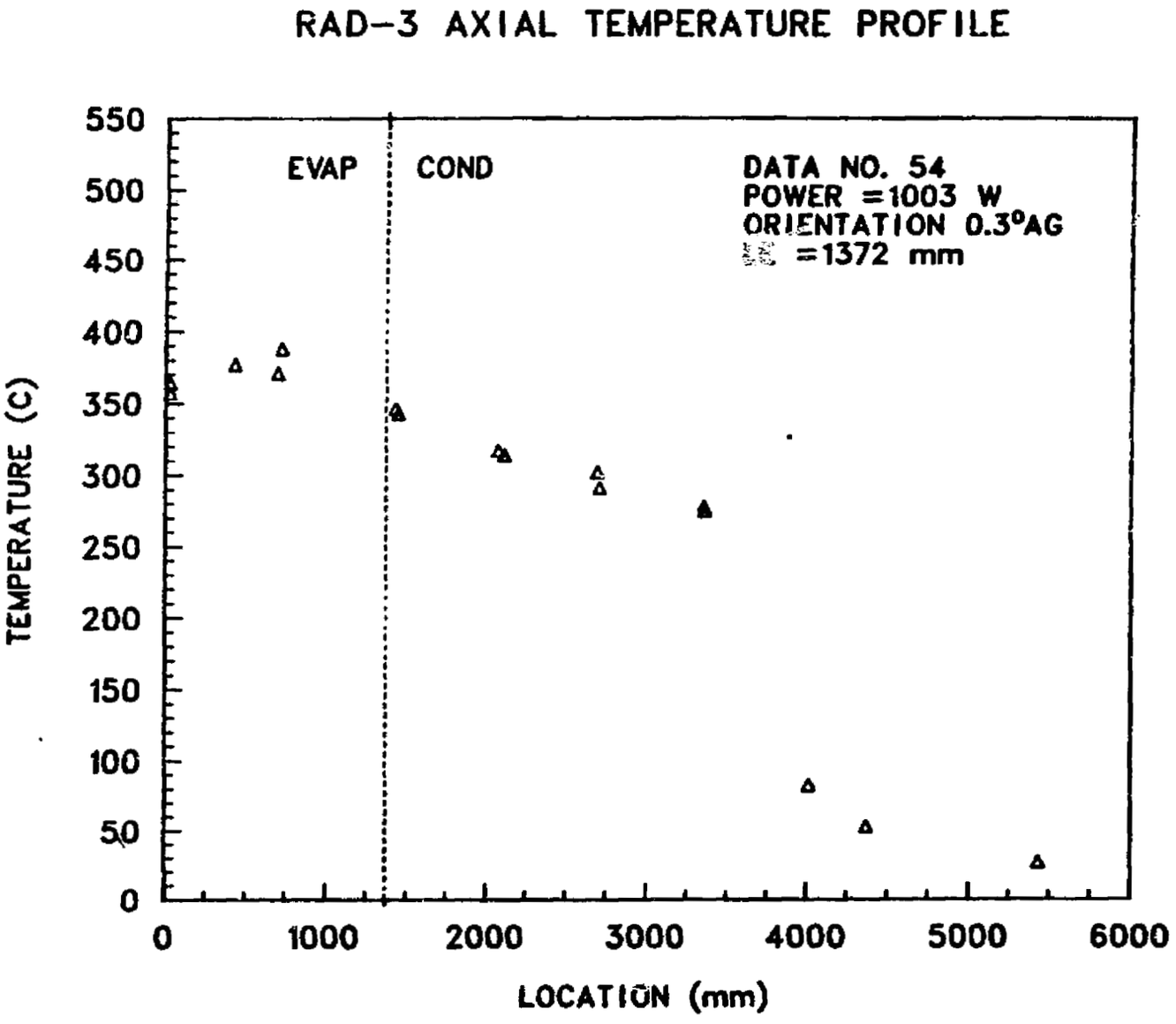

Fig. 28. Start-up temperature profile for data record 54.

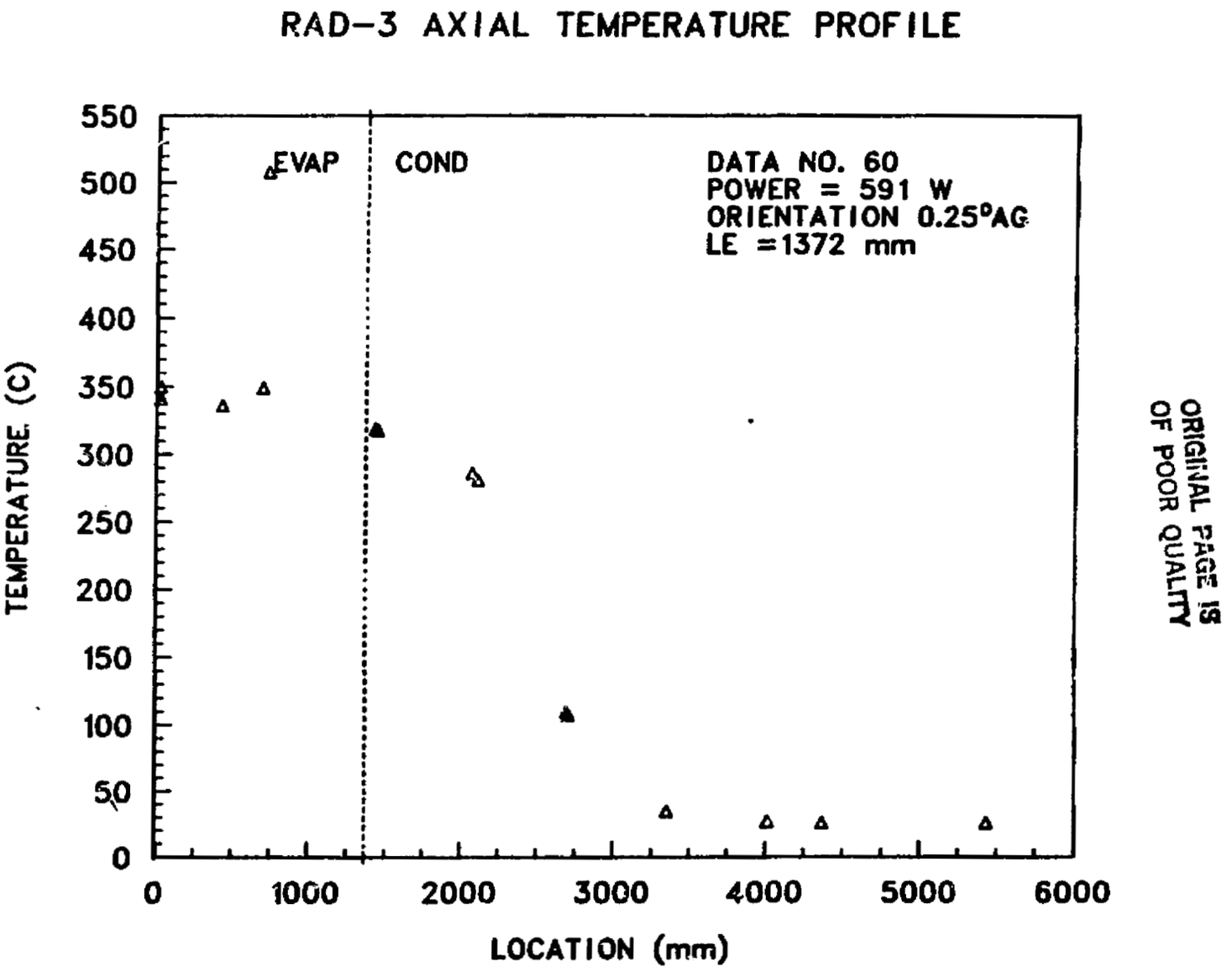

Fig. 29. Start-up temperature profile for data record 60.

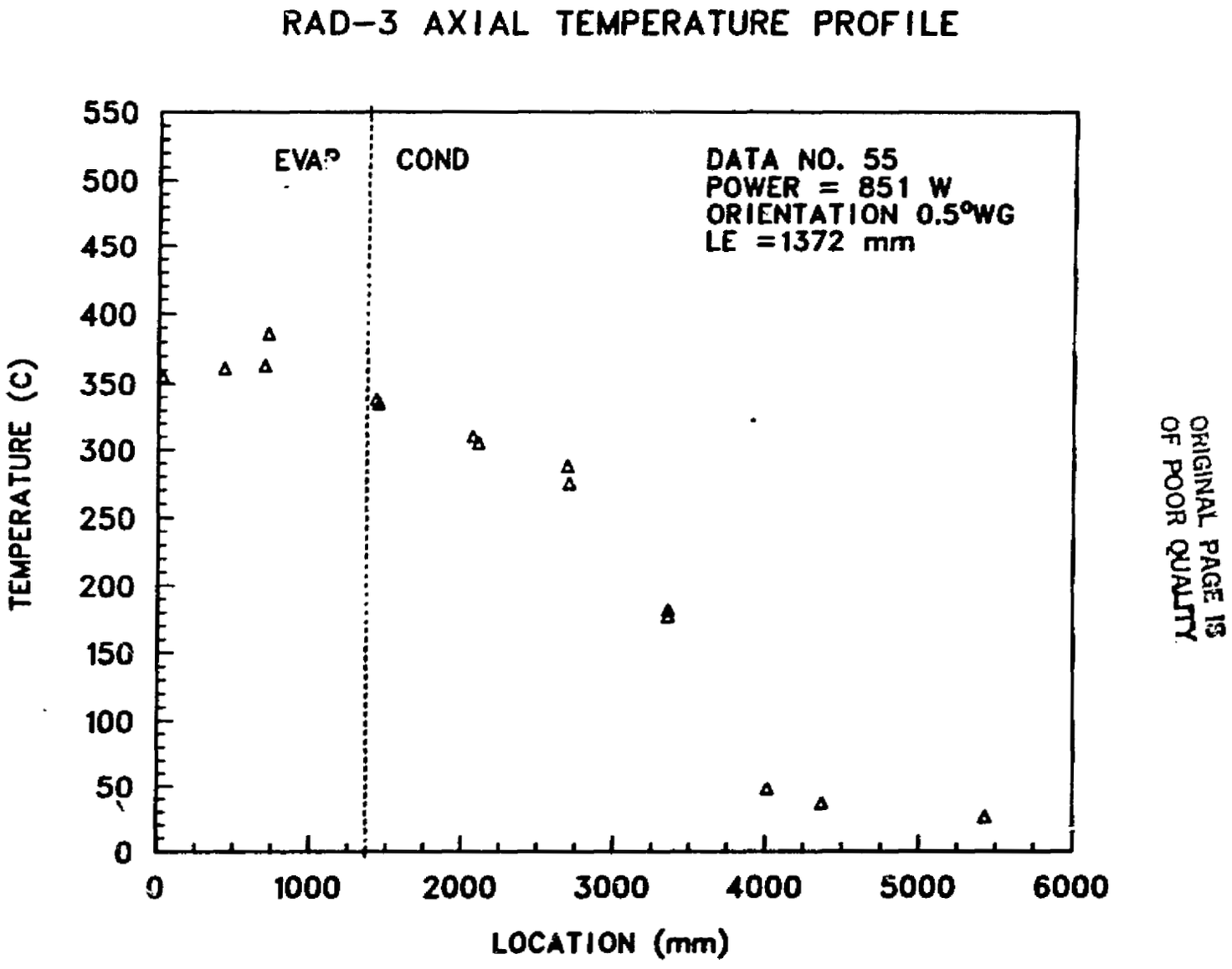

Fig. 30. Start-up temperature profile for data record 55.

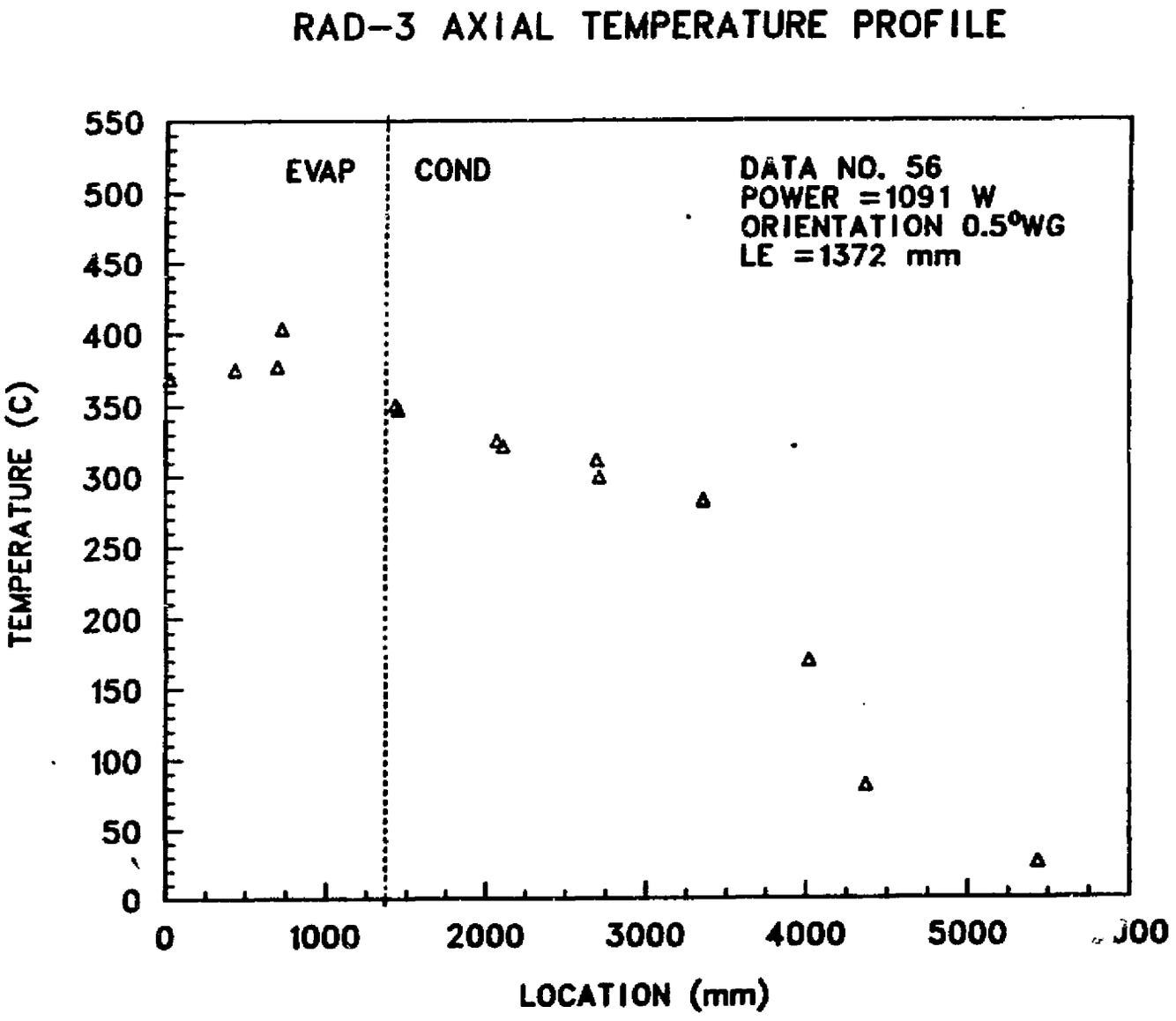

Fig. 31. Startup temperature profile for data record 56.

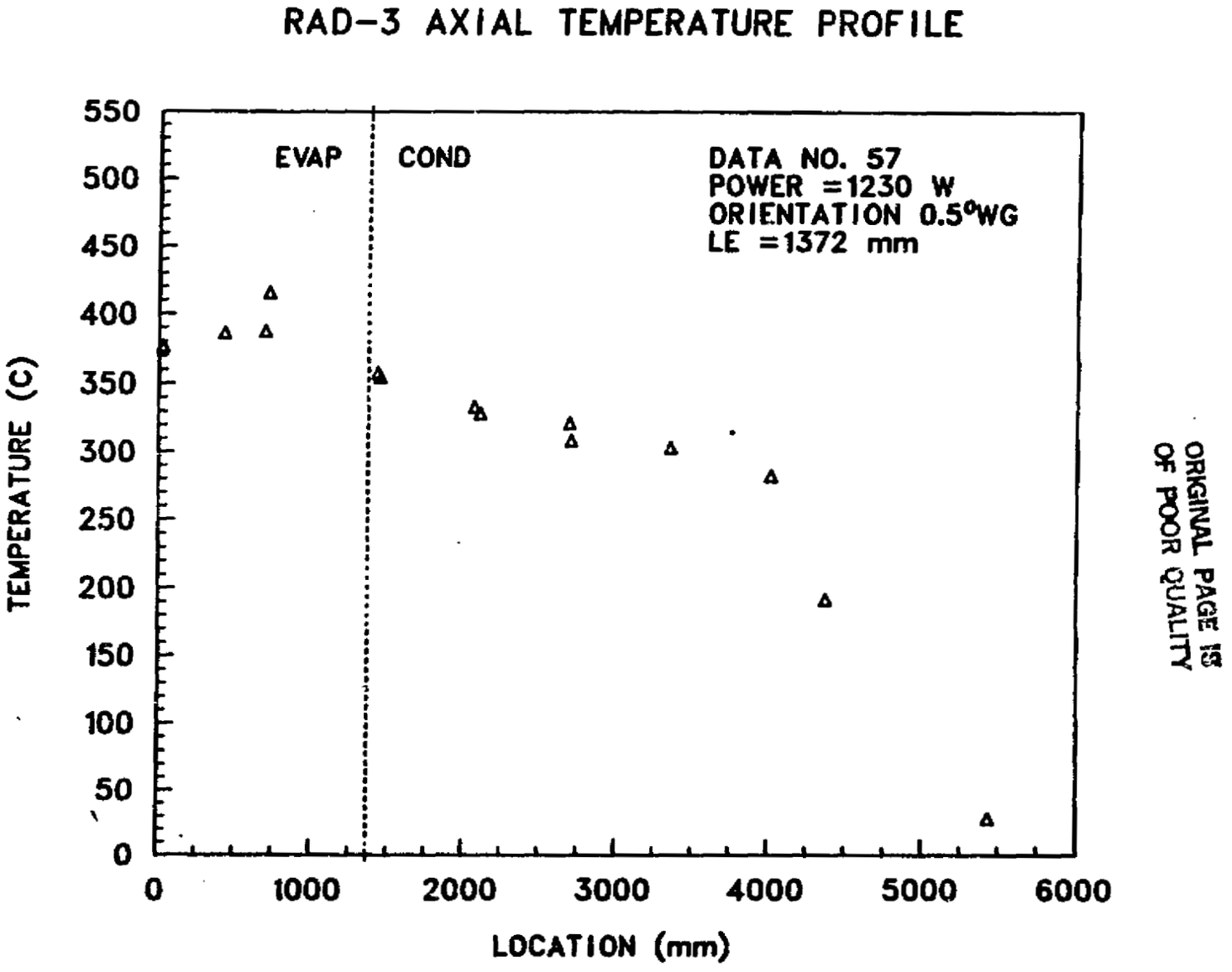

Fig. 32. Start-up temperature profile for data record 57.

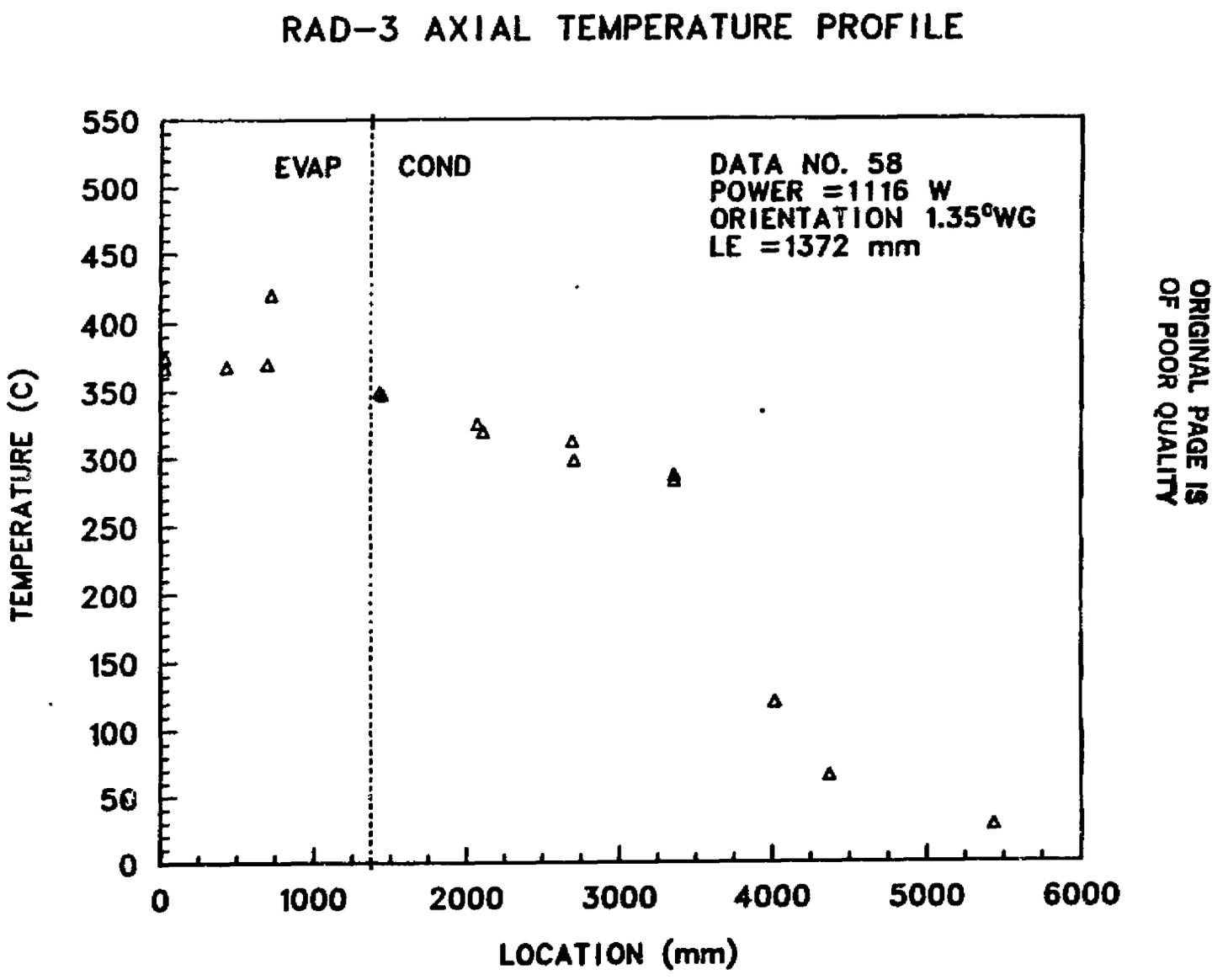

Fig. 33. Start-up temperature profile for data record 58.

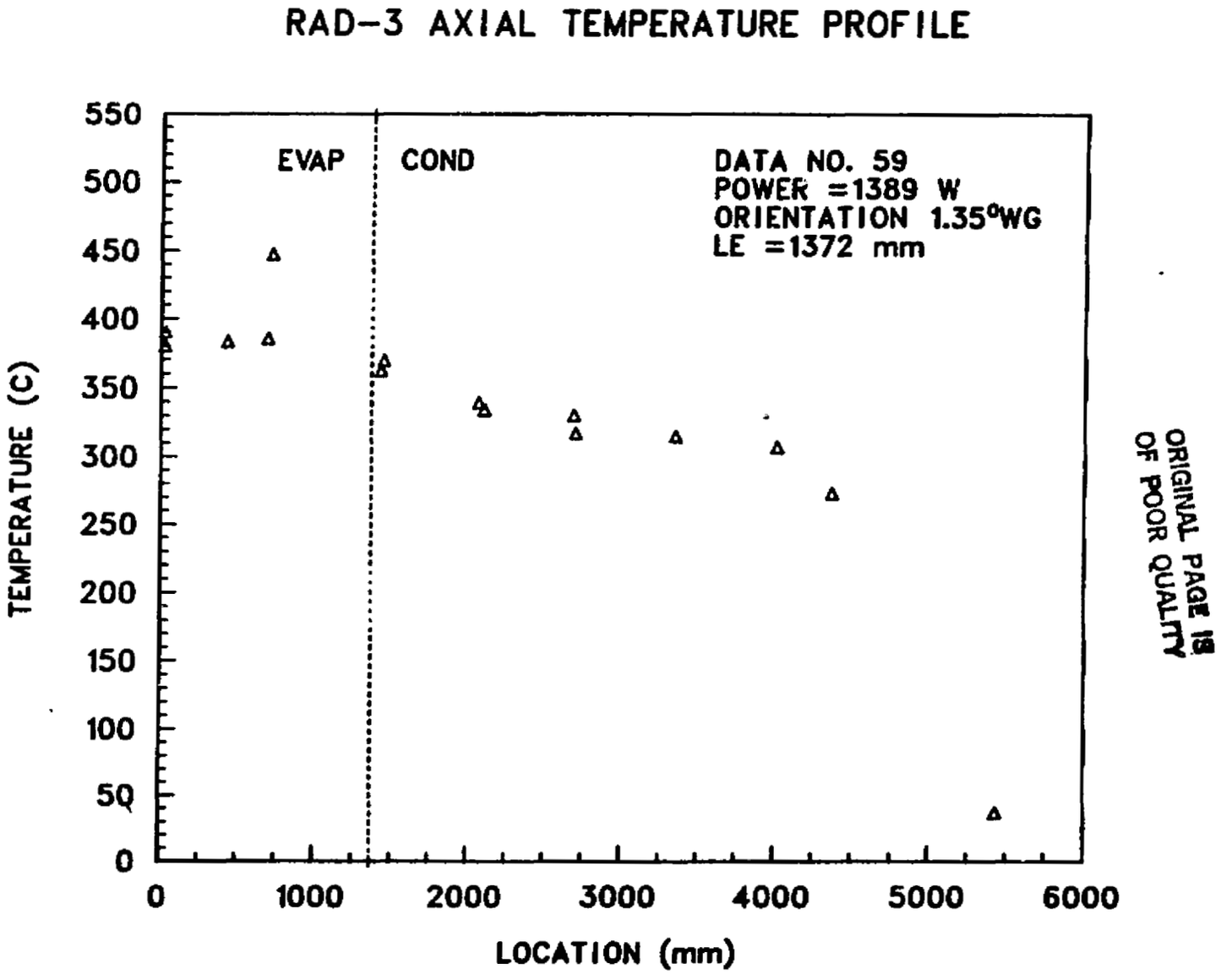

Fig. 34. Start-up temperature profile for data record 59.

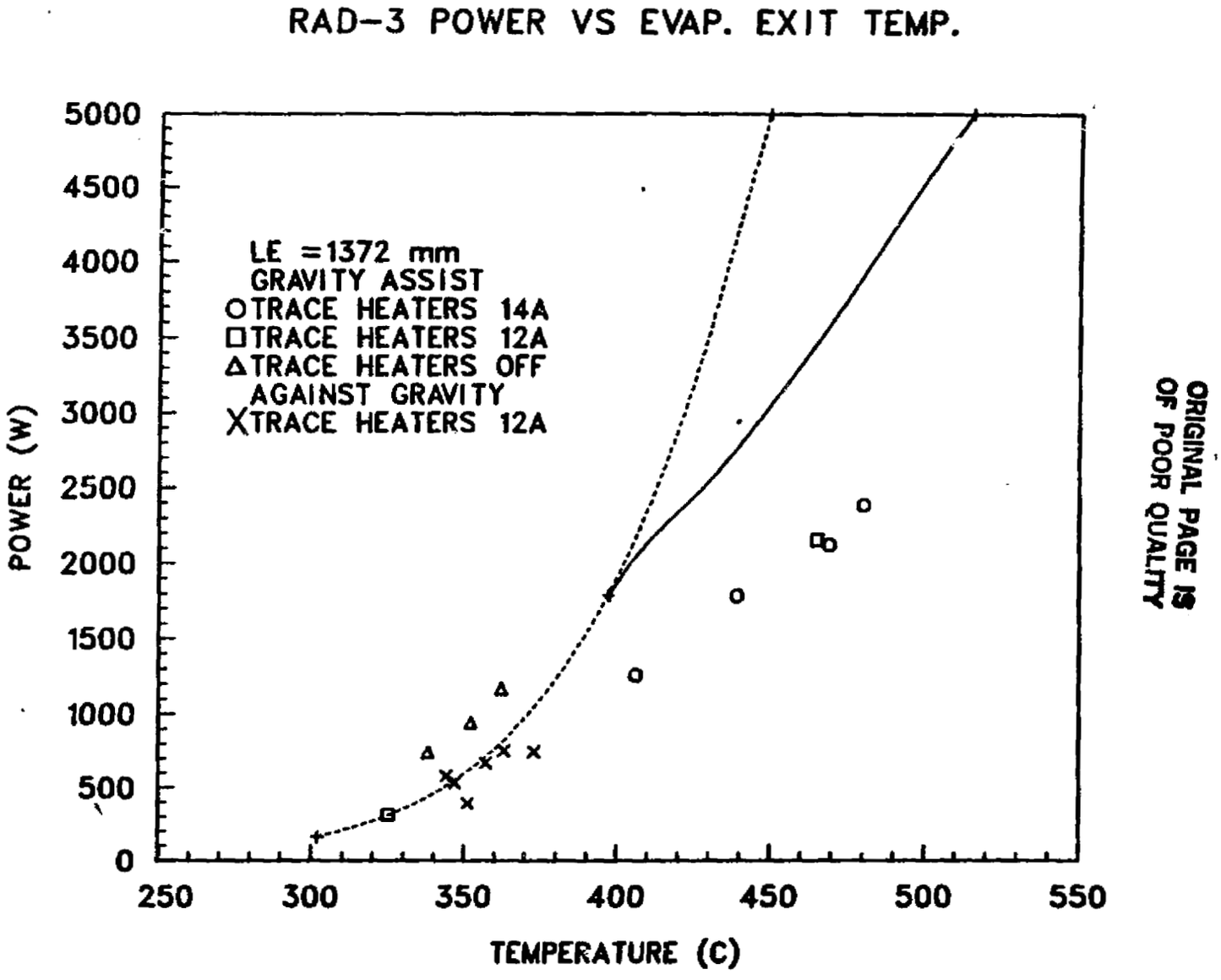

Fig. 35. Measured heat pipe power vs evaporator exit temperature.

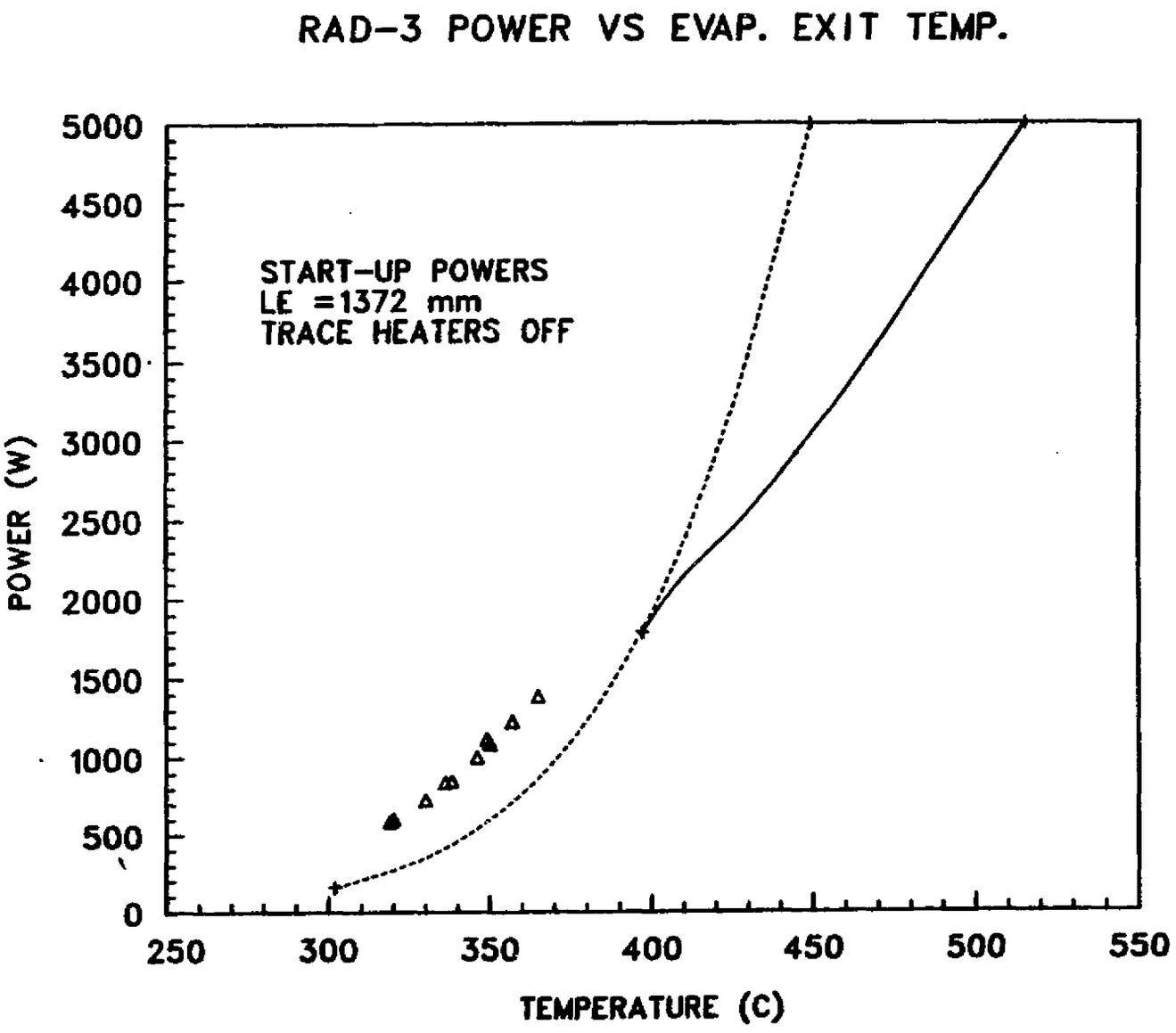

Fig. 36. Measured heat pipe power vs evaporator exit temperature during start-up.

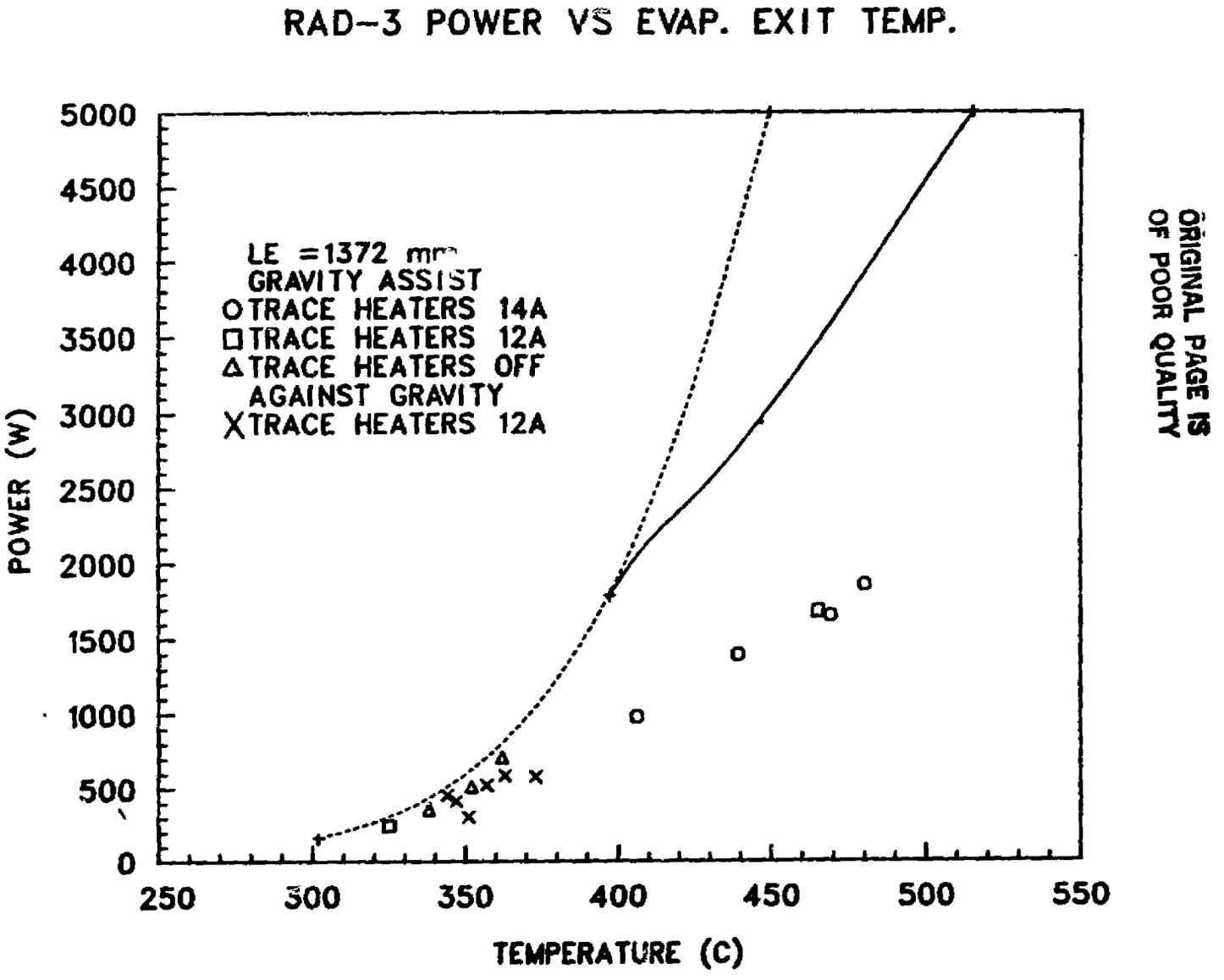

Fig. 37. Heat pipe power vs temperature after reduced power correction.

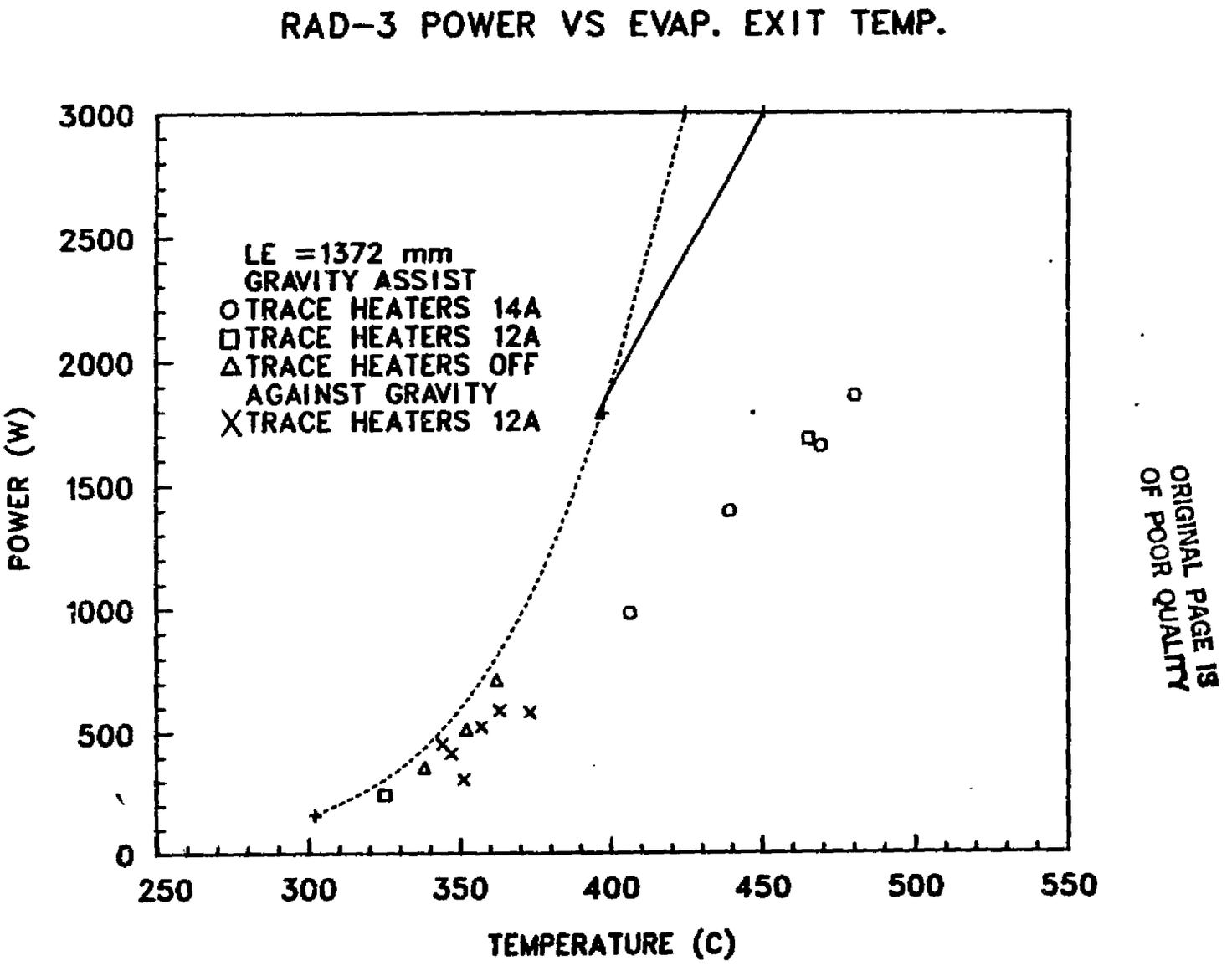

Fig. 38. Expanded scale of reduced power vs temperature.

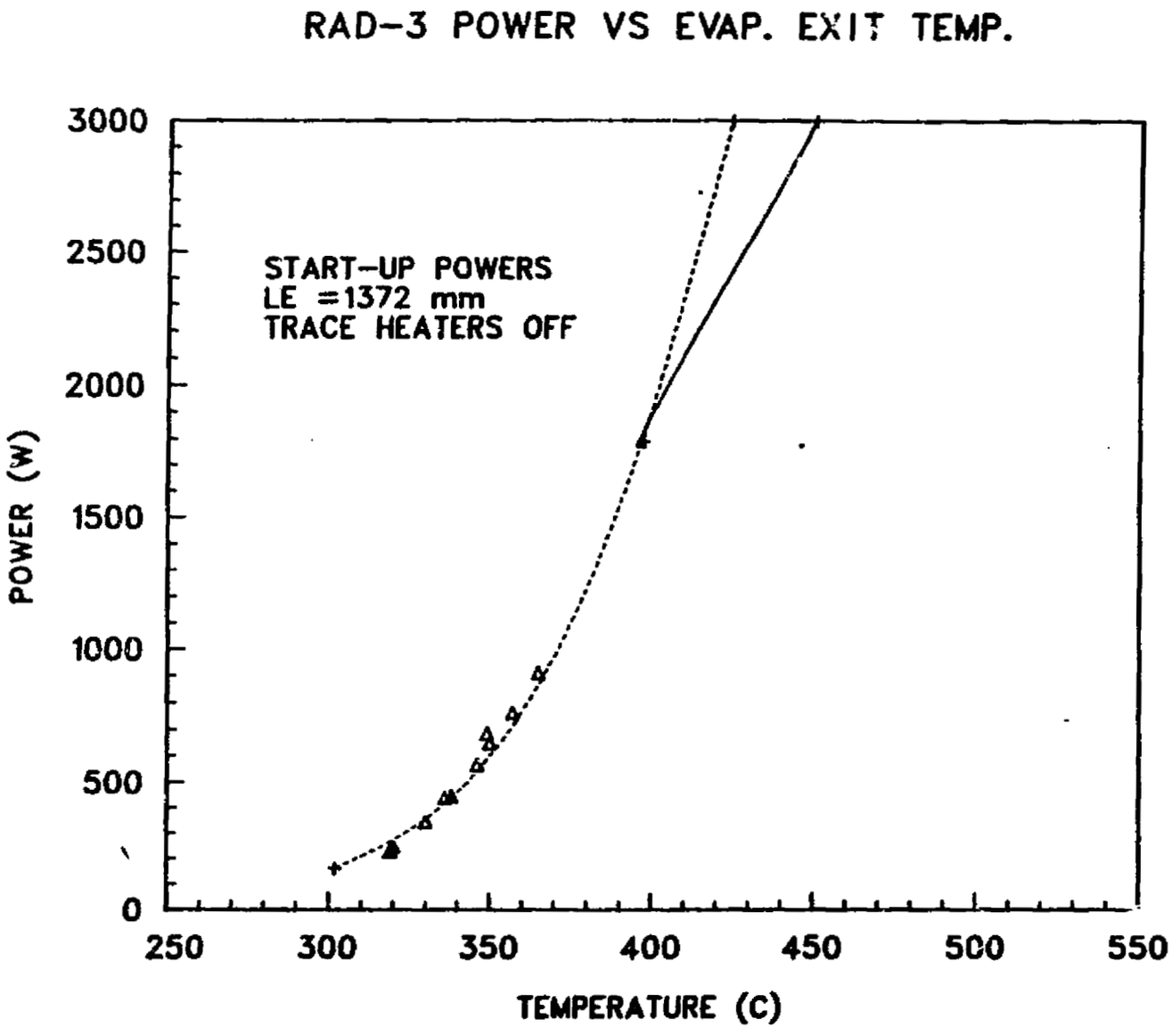

Fig. 39. Reduced start-up powers vs evaporator exit temperature.

APPENDIX I - TEMPERATURE RECORD OF DISTILLATION FILL FOR RAD-3.

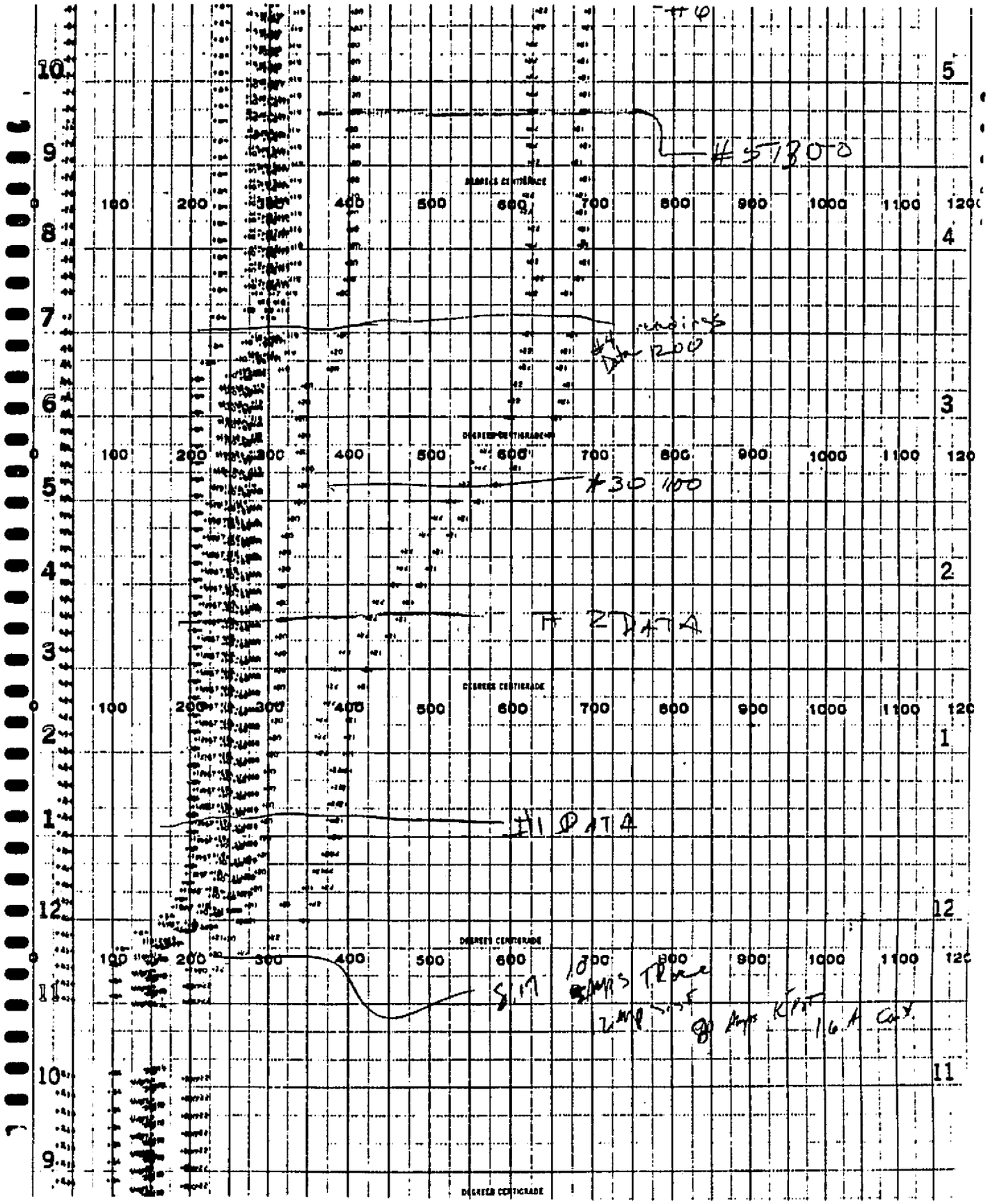

ORIGINAL PAGE IS
OF POOR QUALITY

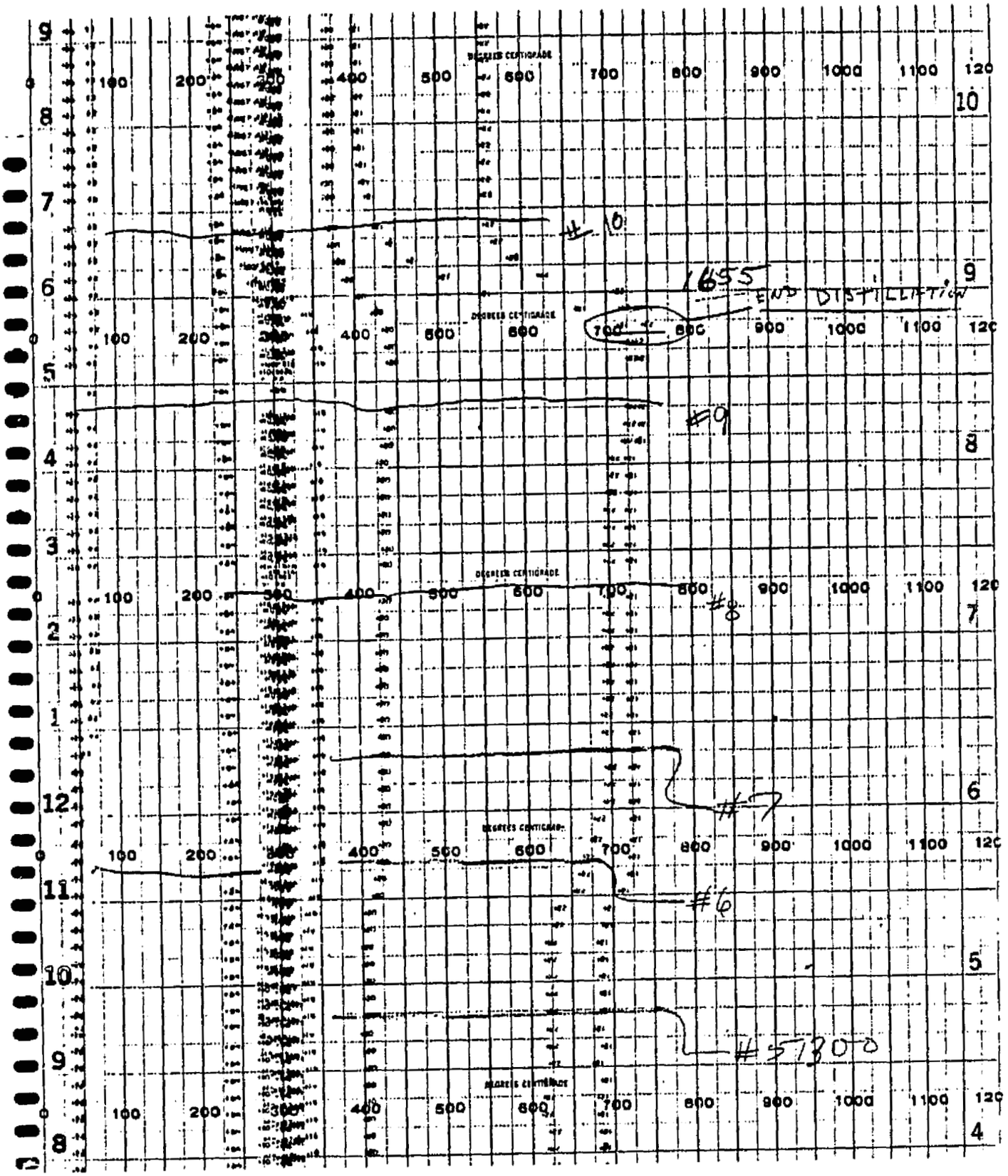

ORIGINAL PAGE IS
OF POOR QUALITY

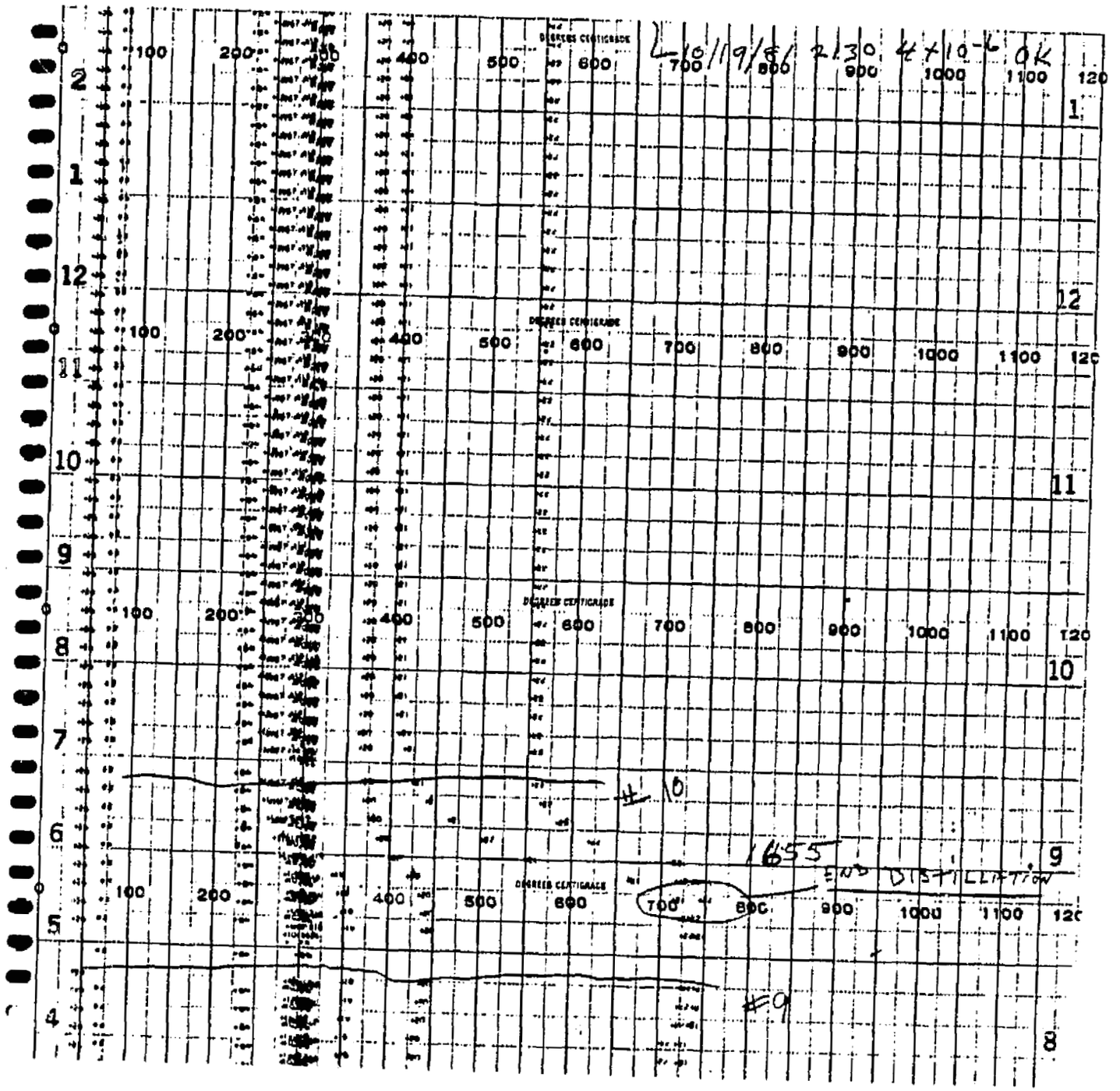

RAD-3 SPAR 5.5M TEST HEAT PIPE (12-8-81 MFPD)

HEAT PIPE ANALYSIS: POWER VS TEE

NO. OF ARTERIES OPERATING	8
ARTERY DIMENSION	.19000E+00
ARTERY PUMPING RADIUS	.25400E-01
ARTERY GEOMETRY	1 CIRCULAR
NO. OF ART. NOT OPERATING	0
ARTERY SCREEN THICKNESS	.20320E-01
DISTRIB. SCREEN THICKNESS	.12700E-01
EVAPORATOR LENGTH	.13700E+03
ADIABATIC LENGTH	0.
CONDENSER LENGTH	.41000E+03
ANGLE FROM HORIZONTAL	0.
PIPE INSIDE RADIUS	.14606E+01
WORKING FLUID NO.	3 K
A-RATIO(LAMIN OR TURB)	.12344E+01
PIPE EFFECTIVE LENGTH	.27350E+03
VAPOR PASSAGE AREA	.63027E+01
TOTAL LIQUID FLOW AREA	.22682E+00

TEE POWER	PRESSURE DROPS: LIQUID HYDROSTATIC	VAPOR(L) VAPOR(T)	INERTIAL CAPILLARY	EVAPORATOR ADIABATIC CONDENSER	TEMPERATURE TBE TBESON	TBC TBCSON	LIMITS QSONIC QENTRN
575.	148.	8516.	4119.	6252.	681.	575.	161.
-473.	0.	0.	7788.	0.	690.	575.	905.
				1388.			
600.	219.	6781.	4797.	6495.	686.	600.	328.
-717.	0.	0.	7661.	0.	627.	660.	1262.
				947.			
625.	387.	5754.	6011.	7452.	696.	625.	630.
-1097.	0.	0.	7634.	0.	654.	625.	1710.
				-879.			
650.	434.	4528.	6166.	7299.	703.	650.	1150.
-1488.	0.	0.	7407.	0.	682.	650.	2261.
				-1944.			
675.	559.	3665.	6238.	7140.	713.	675.	2003.
1948.	0.	0.	7281.	0.	709.	675.	2922.
				-2701.			
700.	705.	2913.	6248.	6977.	726.	700.	3358.
2484.	0.	0.	7154.	0.	737.	700.	3781.
				-3238.			
725.	871.	2384.	6211.	6808.	743.	725.	5407.
3109.	0.	0.	7027.	0.	765.	725.	4604.
				-3698.			
750.	1058.	1975.	6148.	6635.	763.	750.	8442.
3819.	0.	0.	6900.	0.	793.	750.	5637.
				-3858.			
775.	1268.	1654.	6041.	6456.	784.	775.	18797.
4614.	0.	0.	6773.	0.	821.	775.	6801.
				-4019.			
800.	1494.	1399.	5921.	6271.	806.	800.	18884.
5490.	0.	0.	6646.	0.	849.	800.	8098.
				-4111.			
825.	1748.	1195.	5783.	6082.	829.	825.	87198.
6446.	0.	0.	6519.	0.	877.	825.	9526.
				-4149.			

[61,]

61	850.	2000.	1029.	5631.	5889	853.	850.	38312.
62	7473.	0.	0.	6392.	0	905.	850.	11086.
63					-4146.			
64	875.	2892.	893.	5467.	5691.	877.	875.	52815.
65	8568.	0.	0.	6265.	0.	934.	876.	12768.
66					-4108.			
67	900.	2592.	780.	5293.	5489.	902.	900.	71658.
68	9722.	0.	0.	6138.	0.	962.	900.	14575.
69					-4044.			

*